



HAL
open science

Analysis of Electrocardiogram signals: from modelling to classification through signal processing

Julien Oster

► **To cite this version:**

Julien Oster. Analysis of Electrocardiogram signals: from modelling to classification through signal processing. Signal and Image processing. Université de Lorraine, 2022. tel-03908656

HAL Id: tel-03908656

<https://hal.univ-lorraine.fr/tel-03908656v1>

Submitted on 20 Dec 2022

HAL is a multi-disciplinary open access archive for the deposit and dissemination of scientific research documents, whether they are published or not. The documents may come from teaching and research institutions in France or abroad, or from public or private research centers.

L'archive ouverte pluridisciplinaire **HAL**, est destinée au dépôt et à la diffusion de documents scientifiques de niveau recherche, publiés ou non, émanant des établissements d'enseignement et de recherche français ou étrangers, des laboratoires publics ou privés.

Mémoire de recherche
présenté pour l'obtention du diplôme
d'Habilitation à diriger des Recherches
de l'Université de Lorraine
par **Julien OSTER**

Analysis of Electrocardiogram signals: from modelling to classification through signal processing

Le 19 décembre 2022

Membres du jury :

Rapporteurs:	M. Rémi Dubois	Professeur, Université de Bordeaux
	M. Christian Jutten	Professeur, Université de Grenoble
	Mme. Sabine VanHuffel	Professeure, KU Leuven

Examineurs:	M. Guy Carrault	Professeur, Université de Rennes
	M. Jacques Felblinger	Professeur, UL, Nancy
	Mme. Frida Sandberg	Professeure associée, Lund University

À Anatole...

A heart without dreams is like a bird without feathers.
Suzy Kassem

Résumé

Mes recherches ont essentiellement porté sur l'utilisation de méthodes de modélisation et de traitement des signaux pour extraire de nouveaux paramètres cliniques de grandes bases de données de signaux physiologiques, et sur l'utilisation de techniques d'apprentissage automatique pour l'aide à la décision clinique. J'applique ces techniques aux données électrocardiographiques (ECG) depuis plus de 10 ans.

Mon projet de recherche consiste à développer de nouvelles techniques d'apprentissage automatique combinées à et/ou inspirées par la modélisation afin de créer des systèmes de décision automatique interprétables dans le domaine des soins de santé cardiovasculaire. L'évaluation clinique de la santé cardiovasculaire nécessite l'acquisition de données multimodales, deux des modalités les plus importantes étant l'imagerie par résonance magnétique (IRM) et l'ECG. Mon objectif sera donc de développer des outils pour l'analyse conjointe de données électrophysiologiques et d'imagerie. Ces techniques et représentations de données offriront des solutions à des problèmes cliniques concrets tels que pour la prédiction des résultats de l'ablation par catheter de la fibrillation auriculaire, ou la stratification de risque de présenter une tachycardie ventriculaire.

Abstract

The focus of my research is the use of modeling and signal-processing methods to extract novel clinical parameters from large databases of physiological signals, and the use of machine-learning techniques to provide predictive actionable information to clinicians. I have been applying these techniques to electrocardiographic (ECG) (and other physiological) data for more than 10 years.

My research project consists in developing novel machine-learning techniques combined with and/or inspired by modelling in order to create interpretable automatic decision-making systems in healthcare, with a particular focus to cardiovascular health data. Clinical assessment of the cardiovascular health requires the acquisition of multimodal data, two of the most important modalities being Magnetic Resonance Imaging (MRI) and ECG. I therefore aim at developing tools for the joint analysis of electrophysiological and imaging data. These techniques and representations of data will offer solutions for concrete clinical problems such as better risk stratification for patients, whether for Atrial Fibrillation catheter ablation outcome prediction, and the risk of presenting Ventricular Tachycardia.

Contents

Résumé	9
Abstract	11
Introduction	19
I Work Experience	21
1 Curriculum Vitae	25
2 PhD Diploma	27
3 Teaching Activity	29
3.1 CentraleSupélec	29
3.2 University of Oxford	30
3.3 Université de Lorraine	30
3.4 Current Teaching Activities	30
4 Research Experience	31
4.1 Scientific Career	31
4.2 Publications	38
II Research Activities	45
5 Modelling	49
5.1 A morphological model for ECG signals	51
5.2 Considering pathological rhythms	53
5.3 Adding other pseudo-periodic components	56
5.4 Incorporating imaging information	59
5.5 Synthesis	63
6 Processing	65
6.1 Introduction of Bayesian filtering	65
6.2 Denoising	67
6.3 Signal Extraction	68
6.4 Synthesis	71

Table des matières

7	Classification	73
7.1	Detection of pathological beats	73
7.2	Rhythm classification: AF detection	76
7.3	Synthesis	80
III	Research Proposal	81
8	Analysis of electrophysiological data	85
8.1	Electrocardiogram	85
8.2	Representation Learning	86
8.3	Interpretability	87
8.4	Electrogram	88
8.5	Synthesis	89
9	MRI image analysis and reconstruction integrating the motion	91
9.1	Cardiac segmentation and heart model extraction	91
9.2	Cardiac image reconstruction pipelines	92
9.3	Autonomous cardiac MRI acquisition	93
9.4	Synthesis	94
10	Multimodal Deep Learning	95
10.1	Smart fusion of the multimodal information	95
10.2	ECG Imaging	96
10.3	Synthesis	97
	Bibliography	107

List of Figures

5.1	Famous picture of Einthoven during his ECG recording experiment. . . .	49
5.2	Drawing representing an entire cardiac cycle. The bottom row represents the equivalent dipole through the cardiac cycles and how it is projected on the the three limb leads (Netter, 1992).	50
5.3	Representation of an ECG cycle, the five characteristics waves, and the main biomarkers.	50
5.4	Simulation of an ECG signal using the model. (left) 3D representation of ten simulated cycles. Red circles represent the position of the five main waves. (right) Simulation of ten noisy ECG cycles, in red the representation of the scaled phase signal.	52
5.5	State transition graph for a first order Markov model with three modes. p_{ij} being the probability of the system to transition from mode i to mode j at any time t	54
5.6	Simulation of an ECG signal with Paroxysmal AF (PAF) using the model. (a) Simulated f waves. (b) Simulated ECG with a brief AF episode, indicated on top of the plot. (Petrenas et al., 2017)	56
5.7	From top to bottom: chest ECG (largely dominated by maternal ECG – mECG–), scalp EEG (sECG), and abdominal ECG (mixture of mECG and foetal ECG (fECG) (Clifford et al., 2014)	57
5.8	Amplitude and frequency range of different electro-physiological signals: maternal ECG (mECG), maternal EEG (mEEG), maternal Electrooculogram (mEOG), electromyogram (mEMG), electrohystogram (mEHG) and foetal ECG (fECG) (Sameni and Clifford, 2010)	58
5.9	Simple cylindrical model representing the mother torso. The two red circles represent the mother and the foetal hearts. The axis for each heart represent the orientation for the electrical dipole. The blue rectangles represent the location of the electrodes and their number denomination.	59
5.10	Influence of the synchronisation on image quality. Example of failed synchronisation (left) and good synchronisation (right).	60
5.11	Simplified flowchart of induction voltage due to MHD effect.	61
5.12	Distortion of the ECG signal by the MRI environment, with clean ECG signal (left) distortion of the ECG by the MHD effect (centre) and distortions by the gradients $G_{\{X,Y,Z\}}$ (right).	61
5.13	Multiple view of the geometrical models, torso in grey, heart in black and aortic arch in red. a) frontal view, b) lateral view, c) top view, d) lateral view.	62

LIST OF FIGURES

5.14	MRI image of the chest region (left), with the four hand selected planes for the measurement of the blood flow, in the ascending aorta (cyan) ascending aortic arch (blue) descending aortic arch (green) and descending aorta (red). The four corresponding flow rate measurements over one cardiac cycle, with the time $t = 0$ corresponding the QRS trigger point (right).	63
5.15	Template of the estimated and simulated MHD effects on the standard 12-lead derivations. (blue: extracted MHD effect, green: theoretical solution, black: INRIA's model, red: proposed model)	63
6.1	Flowchart of Bayesian filtering. The recursive process is depicted, starting from a prior knowledge of the state one get updated statistics of the hidden variabl, which are finally updated when new measurements come in. (source Wikipedia).	66
6.2	Results of ECG signal extraction, and automatic detection of a simulated T wave inversion. The annotations were obtained by using an automatic technique (ecgpuwave) Jané et al. (1997).	71
7.1	Example of the SKF filtering. The top row contains the ECG signal with both the raw signal (solid line) and the denoised signal (dashed line). The second row shows the class likelihood for each mode: normal beat (solid line), ventricular beat (dashed line) and X-factor (dash-dotted line). The example on the bottom highlights an example of ventricular beat classification, and the example on the top highlights an example of a noisy segment classified as X-factor.	77
7.2	Flowchart of the proposed methodology. The top row illustrates the expert annotation process including the manual subset selection, while the bottom row represents the automated identification of AF patients with the evaluation performed on a subset of the UK Biobank database, and the training of the evaluated techniques performed on the 2017 PhysioNet/Cinc challenge database.	78
8.1	Architecture of the CNN-LSTM network developed for ECG rhythm analysis3. The CNN network extracts multilevel morphological features at different time-steps, which are inputted in a LSTM network extracting temporal information, and returns the final rhythm label.	85
8.2	Illustration of the temporal and spatial invariance properties of the ECG signals. These properties allows for elegant and realistic data augmentation. Figure provided from Kiyasseh et al. (2021a).	87
8.3	Examples of SHAP values, and most important features for the decision on local ECG recordings, with examples from top to bottom of AF, Sinus rhythm, other abnormal rhythm or a noisy recording. On the examples A and B, it can be seen that the features lv_{rr} and PSS are contributing the most to the decision making, while $medPR$, in the example A, is the one contributing the most negatively (that is by decreasing the msot the confidence of the decision). Figure extracted from Rouhi et al. (2021).	88
8.4	Example of the use of active learning scheme for optimal placement of intracardiac measurements. Figure is extracted from Sahli Costabal et al. (2020)	89

9.1	Example of the use of a motion (deformation) model for the simulation of clinical data. Two cases are shown where a pathological deformation is applied on a healthy original heart image, allowing for the simulation of four pathological cases. (figure reproduced from Krebs et al. (2021)). . .	92
9.2	Flowchart of the reconstruction pipeline combining a motion model with external physiological sensor, and an integrated DL-based MRI reconstruction regularisation.	93
9.3	Flowchart of the technique for autonomous pipeline of MR acquisition and reconstruction. Figure reproduced from (Loktyushin et al., 2021).	94
10.1	Flowchart of the use of motion model features (so-called motion fingerprints) for the prediction of survival. Figure reproduced from (Krebs, 2020).	96
10.2	Flowchart of the ECGI technique based on CVAE for the fusion of 3D volumes of myocardial images with Body Surface Potentials. Figure reproduced from (Bacoyannis et al., 2019).	97

Introduction

This manuscript summarises my research career, which started twelve years ago with a PhD at the Imagerie Adaptative Diagnostique et Interventionnelle (IADI) laboratory in Nancy. My PhD was financially supported by an industrial partner, Schiller SA (Wissembourg, France). The collaboration was extremely strong with monthly visits of the company and several algorithms and tools were delivered. The IADI Lab is moreover located inside the University Hospital and strong collaborations with the radiology and cardiology departments were in place. This environment provided me with a better understanding of the challenges of working in an interdisciplinary team. This project was successfully completed and resulted in the development of tools such as a database, containing recordings from both healthy subjects and patients, as well as novel algorithms for improved patient care.

In 2010, I joined the Centre Suisse d'Electronique et de Microtechnique (CSEM) in Neuchâtel (Switzerland) as a Research & Development Engineer. CSEM is an independent, private and non-profit company for applied research. There, I had the opportunity to work on numerous projects involving the development of wearable biomedical devices, with partners such as the European Space Agency, Swiss start-ups or with a big European Consortium. In these projects, I was primarily responsible for the processing of physiological signals and the extraction of respiratory and cardiac features. I was not only in charge of the implementation of algorithms in C (real-time and fixed-point architecture) but was also involved in the development and validation of the electronic components. This experience provided me with exposure to the challenges and expectations in industry.

Subsequently, on the urging of Professor Christian Jutten in Grenoble (my external thesis examiner), I applied for and was awarded a Newton International Fellowship from the Royal Academy of Engineering. I used this fellowship to join the Institute of Biomedical Engineering (IBME) at the University of Oxford in March 2011. My research at the IBME has focused on cardiovascular signal processing. I have been involved in several projects. For instance, I have been leading the signal processing in a project to develop an end-to-end user solution for the management of cardiac arrhythmia using a smart-phone. This project was developed with interests and financial support from ARM and China Mobile. I have also been in charge of the analysis of ($\approx 100,000$) ECG signals on a huge database provided by the UK Biobank initiative. This project was a collaboration between Professor Tarassenko and Professor Barbara Casadei. Furthermore, one of my long running projects lies in improving cardiac monitoring during magnetic resonance imaging (MRI). More specifically I worked on the extraction of clinically useful information from the ECG and other cardiac information in the most hostile electromagnetic environment (the MRI scanner). I have also been awarded several prizes: a couple of poster awards as well as the J.A. Lodge award from the Institute of Engineering and Technology for a "promising early career in biomedical engineering". Joining the IPM group and one of the most prestigious universities has allowed me to conduct my research in a stimulating and enriching environment. Strong overseas collaborations have also been established with researchers

Table des figures

from Harvard Medical School, the Massachusetts Institute of Technology, the University of Valencia, the University of Magdeburg, the University of Dresden, and also with the French engineering school Supélec.

In 2016 I applied successfully for a senior Research Fellowship position from the Inserm Institute, and returned to the IADI laboratory in France. I am in charge of the signal processing and machine learning research undertaken in the lab. My main project consists in providing for a better risk stratification of Ventricular Tachycardia, by fusing information of two modalities: (i) images from an MRI scanner and (ii) ECG signals from multiple locations across the torso. Such an approach is called Electrocardiographic Imaging.

The manuscript is divided in three parts.

1. The first part is devoted to a short summary of my work experience, including a CV, a detailed summary of my teaching activity and of my Research experience.
2. The second part is a detailed presentation of my past research activities. I have been involved in several research projects, with applications ranging from ECG signals acquired during MRI, foetal ECG, detection of pathological rhythms on Big Data or for mHealth applications. These different projects are presented but not according to their applications, but given their research fields. (i) The first chapter presents the modelling of the morphology of the ECG signals. The modelling aspect has been carried out for stress testing analysis techniques in two main circumstances. The first is the generation of synthetic data when real data is scarcely available, which is true for new applications such as foetal ECG or ECG acquired in MRI, or for undiagnosed pathological data such as paroxysmal AF. The second reason stems from the fact that the inherent ground-truth is usually unknown in real data, that is the cleaned version of the ECG cannot be acquired, and quantitative assessment of a denoising technique is therefore impossible. (ii) The second chapter presents how ECG signals can be processed with a Bayesian filtering technique. The underlining theory is explained before two examples of applications are presented, the denoising of the ECG and the extraction of components respectively. (iii) The last chapter is dedicated to machine learning applications, starting with an extension of Bayesian filtering for classification purpose, and some other classification problems.
3. The last part consists in my vision for my future research prospects, and is also divided in three chapters. (i) The first chapter presents future works that will be conducted for the analysis of electrophysiological data (ii) The second chapter will aim at presenting how ML and DL solutions could provide new technique for the analysis and reconstruction of MR images by accounting for motion, maybe allow for the development of an autonomous acquisition of whole heart cardiac MRI. (iii) The final chapter will be investigating how cutting edge machine learning approaches could be used for uncovering a multimodal representation of electrophysiological and imaging data.

Part I
Work Experience

*Engineering: where the noble, semi-skilled laborers execute
the vision of those who think and dream. Hello, Oompa Loompas of science!*
Sheldon Lee Cooper

Chapter 1

Curriculum Vitae

Julien OSTER

PhD - Engineer

Statistical Signal Processing for Biomedical Applications

*IADI U947, Batiment de recherche
CHRU de Nancy Brabois - Rue du Morvan
54511 Vandoeuvre les Nancy, France*

+33 3 83 15 33 97

✉ julien.oster@inserm.fr

Education

- 2006–2009 **PhD, IADI, Nancy-Université, Inserm U947, Nancy, FRANCE.**
Real-time processing of electrophysiological signals acquired in a Magnetic Resonance Environment jointly supervised by Prof. Felblinger and Dr. Pietquin
- 2003–2006 **Master's Degree, Ecole supérieure d'Electricité (Supélec), Metz, FRANCE.**
French leading Engineering School specialized in computer science and electronics.
Specialization: Statistical Signal Processing, Spectral Analysis, Speech/ Image Processing, Pattern recognition.
- 2005–2006 **Master's Degree, Ecole supérieure d'Electricité (Supélec), Metz, FRANCE.**
Fundamental and applied Mathematics

Experience

Vocational

- Oct. 2016 **Personalised ECG Imaging,**
–today *IADI U947, Inserm, Nancy, FRANCE.*
Senior Research Associate,
responsible for the **Biomedical Signal Processing** and **Machine Learning** in the lab.
- 2013–2016 **Cardiovascular signal processing,**
Institute of Biomedical Engineering, University of Oxford, Oxford, UNITED KINGDOM.
Postdoctoral Research Assistant under the supervision of D. Clifford and Prof. Tarassenko
Biomedical Signal Processing
- 2011–2013 **Suppression of the MagnetoHydroDynamic effect on Electrocardiogram in Magnetic Resonance Imaging,**
Institute of Biomedical Engineering, University of Oxford, Oxford, UNITED KINGDOM.
Postdoctoral position under the supervision of D. Clifford
funded through the Newton International fellowship grant scheme
Biomedical Signal Processing
- 2010 **Biomedical signal processing,**
Centre Suisse d'Electronique et de Microtechnique (CSEM), Neuchâtel, SWITZERLAND.
Research & Development Engineer
Biomedical Signal Processing, Wearable Technology
- 2006–2009 **Real-time processing of electrophysiological signals acquired in a Magnetic Resonance Environment,**
Nancy-Université-Inserm, Nancy, FRANCE.
Research engineer. Collaboration with *Schiller Médical, Wissembourg, FRANCE*
Biomedical Signal Processing, Adaptive Magnetic Resonance Imaging Technique
- Teaching activity**
- 2013–2016 **College Lecturer,**
Pembroke College, University of Oxford, Oxford, UNITED-KINGDOM.
Electrical and Information Engineering, 2nd year students
Mathematics, 2nd year students
- 2012–2016 **Lectures,**
CDT for Healthcare Innovation, University of Oxford, Oxford, UNITED-KINGDOM.
Introduction to Digital Filtering, and Event Detection
- 2007–2009 **Labs and Tutorials,**
Ecole supérieure d'Electricité (Supélec), Metz, FRANCE.
Statistical Signal Processing, 3rd year students
Signal Representation and Statistical Analysis, 2nd year students

Chapter 2

PhD Diploma

R É P U B L I Q U E F R A N Ç A I S E
MINISTÈRE DE L'ENSEIGNEMENT SUPÉRIEUR ET DE LA RECHERCHE
UNIVERSITÉ HENRI POINCARÉ, NANCY I
DOCTORAT

Vu le code de l'éducation ;

Vu le code de la recherche et notamment son article L.412-1 ;

Vu le décret n°2002-481 du 8 avril 2002 relatif aux grades et titres universitaires et aux diplômes nationaux ;

Vu l'arrêté du 3 septembre 1998 relatif à la charte des thèses ;

Vu l'arrêté du 7 août 2006 relatif à la formation doctorale ;

Vu les pièces justificatives produites par M. JULIEN OSTER, né le 3 novembre 1983 à HAGUENAU (067), en vue de son inscription au doctorat ;

Vu le procès-verbal du jury attestant que l'intéressé a soutenu, le 5 novembre 2009 une thèse portant sur le sujet suivant : Traitement temps réel des signaux électrophysiologiques

acquis dans un environnement d'imagerie par résonance magnétique, préparée au sein de l'école doctorale Informatique - Automatique - Electronique - Electrotechnique -

Mathématiques (077), devant un jury présidé par PIERRE-YVES MARIE, Prof. des Univ. Praticien Hospitalier et composé de GUY CARRAUDI, Professeur des Universités,

ALAIN DUFAYX, Maître de conférences, JACQUES FEIBLINGER, Prof. des Univ. Praticien Hospitalier, CHRISTIAN JUTTEN, Professeur des Universités, MICHEL

KRAEMER, Ingénieur, OLIVIER PIETQUIN, Maître de conférences ;

Vu la délibération du jury ;

Le **DIPLOME NATIONAL DE DOCTEUR** en AUTOMATIQUE, TRAITEMENT DE SIGNAL ET GÉNIE INFORMATIQUE

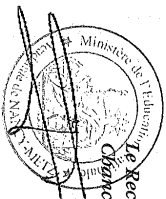
est délivré à **M. JULIEN OSTER**

et confère le **grade de docteur**,

pour en jouir avec les droits et prérogatives qui y sont attachés.

Fait à NANCY, le 3 février 2010

Le titulaire



N° NANCY 1 7857367

Jean-Pierre FINANCE

Jean-Jacques POLLETT

Chapter 3

Teaching Activity

Embracing a research career also necessitates teaching, where one encounters the deepest questions about the foundation of their research and provides the opportunity to test the limits of one's explanatory powers. During my Ph.D., I had the opportunity to give tutorials and supervise labs in Supélec to second and third year engineering students (the equivalent of fourth year undergraduate students and master students respectively). The subjects of these tutorials were Signal Representation and Statistical Analysis, and Statistical Signal Processing. From 2013 to 2016, I was appointed as a Stipendiary Lecturer at Pembroke College (University of Oxford), where I was in charge of the teaching for the Electrical and Information Engineering to the second year students, and also for half of the teaching load in Mathematics (Statistics, Probability and Algebra). This experience was highly enriching. It demonstrated to me the challenges of teaching, but allowed me to learn how to explain difficult concepts and rephrase ideas such that students with varying learning approaches can overcome their difficulties. I was also been giving lectures for the Biomedical Signal Processing module in the Centre for Doctoral Training in Healthcare Innovation at the University of Oxford for three academic years.

3.1 CentraleSupélec

RASS	2006 – 09	Tutorials (6h/year) and laboratory works (45h/year) of the class entitled " <i>Représentation et analyse des signaux statistiques</i> " to second year students (equivalent M1)
Stat. Sign.	2006 – 09	Tutorials (12h/year) of the class entitled " <i>Représentation et analyse des signaux statistiques</i> " to second year students (equivalent M1)
Machine Learning	2016 –	Supervision of End of Year Projects (25h/year) " <i>Machine Learning applied to Health Data</i> " to third year students (equivalent M2)

3.2 University of Oxford

Info. Eng.	2013 – 16	Tutorials (48h/year) of Information Engineering to second year students (equivalent L2)
Math.	2013 – 16	Tutorials (48h/year) of Mathematics to second year students (equivalent L2)
Biosig. Proc.	2012 – 15	Lectures (6h/year) for the Biomedical Signal Processing module in the Centre for Doctoral Training in Healthcare Innovation at the University of Oxford (equivalent M2)

3.3 Université de Lorraine

ECG	2016 – 17	Tutorials (3h/year) of the class entitled " <i>Introduction to the ECG signal</i> " to third year students (equivalent L3)
Mach. Learn.	2017	Lecture (1.5h/year) of the class entitled " <i>Machine Learning</i> " to fifth year students (equivalent M2)

3.4 Current Teaching Activities

A synthesis of my current (as of academic year 22/23) teaching duties in the table 3.1.

Organisation	Title	Info
CentraleSupélec	End of Year Projects "Machine Learning applied to Health Data"	25h/year to M2 students
Université de Lorraine	Artificial Intelligence for Medical Imaging	1.5h/year to M2 students
Université de Lorraine	Introduction to Artificial Intelligence	1h/year to 2nd year Med students

Table 3.1: Synthesis of my current teaching duties.

Chapter 4

Research Experience

4.1 Scientific Career

4.1.1 PhD Student supervision

During my postdoctoral fellowship, I have been offered the opportunity to co-supervise and mentor local and visiting PhD students. I particularly enjoy the interactions with them. These supervisions have been really successful; all three PhD students have defended their thesis successfully. Each of these projects has been accompanied with successes. Both overseas students (J. Krug and F. Andreotti) have won an award for the best poster in international conferences.

Moreover some of the small projects, I have been involved in and managed, finished best entries in two consecutive Physionet/Computing in Cardiology challenges (2013 and 2014). Of particular interest, the 2014 challenge consisted in the robust detection of heartbeats in multimodal data, which demonstrates my expertise in cardiovascular data fusion. Mentoring these students and making them benefit from my experience has reinforced my decision to pursue an academic career.

Chapter 4. Research Experience

Co-supervision

J. Krug 2011 – 15 *Improved cardiac gating and patient monitoring in high field Magnetic Resonance Imaging by means of Electrocardiogram signal processing* co-supervised with **Pr. Georg Rose**.
1 joint journal paper and 4 international conference papers during this PhD

J. Behar 2011 – 14 *Extraction of clinical information from the non-invasive Fetal Electrocardiogram* co-supervised with **Dr. Gari Clifford**.
9 joint journal papers and 8 international conference papers during this PhD

Mentoring

F. Andreotti 2012 – 16 *Extraction and Detection of Fetal Electrocardiograms from Abdominal Recordings* supervised by **Dr. Sebastian Zauneder** and **Pr. Hagen Malberg**.
4 joint journal papers and 4 international conference papers during this PhD

Current PhD co-supervisions

L. Quillien 2022 – .. *IRM cardiaque 3D en respiration libre basée sur des techniques d'apprentissage automatique* co-supervised with **Dr. Pierre-André Vuissoz**.

M. Diaw 2021 – .. *Analyse Approfondie de l'ECG pour l'extraction de biomarqueurs de la Dispersion Mécanique Cardiaque* co-supervised with **Prof. Jacques Felblinger**.
currently 1 joint journal paper submission and 1 joint international conference papers.

P. Aublin 2020 – .. *Analyse approfondie des Electrocardiogrammes acquis en IRM* co-supervised with **Prof. Jacques Felblinger**.
currently 1 joint journal paper and 2 joint international conference paper.

B. Roussel 2018 – 22 *Analyse de champs magnétiques en IRM pour une application d'electro-imaging* co-supervised with **Prof. Jacques Felblinger**.
currently 1 patent application, 1 journal paper submission and 3 joint international conference papers.

Postdoc supervision

S. Mihan-doust 2018 – 22 *Analysis of ECG signals for the prediction of AF Catheter ablation outcome.*
1 joint journal paper.

J.S. Louis 2020 – 22 *Cardiac MRI of pathological rhythms*

4.1.2 Collaborations

Joining the IPM group and one of the most prestigious universities has allowed me to conduct my research in a stimulating and enriching environment. Strong overseas collaborations have also been established with researchers from Harvard Medical School, the Massachusetts Institute of Technology, the University of Valencia, the University of Magdeburg, the University of Dresden, and also with the French engineering school Supélec.

Since returning in France, I have tried to build new collaborations between the IADI lab and international entities.

Some of the collaborations I have been involved are listed below:

Harvard Medical School, USA	2011 – 13	<i>Patient monitoring during interventional MRI with Dr. Ehud Schmidt.</i>
Supélec, France	2011 – 13	<i>Bayesian Filtering with Pr. Olivier Pietquin and Pr. Matthieu Geist.</i>
University of Valencia, Spain	2011 – 13	<i>Modelling of the MagnetoHydroDynamic effect with Dr. Raul Llinares.</i>
Massachusetts Institute of Technology, USA	2013	<i>Help in organising the Physionet/Cinc challenge with Dr. Ikaro Silva and Benjamin Moody.</i>
University of Magdeburg, Germany	2011 – 15	<i>Improved cardiac gating and patient monitoring in high field Magnetic Resonance Imaging by means of Electrocardiogram signal processing with Dr. Johannes Krug and Pr. Georg Rose.</i>
University of Dresden, Germany	2012 – 16	<i>Extraction and Detection of Fetal Electrocardiograms from Abdominal Recordings with Dr. Fernando Andreotti, Dr. Sebastian Zauseder and Pr. Hagen Malberg.</i>
University of Oxford, UK	2015 –	<i>Analysis of ECG signals in UK Biobank with Pr. Lionel Tarassenko, and Pr. Barbara Casadei.</i>
University of Lund, Sweden	2015 – 17	<i>Modeling of ECG with paroxysmal AF with Pr. Leif Sörnmo.</i>
Technion, Haifa, Israel	2015 –	<i>Foetal ECG and Rhythm classification with Dr. Joachim Behar.</i>
University of Applied Sciences and Arts Northwestern Switzerland	2016 –	<i>Magnetic Tracking and magnetic field mapping with Pr. Joris Pascal.</i>
University of Luebeck, Germany	2017 –	<i>Heart segmentation with Pr. Mattias Heinrich.</i>

4.1.3 External Visibility

4.1.3.1 Prizes and awards

- 2020** *top 10 % of high-scoring reviewers for NeurIPS 2020*
- 2016** *Highlights of 2016 "Evaluation of the foetal QT interval using non-invasive foetal ECG technology" selected by Physiological Measurement*
- 2016** *Highlights of 2016 "A practical guide to non-invasive foetal ECG extraction and analysis" selected by Physiological Measurement*
- 2014** *Winner of Phase 3 of the Physionet/Computing in Cardiology Challenge: Robust Detection of Heart Beats in Multimodal Data*
- 2014** *Best poster award at Computing in Cardiology*
- 2013** *Unofficial winner of events 1 and 2 of the Physionet/Computing in Cardiology Challenge: Noninvasive Fetal ECG*
- 2013** *Best poster award at the SCMR/ISMRM Jointly Sponsored Workshop: New Horizons in High Field Cardiovascular MR: Promises and Progress*
- 2012** **J.A. Lodge Award** from the Institute of Engineering and Technology (IET), for recognition of promising early career in Biomedical engineering
- 2012** *2nd prize for the best poster award at the Workshop of Biomedical Signal Interpretation*
- 2010** **Newton International Fellowship** Royal Academy of Engineering, (126,000 pounds)
- 2008–2009** *PhD Scholarship* Received the Région Lorraine PhD Scholarship

4.1.3.2 Invited Talks and Editorships, and Session chair

Invited Editor

- 2017** focus issue on Wearables and mHealth in mental health and neurological disorders, *Physiological Measurement*
- 2015** focus issue on the 2014 Physionet/Cinc Challenge, *Physiological Measurement*

Session Chair

- 2021** Computing in Cardiology, Brno, Czech Republic
- 2017** Computing in Cardiology, Rennes, France
- 2015** Computing in Cardiology, Nice, France
- 2015** International Society of Computerized Electrocardiography, San Jose, USA

Invited Talks

- 2019** *Workshop of Consortium of ECG Imaging*, Bordeaux, France
 Preceding to Functional Imaging and Modeling of the Heart (FIMH), the Consortium for ECG Imaging organized a one-day workshop to improve the interaction between engineers and clinicians in the field of ECGI. This CEI satellite workshop took place on the 5th June 2019 at the LIRYC institute amphitheatre in Bordeaux, the day before the FIMH conference begins. The format included a mixture of clinical and engineering presentations as well as time for open discussion.
- 2015** *EHRA Europace Cardiostim*, Milano, Italy
 EHRA Congress is a truly international event with healthcare professionals from over 100 countries. It expands boundaries of arrhythmia management and gather physicians, nurses, allied professionals and healthcare industry representatives to gain valuable insight from these prominent professionals.
- 2015** *International Society of Computerized Electrocardiography*, San Jose, USA
 The Society is devoted to the advancement of electrocardiography through the application of computer methods. Its annual scientific conference, designed in the Gordon format, brings together scientists, clinicians, engineers and policy makers working in the field. Since the conference is designed to stimulate the informal exchange of ideas and information, there is ample allocated time for the 125 or so participants to mingle and discuss ideas of mutual interest.
- 2014** *Computational Cardiovascular Science Workshop*, Oxford, UK
 The Computational Cardiovascular Science Workshop was hosted in Oxford, organised by Prof Blanca Rodriguez. It created an international, interdisciplinary and inter-sectorial forum to discuss current trends in computational technologies to augment cardiovascular physiology, pharmacology and medicine, and to replace, refine and reduce animal experimentation. Participants included experts in cardiology, computer science, physiology, pharmacology, philosophy, and biomedical engineering from academia and industry, from 11 Universities and 12 companies, from the UK, several countries in Europe, the USA and Japan.

Chapter 4. Research Experience

4.1.3.3 Reviewing activity

Journals IEEE Transactions on Biomedical Engineering, IEEE Journal of Biomedical and Health Informatics, Physiological Measurement, Signal Processing, Biomedical Signal Processing and Control, Biomedical Engineering Online, Royal Society Open Science, Medical and Biological Engineering and Computing, Computers in Biology and Medicine, Plos One...

Conferences NeurIPS, ICML, ICLR, Computing in Cardiology, CHIL, IEEE NEWCAS

Thesis

PhD *Thimothée Zaragori* (Nancy, France), 2021 (as an examiner).

PhD *Soumaya Khreis* (Rennes, France), 2019.

PhD *Matthieu Doyen* (Rennes, France), 2018.

PhD *Johannes Krug* (Magdeburg, Germany), 2015.

Licentiate *Mikael Henrikson* (Lund, Sweden), 2016.

BsC *Patrick Rotach* (MuttENZ, Switzerland), 2022.

BsC *Ralph Rechsteiner* (MuttENZ, Switzerland), 2019.

BsC *Dominic Jeker* (MuttENZ, Switzerland), 2019.

BsC *Felix Yeung* (MuttENZ, Switzerland), 2017.

4.1.4 Project Management

Since the beginning of my career, I have managed to secure funding for several projects. This funding allowed for the recruitment of all the PhD students and postdocs I am currently supervising.

2010–2020 126k£ PI *Newton International Fellowship*, Royal Academy of Engineering,

This fellowship allowed to join the Intelligent Patient Monitoring group led by Prof. Gari Clifford. The funding scheme paid for my salary over a two-year period plus a generous relocation package. During this period, my research focuses on the development of statistical signal processing techniques for the removal of blood flow artifacts in cardiac electrophysiological data recorded during magnetic resonance imaging.

2018–2021 100k PI *Bourse doctorale (B. Roussel)*, Région Grand Est – Université de Lorraine

This grant secured funding Benjamin Roussel's PhD, with an equal contribution from the Région Grand Est and the Ecole doctorale (IAEM). Benjamin worked on the analysis of the varying magnetic fields in MRI for two applications, first the magnetic tracking of ECG sensors during MRI acquisitions, and second the development of a machine-learning based Electrical Impedance Tomography, fusing prior imaging information and electrical measurements.

2019–2021 150k (75k) co-PI *AIHD*, Projet Mirabelle+, Lorraine Université d'Excellence

This project stemmed from a collaboration between three institutes from the Université de Lorraine (Loria, IECL and IADI). The goal of the project was to develop machine-learning based techniques for the analysis of ECG signals for the early detection of Atrial Fibrillation, and the outcome prediction of AF ablation procedures.

2020–2023 630k (275k) PI *MEIDIC-VTACH*, ERA-CVD JTC 2019

This project is an international collaboration between three institutes the University of Luebeck (Germany), the Technion Institute (Israel) and the IADI lab. Our main objective is to develop a novel technique for the fusion of information provided by Electrocardiogram (ECG) data, mechanical information of the heart provided by Magnetic Resonance Imaging (MRI), and rhythm information provided by long-term portable ECG, which will be denoted mobile ECGI. ECGI is an exciting avenue of research for several cardiovascular applications, including risk stratification for VT.

2021–2023 160k (80k) PI *LIBI*, PHC Maimonide, MAE et MESRI

This project is a collaboration between the Technion Institute (Israel) and the IADI lab. One aims to develop novel ML classification algorithms for the purpose of physiological time series analysis within the context of AF diagnosis and personalized therapy. This research objective is two-fold: (i) generalization of ML algorithms for AF diagnosis (ii) the extraction morphological and rhythms variability biomarkers for catheter ablation outcome prediction.

2021–2025 400k (200k) PI *MEDICARE*, 1st German French Call on AI, ANR.

This project is a collaboration between the University of Luebeck (Germany) and the IADI lab. The overall goal of developing a Motion-Integrated AI-based cardiac reconstruction technique will be achieved through the following four sub-objectives: (i) Develop accelerated AI-based MRI reconstruction that incorporate uncertainty modelling into the analysis to enhance the trustworthiness of image quality(ii) Advance MRI reconstruction of subtle abnormal anatomical details to avoid bias of healthy tissues in AI-models and improve clinical reliability (iii) Develop and incorporate AI-based 4D motion prediction without full reconstruction for faster sparse k-space sampling for MRI acquisition (iv) Enhance the explainability of AI methods for MR image processing by combining AI based feature extraction with robust graph-based optimization strategies.

4.2 Publications

4.2.1 Patents

2013 **G. D. Clifford, J. Behar, J. Oster**, Signal Extraction, US patent application 61/803,004, March 2013.

G. D. Clifford, J. Oster, O. Pietquin, M. Geist, Periodic artifact reduction from biomedical signals, WO 2 013 052 944, April 2013.

4.2.2 Thesis

2009 **J. Oster**, "Real-Time Processing of Electrophysiological Signals Acquired in a Magnetic Resonance Imaging Environment", PhD Thesis.

4.2.3 Book Chapter

2015 **J. Oster, and G.D. Clifford**, "Signal quality indices for state-space electrophysiological signal processing and vice versa", *Advanced State Space Methods for Neural and Clinical Data*, Cambridge University Press, 2015.

2016 **Q. Liu, C. Liu, J. Oster, and G.D. Clifford**, "Signal Processing and Feature Selection pre-processing for classification in noisy Healthcare Data", *Machine Learning in Healthcare*, IET, 33, 2016.

2016 **J. Oster**, "ECG model-based Bayesian filtering", *Machine Learning in Healthcare*, IET, 59, 2016.

4.2.4 Journals

2022 **P. Aublin, M. Ammar, J., Fix, M., Barret, J., Behar and J. Oster**, "Predict alone, decide together: cardiac abnormality detection based on single lead classifier voting." *Physiological Measurement*, 2022.

K. Isaieva, M. Fauvel, N. Weber, P.-A. Vuissoz, J. Felblinger, J. Oster and F. Odille, "A hardware and software system for MRI applications requiring external device data." *Magnetic Resonance in Medicine*, 2022.

T. Zaragori, J. Oster, V. Roch, G. Hossu, M.B. Chawki, R. Grignon, C. Pouget, G. Gauchotte, F. Rech, M. Blonski, L. Taillandier, L. Imbert and A. Verger, "18F-FDOPA PET for the non-invasive prediction of glioma molecular parameters: a radiomics study." *Journal of Nuclear Medicine*, 63 (1), 147-157, 2021.

2021 **R. Rouhi, M. Clausel, J. Oster, and F.Lauer**, "An Interpretable Hand-Crafted Feature-Based Model for Atrial Fibrillation Detection." *Frontiers in Physiology* 12: 581, 2021.

Y. Xie, J. Oster, E. Micard, B. Chen, I.K. Douros, L. Liao, ... and THRACE Investigators, "Impact of Pretreatment Ischemic Location on Functional Outcome after Thrombectomy". *Diagnostics*, 11(11), 2038, 2021.

S. Ahrari, T. Zaragori, L. Rozenblum, J. Oster, L. Imbert, A.Kas and A. Verger. "Relevance of dynamic 18F-DOPA PET radiomics for differentiation of high-grade glioma progression from treatment-related changes." *Biomedicines*, 9(12), 1924, 2021.

- 2020** **P. Hoyland, N. Hammache, A. Battaglia, J. Oster, J. Felblinger, C. de Chillou, and F. Odille**, "A Paced-ECG Detector and Delineator for Automatic Multi-Parametric Catheter Mapping of Ventricular Tachycardia" *IEEE Access* 8: 223952-60, 2020.
- A. Chocron, J. Oster, S. Biton, F. Mendel, E. Meyer, Y. Zeevi, and J. Behar**, "Remote atrial fibrillation burden estimation using deep recurrent neural network." *IEEE Transactions on Biomedical Engineering*, 2020.
- J. Oster, J.C. Hopewell, K. Ziberna, R. Wijesurendra, C.F. Camm, B. Casadei, L. Tarassenko**, "Identification of patients with Atrial Fibrillation, a Big Data exploratory analysis of the UK Biobank," *Physiological Measurement*, in Press, 2021.
- J. Dos Reis, F. Odille, G. Petitmangin, A. Guillou, P.A. Vuissoz., J. Felblinger and J. Oster**, "Broadband electrocardiogram acquisition for improved suppression of MRI gradient artifacts," *Physiological Measurement*, 41(4), p.045004, 2020.
- F. Dore, J.M. Sellal, E. George, J. Oster, C. De Chillou**, "Non-invasive prediction of first catheter ablation outcome in persistent atrial fibrillation," *Archives of Cardiovascular Diseases Supplements*, 1;12(1):105, 2020.
- 2019** **J. Dos Reis, P. Soullie, J. Oster, E. Palmero Soler, G. Petitmangin, J. Felblinger and F. Odille**, "Reconstruction of the 12-lead ECG using a novel MR-compatible ECG sensor network," *Magnetic resonance in medicine*, 2019.
- J. Behar, J. Oster, M. De Vos and G.D. Clifford**, "Wearables and mHealth in mental health and neurological disorders," *Physiological measurement*, 2019.
- J. Behar, L. Bonnemains, V. Shulgin, J. Oster, O. Ostras and I. Lakhno**, "Noninvasive fetal electrocardiography for the detection of fetal arrhythmias," *Prenatal diagnosis*, 39(3), pp.178-187, 2019.
- 2018** **J. Behar, L. Bonnemains, V. Shulgin, J. Oster, O. Ostras, and L. Lakhno**, "Non-invasive fetal electrocardiography for the detection of fetal arrhythmias: Toward a fetal Holter" *Archives of Cardiovascular Diseases Supplements*, 10(3-4), p.281, 2018.
- C. Liu, J. Oster, E. Reinertsen, Q. Li, L. Zhao, S. Nemati, S. and G. Clifford**, "A comparison of entropy approaches for AF discrimination," *Physiological measurement*, 39(7), p.074002, 2018.
- C. Aye, A. Lewandowski., J. Oster, R. Upton, E. Davis, Y. Kenworthy, H. Boardman, Z. Grace, T. Siepmann, S. Adwani, and K. McCormick**, "Neonatal autonomic function after pregnancy complications and early cardiovascular development," *Pediatric research*, 84(1), p.85, 2018.
- 2017** **A. Petr nas, V. Marozas, A. Solosenko, R. Kubilius, J. Skibarkien , J. Oster, L. S rnmo**, "Electrocardiogram modeling during paroxysmal atrial fibrillation: application to the detection of brief episodes", *Physiological Measurement*, 2017.
- I. Lakhno, J.A. Behar, J. Oster, V. Shulgin, O. Ostras, F. Andreotti** "The use of non-invasive fetal electrocardiography in diagnosing second-degree fetal atrioventricular block", *Maternal Health, Neonatology and Perinatology*, 3(1):14, 2017.
- J. Oster, G.D. Clifford** "Acquisition of electrocardiogram signals during magnetic resonance imaging", *Physiological Measurement*, 38(7):R119, 2017.
- 2016** **J. Behar, T. Zhu, J. Oster, A. Niksch, D.Y. Mah, J. Greenberg, C. Tanner, J. Harrop, R. Sameni, J.Ward, A.J. Wolfberg, G.D. Clifford** , "Evaluation of QT interval using non-invasive fetal ECG technology", *Physiological Measurement*, 37(9), 1392, 2016.
- F. Andreotti, J. Behar, S. Zaunseeder, J. Oster, G.D. Clifford**, "An Open-Source Framework for Stress- Testing Non-Invasive Foetal ECG Extraction Algorithms", *Physiological Measurement*, 37(5), 627, 2016.
- J. Behar, F. Andreotti, S. Zaunseeder, J. Oster and G.D. Clifford**, "A Practical Guide to Non-Invasive Foetal Electrocardiogram Extraction and Analysis", *Physiological Measurement*, 37(5), R1, 2016.

Chapter 4. Research Experience

- 2015** **J. Oster, J. Behar, O. Sayadi, S. Nemati, A.E.W. Johnson, G.D. Clifford**, "Semi-supervised ECG Ventricular Beat Classification with Novelty Detection Based on Switching Kalman Filters," *IEEE Transactions on Biomedical Engineering*, 62(9), 2125-2134, 2015.
- J. Oster, G.D. Clifford**, "Impact of the presence of noise on RR interval-based Atrial Fibrillation," *Journal of Electrocardiology*, 48(6), 947-951, 2015.
- A.E.W. Johnson, J. Behar, F. Andreotti, G.D. Clifford and J. Oster**, "Multimodal heart beat detection using signal quality indices," *Physiological Measurement*, 36(8), 1665-1677, 2015.
- I. Silva, B. Moody, J. Behar, A.E.W. Johnson, J. Oster and G.D. Clifford**, "Detection of Heart Beats in Multimodal Data," *Physiological Measurement*, 36(8), 1629-1644, 2015.
- J. Oster, R. Llinares, S. Payne, Z. Tse, E.J. Schmidt and G.D. Clifford**, "Comparison of three artificial models of the MHD effect on the electrocardiogram," *Computers Methods in Biomechanics and Biomedical Engineering*, 18(13), 1400-1417, 2015.
- B. Rodriguez, A. Carusi, N. Abi-Gerges, R. Ariga, O. Britton, G. Bub, A. Bueno-Orivio, R. Burton, V. Carapella, L. Cardone-Noot, M. Daniels, M. Davies, S. Dutta, A. Ghetti, V. Grau, S. Harmer, I. Kopjar, P. Lambiase, H. Lu, A. Lyon, A. Minchile, A. Muszkiewicz, J. Oster, M. Paci, E. Passini, S. Severi, P. Taggart, A. Tinker, J-P. Valentin, A. Varro, M. Wallman, X. Zhou**, "Human-based approaches to pharmacology and cardiology: an interdisciplinary and intersectorial workshop", *Europace*, euv320, 2015.
- 2014** **J. Behar, A. Jonhson, G.D. Clifford, J. Oster**, "A Comparison of Single Channel Foetal ECG Extraction Methods," *Annals of Biomedical Engineering*, 42(6), 1340-53, 2014
- J. Behar, J. Oster, G.D. Clifford**, "Combining and Comparing Benchmarking Methods of Foetal ECG Extraction Without Maternal or Scalp Electrode Data," *Physiological Measurement*, 35, 1569-89, 2014.
- J. Behar, F. Andreotti, S. Zaunseeder, Q. Li, J. Oster, G.D Clifford**, "An ECG Model for Simulating Maternal-Foetal Activity Mixtures on Abdominal ECG Recordings," *Physiological Measurement*, 35, 1537-50, 2014.
- Z. Tse, C. Dumoulin, G.D. Clifford, J. Schweitzer, L. Qin, J. Oster, M. Jerosch-Herold, R. Kwong, G. Michaud, W. Stevenson, E. Schmidt**, "1.5 Tesla MRI-Conditional 12-lead ECG for MR Imaging and Intra-MR Intervention," *Magnetic Resonance in Medicine*, 71(3), 1336-1347, 2014.
- 2013** **J. Oster, M. Geist, O. Pietquin and G. D. Clifford**, "Filtering of pathological rhythms during MRI scanning," *International Journal of Bioelectromagnetism*, 15, 54-59, 2013.
- J.W. Krug, G. Rose, G.D. Clifford and J. Oster**, "ECG-Based Gating in Ultra High Field Cardiac MRI using an Independent Component Analysis Approach," *Journal of Cardiovascular Magnetic Resonance*, 15, 1:104, 2013.
- J. Behar, J. Oster, Q. Li and G.D. Clifford**, "ECG signal quality during arrhythmia and its application to False Alarm reduction," *IEEE Transactions on Biomedical Engineering*, 60, 1660-1666, 2013.
- 2010** **B. Fernandez, J. Oster, M. Lohezic, D. Mandry, O. Pietquin, P.-A. Vuissoz and J. Felblinger**, "Adaptive Black Blood Fast Spin Echo for End-Systolic Rest Cardiac Imaging," *Magnetic Resonance in Medicine*, 64, 1760-71, 2010.
- J. Oster, O. Pietquin, M. Kraemer and J. Felblinger**, "Nonlinear Bayesian Filtering for Denoising of Electrocardiograms acquired in a Magnetic Resonance Environment," *IEEE Transactions on Biomedical Engineering*, 57, 1628-38, 2010.
- 2009** **J. Oster, O. Pietquin, R. Abächerli, M. Kraemer and J. Felblinger**, "Independent Component Analysis based Artefact Reduction: Application to electrocardiogram for improved magnetic resonance imaging," *Physiological Measurement*, 30, 1381-97, 2009.

4.2.5 International Conferences

- 2022** **P. Aublin, J. Felblinger and J. Oster**, "Automated Detection of Ventricular Heartbeats from Electrocardiogram (ECG) acquired during Magnetic Resonance Imaging (MRI)." *in Proc. of Computing in Cardiology (Cinc)*, Tampere (Finland), 2022.
- M. Diaw, S. Papelier, A. Durand-Salmon, J. Felblinger and J. Oster**, "A QT Interval Inaccuracy Index (QTI) for Highly Automated TQT Studies." *in Proc. of Computing in Cardiology (Cinc)*, Tampere (Finland), 2022.
- 2021** **P. Aublin M. BenAmmar, M. Barret, J. Fix and J. Oster**, "Cardiac Abnormality Detection based on an Ensemble Voting of Single-Lead Classifier Predictions." *in Proc. of Computing in Cardiology (Cinc)*, Brno (Czech Republic), 2021.
- 2020** **T. Zaragori, J. Oster, M. B. Chawki, B. Chen, V. Roch, L. Taillandier, G. Karcher, L. Imbert, and A. Verger**, "Textural features combined with static and dynamic parameters of F-18-FDopa PET imaging for the non-invasive prediction of the IDH mutation status in glioma." *In EUROPEAN JOURNAL OF NUCLEAR MEDICINE AND MOLECULAR IMAGING*, (47, no. SUPPL 1), pp. S334-S335. 2020.
- 2019** **B. Roussel, J. Pascal, J. Felblinger, and J. Oster**, "Magnetic tracking of ECG sensors for respiratory motion correction," *in Proc. of the annual meeting of the International Society for Magnetic Resonance in Medicine*, Montreal, 2019.
- B. Roussel, J. Oster and M. Heinrich**, "Propagation Neural Network for Cardiac Segmentation," *in Proc. of the annual meeting of the International Society for Magnetic Resonance in Medicine*, Montreal, 2019.
- B. Roussel, J. Behar and J. Oster**, "A Recurrent Neural Network for the Prediction of Vital Sign Evolution and Sepsis in ICU," *in Proc. of Computing in Cardiology (Cinc)*, Singapore, 2019.
- 2018** **C. Robert, E. Micard, and J. Oster**, "Uncalibrated Real-Time Stroke Volume Estimation in MRI Using the Magnetohydrodynamic Effect?," *in Proc. of Computing in Cardiology (Cinc)*, Maastricht (Netherlands), 2018.
- 2017** **J.A. Behar, A.A. Rosenberg, Y. Yaniv, J. Oster**, "Rhythm and Quality Classification from short ECGs recorded using a Mobile Device," *in Proc. of Computing in Cardiology (Cinc)*, Rennes (France), 2017.
- M. Heinrich, J. Oster**, "MRI Whole Heart Segmentation using Discrete Nonlinear Registration and Fast Non-Local Fusion", *in Proc. of STACOM workshop and ACDC & MM-WHS challenges, MICCAI*, Québec (Canada), 2017.
- 2016** **J. Oster and L. Tarassenko**, "Automated ECG Ventricular Beat Detection with Switching Kalman Filters," *in Proc. of Computing in Cardiology (Cinc)*, Vancouver (Canada), 37-40, 2016.
- 2014** **A.E.W Johnson, J. Behar, F. Andreotti, G.D. Clifford and J. Oster**, "R-Peak Estimation using Multimodal Lead Switching," *in Proc. of Computing in Cardiology (Cinc)*, Cambridge (MA, USA), 2014.
- G.D. Clifford, C. Arteta, T. Zhu, M. Pimentel, M. Santos, J. Domingos, A. Maraci, J. Behar, J. Oster**, "A Scalable mHealth System for Non-Communicable Disease Management," *in Proc. of IEEE Global Humanitarian Technology Conference*, San Jose (CA, USA), 2014.
- J. Behar, F. Andreotti, J. Oster and G.D. Clifford**, "A Bayesian Filtering Framework for Accurate Extracting of the Non Invasive FECG Morphology," *in Proc. of Computing in Cardiology (Cinc)*, Cambridge (MA, USA), 2014.
- F. Andreotti, J. Behar, J. Oster, G.D. Clifford, H. Malberg and S. Zaunseeder**, "Optimized Modelling of Maternal ECG Beats using the Stationary Wavelet Transform," *in Proc. of Computing in Cardiology (Cinc)*, Cambridge (MA, USA), 2014.
- M.S. Alvi, F. Andreotti, J. Oster, S. Zaunseeder, G.D. Clifford, and J. Behar**, "fecgsyn-gui: A GUI Interface to fecgsyn for Simulation of Maternal-Foetal Activity Mixtures on Abdominal Electrocardiogram Recordings," *in Proc. of Computing in Cardiology (Cinc)*, Cambridge (MA, USA), 2014.

Chapter 4. Research Experience

- 2014 **T. Zhu, M. Osipov, T. Papastylianou, J. Oster, D. Clifton and G.D, Clifford**, "The intelligent cardiac health monitoring and review system," in *Proc. of the IET Appropriate Healthcare Technologies for Low Resource Settings (AHT2014)*, London, 2014.
- 2013 **J. Oster, M. Geist, Z. Tse, E.J. Schmidt, O. Pietquin and G.D. Clifford**, "Non-linear Bayesian suppression of Magnetohydrodynamic effect for accurate Electrocardiogram analysis during MRI", in *Proc. of the annual meeting of the annual meeting of the International Society for Magnetic Resonance in Medicine*, Salt-Lake-City, 2013
- J. Oster and G.D. Clifford**, "An artificial model of the Electrocardiogram during paroxysmal Atrial Fibrillation", in *Proc. of Computing in Cardiology (Cinc)*, Zaragoza, 2013.
- J. Oster, J. Behar, R. Colloca, Q. Li and G.D. Clifford**, "Open source Java-based ECG analysis software and Android app for Atrial Fibrillation screening", in *Proc. of Computing in Cardiology (Cinc)*, Zaragoza, 2013.
- J. Behar, J. Oster and G.D. Clifford**, "Non invasive FECG Extraction from a set of Abdominal sensors", in *Proc. of Computing in Cardiology (Cinc)*, Zaragoza, 2013.
- J.W. Krug, G. Rose, D. Stucht, G.D. Clifford and J. Oster**, "Limitations of VCG based gating methods in ultra high field cardiac MRI", *Journal of Cardiovascular Magnetic Resonance*, 15 (Suppl 1), W19, 2013.
- J.W. Krug, G. Rose, D. Stucht, G.D. Clifford and J. Oster**, "Improved ECG based gating in ultra high field cardiac MRI using an independent component analysis approach", *Journal of Cardiovascular Magnetic Resonance*, 15 (Suppl 1), W33, 2013.
- 2012 **J. Oster, R. Linares, Z. Tse, E. Schmidt and G. D. Clifford**, "Realistic MHD modeling based on MRI blood flow measurements," in *Proc. of the annual meeting of the annual meeting of the International Society for Magnetic Resonance in Medicine*, Melbourne, 2012
- J. Oster, M. Geist, O. Pietquin and G. D. Clifford**, "Filtering of pathological rhythms during MRI scanning," in *Workshop of Biomedical Signal Interpretation*, Como, 2012
- J. Krug, G. D. Clifford, G. Rose and J. Oster**, "The limited applicability of Wiener Filtering to ECG signals disturbed by the MHD effect," in *Proc. of European Signal Processing Conference*, Bucharest, 2012
- J.W. Krug, G.H. Rose, D. Stucht, G.D. Clifford and J. Oster**, "Filtering the Magneto-hydrodynamic Effect from 12 lead ECG Signals using Independent Component Analysis", in *Proc. of Computing in Cardiology (Cinc)*, Krakow, 2012.
- J. Behar, J. Oster, Q. Li and G. Clifford**, "A single channel ECG quality metric," in *Proc. of Computing in Cardiology*, Krakow, 2012.
- Z. Tse, C. Dumoulin, G. Clifford, J. Oster, M. Jerosch-Herold, R. Kwong, W. Stevenson and Ehud J Schmidt**, "Cardiac MRI with Concurrent Physiological Monitoring using MRI-compatible 12-lead ECG," *Journal of Cardiovascular Magnetic Resonance*, 14(Suppl 1),231, 2012
- 2011 **J. Oster, R. Linares, Z. Tse, E. Schmidt and G. D. Clifford**, "An artificial model for the MHD effect on the surface ECG," in *Proc. of the annual meeting of the European Society for Magnetic Resonance in Medicine and Biology (ESMRMB 11)*, Leipzig, 2011
- 2010 **J. Oster, O. Pietquin, M. Kraemer and J. Felblinger**, "Bayesian framework for artifact reduction on ECG in MRI," in *Proc. of the IEEE International Conference on Acoustics, Speech and Signal Processing*, Dallas, 2010
- J. Oster, O. Pietquin, M. Kraemer, and J. Felblinger**, "Magnetic field gradient artifact reduction on ecg for improved triggering," in *Proc. of the annual meeting of the International Society for Magnetic Resonance in Medicine*, Stockholm, 2010
- 2009 **J. Oster, O. Pietquin, R. Abächerli, M. Kraemer and J. Felblinger**, "A specific QRS detector for Electrocardiography during MRI: using Wavelets and Local Regularity Characterization," in *Proc. of the IEEE International Conference on Acoustics, Speech and Signal Processing*, Taipei, 2009
- J. Oster, J. Pascal, O. Pietquin, M. Kraemer, J. P. Blondé and J. Felblinger**, "Real-Time Adaptive Suppression of MR Gradient Artifacts on Electrocardiograms using a new 3D Hall Probe," in *Proc. of the annual meeting of the International Society for Magnetic Resonance in Medicine*, Honolulu, 2009

- 2009** **J. Oster, B. Fernandez, M. Lohezic, D. Mandry, P.-A. Vuissoz, O. Pietquin and J. Felblinger**, "Adaptive Heart Rate Prediction for Black-Blood Systolic Imaging," in *Proc. of the annual meeting of the International Society for Magnetic Resonance in Medicine*, Honolulu, 2009
- B. Fernandez, J. Oster, M. Lohezic, D. Mandry, O. Pietquin, P.-A. Vuissoz and J. Felblinger**, "Adaptive Trigger Delay Using a Predictive Model Applied to Black Blood Fast Spin Echo Cardiac Imaging in Systole," in *Proc. of the annual meeting of the International Society for Magnetic Resonance in Medicine*, Honolulu, 2009
- M. Lohezic, B. Fernandez, J. Oster, D. Mandry, O. Pietquin, P.-A. Vuissoz and J. Felblinger**, "Free breathing black-blood systolic imaging using heart rate prediction and motion compensated reconstruction," in *Proc. of the annual meeting of the International Society for Magnetic Resonance in Medicine*, Honolulu, 2009
- L. Zhou, M. Ayachi, J. Oster, R. Abächerli, O. Fokapu, M. Kraemer, J.-J. Schmid, J.-P. Blondé and J. Felblinger**, "Dedicated MR ECG amplifier," in *Proc. of the annual meeting of the International Society for Magnetic Resonance in Medicine*, Honolulu, 2009
- 2008** **J. Oster, O. Pietquin, G. Bosser and J. Felblinger**, "Adaptive RR Prediction for Cardiac MRI," in *Proc. of the IEEE International Conference on Acoustics, Speech and Signal Processing*, Las Vegas, 2008
- J. Oster, O. Pietquin, M. Kraemer, and J. Felblinger**, "Independent Component Analysis based Artifact Reduction Method for ECG in MR," in *Proc. of the annual meeting of the European Society for Magnetic Resonance in Medicine and Biology (ESMRMB 08)*, Valencia, 2008
- J. Pascal, L. Hebrard, V. Frick, J.-P. Blondé, J. Felblinger and J. Oster**, "3D Hall probe in 0.35 μm CMOS technology for magnetic field monitoring in MRI environment," in *Proc. of the European Magnetic Sensors and Actuators Conference (EMSA'08)*, Caen, 2008
- 2007** **J. Oster, F. Odille, G. Bosser, O. Pietquin, C. Pasquier, P.-A. Vuissoz and J. Felblinger**, "Adaptive Prediction of RR interval for online MR parameters changes," in *Proc. of the Joint annual meeting International Society for Magnetic Resonance in Medicine and European Society for Magnetic Resonance in Medicine and Biology*, Berlin, 2007
- H. Berviller, V. Frick, L. Zhou, J. Pascal, J.-P. Blondé, J. Oster and J. Felblinger**, "ECG signal artifacts suppression in MRI environment by means of LMS filtering," in *Proc. of the Workshop on Design and Architectures for Signal and Image Processing (DASIP 07)*, Grenoble, 2007
- V. Frick, H. Berviller, J. Pascal, P. Bougeot, J.-P. Blondé, J. Oster and J. Felblinger**, "ECG signal artifacts suppression system based on an MRI environment dedicated CMOS magnetic field monitor and FPGA implementation," in *Proc. of the 14th IEEE International Conference on Electronics, Circuits and Systems (ICECS 2007)*, Morocco, 2007
- L. Zhou, H. Berviller, V. Frick, P. Bougeot, J.-P. Blondé, J. Oster and J. Felblinger**, "FPGA implementation of an adaptive filtering: Application on ECG signal artifact suppression in MRI environment," in *Proc. of the 3rd International Workshop on Reconfigurable Communication-centric Systems-on-Chip (ReCoSoC'07)*, Montpellier, 2007

Part II

Research Activities

*The model should only serve the very private function for the painter
of providing the starting point for his excitement.*

Lucian Freud

As stated in this quote, a model was the starting point of my excitement during my research career. The model in my case was a simplified representation of the morphology of the ECG. It was introduced just as a way of representing the ECG signal, but turned out to be a powerful and versatile tool for the analysis of the cardiac electrophysiology. This representation of the ECG signal has been binding my work together throughout my research career.

This part is devoted to the presentation of my past research activities, and is divided in three chapters. The first chapter is introducing the notion of modelling of physiological signals, and how such models can be used for stress-testing analysis or processing techniques. Such models are particularly useful when real data are scarce or in circumstances for which the ground-truth cannot be extracted from real recordings. The second chapter is presenting a class of signal processing techniques, based on a Bayesian filtering approach. These techniques are taking profit of the models being introduced earlier in order to enable a robust and accurate extraction of the relevant part of the signal. Finally, the last chapter is dedicated to the classification task, starting with an extension of the Bayesian approach for beat classification. Other classification applications are also presented.

Chapter 5

Modelling

In science, it is generally customary to try to explain or understand a phenomenon by building a (mathematical) model of the complex system mimicking its behaviour, and which is able to produce the same observations. The field of cardiology and more precisely of Electrocardiography is in that way no different, and many models have been suggested since the first observation and interpretation of this amazing signal by [Einthoven \(1912\)](#) (cf. figure 5.1).

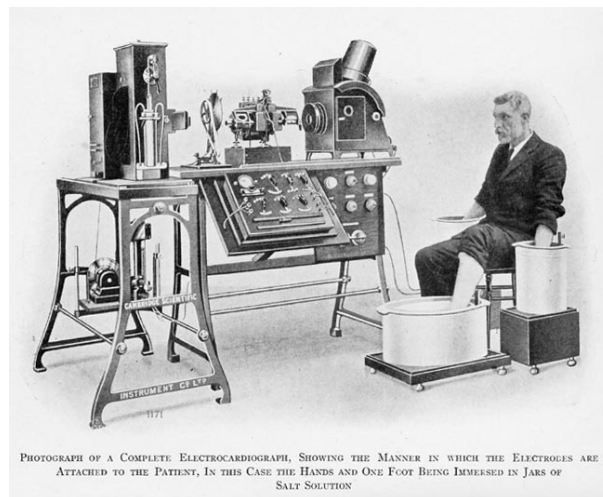


Figure 5.1: *Famous picture of Einthoven during his ECG recording experiment.*

The level of complexity or scale of the model depends of the depth at which the phenomenon is studied. The deepest scale of ECG modelling, and probably the most studied, consists of cardiac cell models, where one is interested in the generation and propagation of electricity at a microscopic level. Such studies started in the sixties, and is still very active today ([Noble, 1960](#), [Noble et al., 2012](#)), and the Hodgkin-Huxley equations ([Hodgkin and Huxley, 1952](#)) have been used and manipulated by thousands of scientists ever since. If one steps up one level, one start studying the cardiac electrophysiology at the tissue level. The cardiac electrical activity is then often depicted as an electrical wave propagating through the atria and the ventricles. The most common approach is known as the bi-domain approach ([Schmitt, 1969](#), [Tung, 1978](#)), but other solutions or variants have obviously also been suggested. These modellings along with the explosion of computational power have led to the development of simulation software, some of which having been made freely available ([Pitt-Francis et al., 2009](#), [van Oosterom and Oostendorp, 2004](#)). The models that are presented in this chapter are not this kind of models, and are among the most simplistic modelling class, which was used by Einthoven for the interpretation of the ECG signal. It assumes that the heart electrical activity is a single time-varying electrical dipole, which is a vector characterized by its strength, direction and position. The ECG signal is then the projection of this dipole on the lead, which is mathematically equivalent to a scalar product. A depiction of the phenomenon and the dipole interpretation is given in figure 5.2.

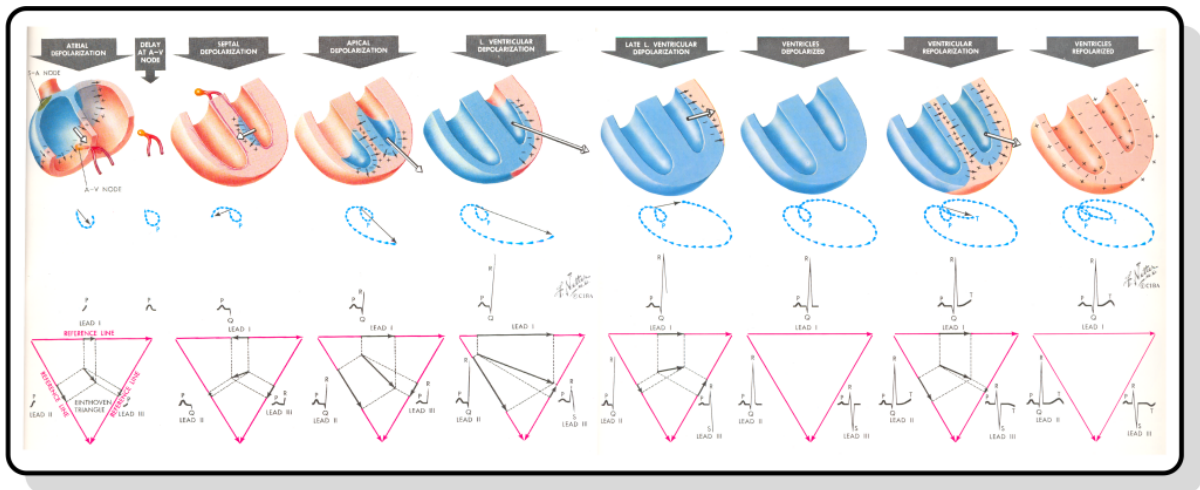


Figure 5.2: Drawing representing an entire cardiac cycle. The bottom row represents the equivalent dipole through the cardiac cycles and how it is projected on the three limb leads (Netter, 1992).

Einthoven introduced the notation of the main five deflections (P, Q, R, S, and T waves) characterising a typical cardiac cycle on the ECG signal. Figure 5.3 depicts the morphology of an ECG signal, with the location of the different waves along with some of the biomarkers commonly analysed.

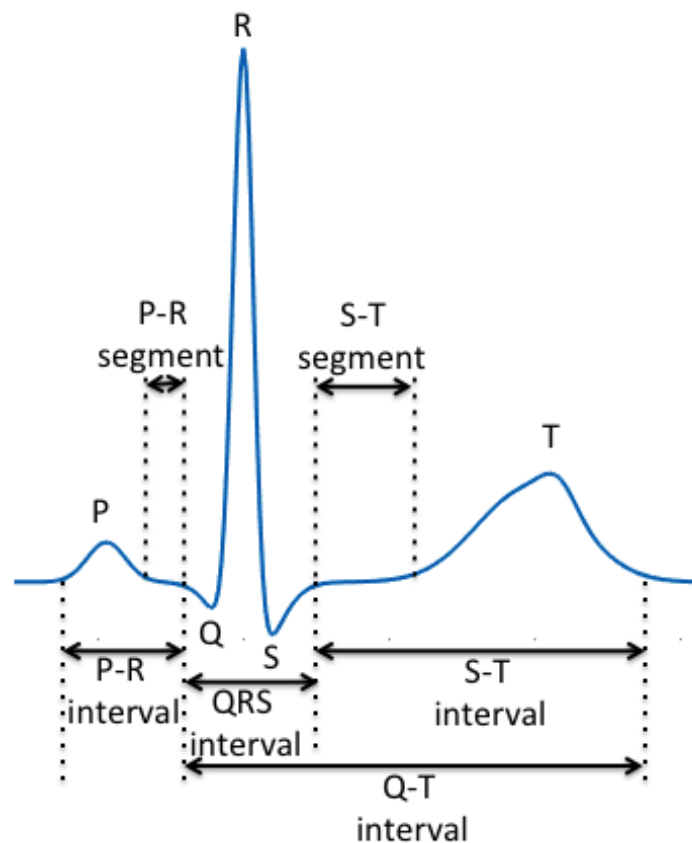


Figure 5.3: Representation of an ECG cycle, the five characteristics waves, and the main biomarkers.

In this chapter, the focus is on the modelling of the morphology of the ECG signal on a single lead (or one of the three components of the equivalent dipole model). The first application of building a morphological model of the ECG signal is the possibility of using it as synthetic signal

generator. These synthetic data will then be mainly used for stress testing new or existing analysis techniques. Stress-testing on such synthetic data is particularly useful in two situations: (i) when the ground-truth cannot be extracted for a given application due to the presence of noise, (ii) when real clinical data is not available because of a new recording method or application (as is the case for foetal ECG or ECG acquired in MRI), or because of an undiagnosed pathology (as is the case for paroxysmal AF).¹

5.1 A morphological model for ECG signals

Many mathematical models have been introduced for representing the morphology of the ECG signal or parts of it, one can for example cite the use of Hermite functions [Sornmo et al. \(1981\)](#). But, [McSharry et al. \(2003\)](#) introduced a dynamical modelling of the ECG signal, which had a huge impact on the community (with more than a thousand citations according to Google scholar). This model was developed and introduced to simulate artificial signals, which could be used for the evaluation of different analysis techniques with a complete knowledge of the ground-truth of the underlying physiological signals. It also allowed not only for precise measurements of Signal to Noise Ratio (SNR), but also accurate physiologically meaningful measurements such as QT, PR, or QRS intervals, or ST levels for example. As the end-point of ECG analysis is the extraction of meaningful physiological parameters, processing techniques should always be evaluated according to how precise these parameters are (and not only with a SNR measure). As will be seen later in the document, the success of this modelling stems from its versatility as it could be used as the basis of many analysis techniques.

5.1.1 Mathematical representation

The ECG is a pseudo-periodic signal, with a pattern (cardiac cycle) repeating itself with a relative stability. [McSharry et al. \(2003\)](#) showed that each heartbeat (or cycle) can be modelled as a sum of Gaussian waves, and are therefore governed by a set of dynamical equations.

The first part of the modelling paper was dedicated to the creation of a realistic heart rhythm, or the pseudo-periodicity of the ECG. The simulation of such rhythm has been the focus of the 2002 Physionet/CinC challenge. Interested readers are referred to the original paper ([McSharry et al., 2003](#)). The most important point for the ECG modelling is the creation of a variable ω , which represented the speed of the dynamical system.

As explained earlier, a typical heartbeat consists in a series of deflections.

Each of these characteristic waves or components can be modelled as sum of multiple Gaussian waves, and it has been shown that two Gaussians can represent accurately each of the P and T waves, while three Gaussians are necessary for the modelling of the most easily distinguishable peak of the ECG, namely the QRS complex. A total of seven Gaussian waves have therefore been shown to be required for a proper approximation of the ECG morphology ([Clifford et al., 2005](#)).

An ECG signal can therefore be written down as a set of equations, and modelled with a finite set of parameters:

¹On a side note, it should be emphasized that the use of synthetic data for stress-testing analysis techniques is less and less frequent. One should thank the Physionet team, and more specifically their founders (Ary L. Goldberger, MD; Roger G. Mark, MD, PhD; and George Moody). They had the visionary idea of freely providing the research community with clinical research data (but also software) in order to allow for a fair comparison of the different analysis techniques. Their vision has allowed many researchers around the world to work and develop novel and innovative approaches. One should be thankful for such a great initiative and hope that it will be replicated in many other medical research fields.

$$\begin{cases} \dot{x} = \rho x - \omega y \\ \dot{y} = \rho y - \omega x \\ \dot{z} = -\sum_{i=1}^7 \frac{\omega \Delta\theta_i}{b_i^2} g(\alpha_i, \Delta\theta_i, b_i) - (z - z_0) \end{cases}, \quad (5.1)$$

where $\rho = 1 - \sqrt{x^2 + y^2}$, ω is the angular speed or the speed of the dynamical system (given by the heart rhythm). z represents the ECG value in mV and α_i, b_i, ξ_i are the amplitude, width and angular position of the i^{th} Gaussian respectively, with $\Delta\theta_i = (\theta - \xi_i) \pmod{2\pi}$, where $\pi < \theta = \arctan(\frac{y}{x}) \leq \pi$ and with $g(a, b, c) = a \exp(-\frac{b^2}{2c^2})$ representing one Gaussian wave. z_0 represents the baseline, and models the baseline wander by letting the signal evolve following a pseudo-periodical rhythm at the respiratory frequency (which is usually the main contribution of the baseline wander).

As depicted in figure 5.4, a synthetic ECG signal can be realistically generated by selecting a few parameters for the morphology of the heartbeat, more precisely twenty one (three per Gaussian wave), along with a function simulating the heart rhythm.

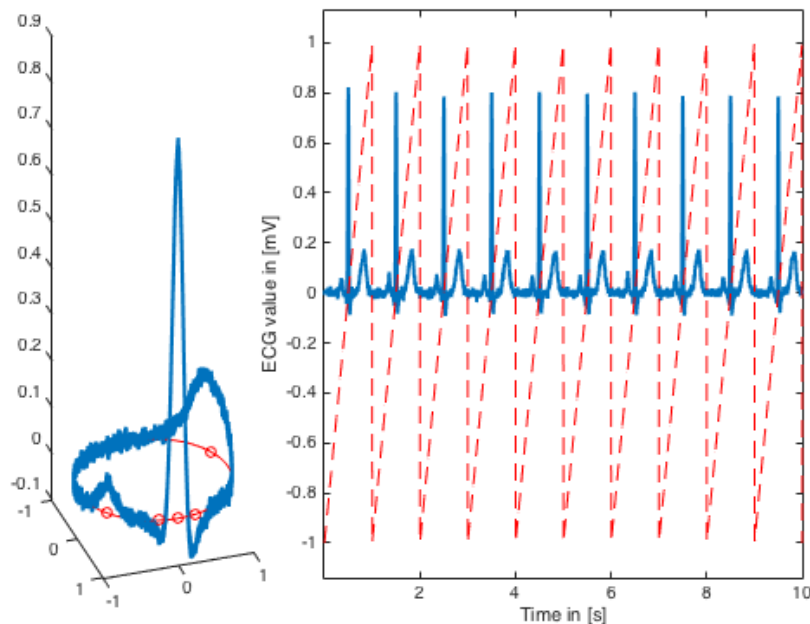


Figure 5.4: Simulation of an ECG signal using the model. (left) 3D representation of ten simulated cycles. Red circles represent the position of the five main waves. (right) Simulation of ten noisy ECG cycles, in red the representation of the scaled phase signal.

In order to improve the realism of the generated signal it is also necessary to add one or multiple noise components. The use of Gaussian white noise has widely been suggested, for sake of simplicity. Such an approach has a huge drawback, first real physiological noise can usually not be modelled as a Gaussian white noise as it is usually a coloured noise, but also many denoising or processing techniques assume the noise to be Gaussian white noise and stress-testing them in these ideal conditions will bias the results. A multi-lead noise simulator has been suggested by [Oster and Clifford \(2013\)](#), by using data provided in the noise stress dataset available on Physionet. The real data is used to estimate parameters of spectrum of short portions of the noise. These parameters are then used to generate synthetic, but realistic noise. This approach has been used in FECGSyn, a freely available software for the generation of synthetic foetal ECG data ([Andreotti et al., 2016](#), [Behar et al., 2014b](#)).

This model could be used in order to simulate realistic 12-lead ECG recordings. The model was duplicated three times in order to generate the three components of the equivalent dipole (or the VectoCardioGram i.e. the Frank leads derivations) and was projected onto a 12-lead system using a simple matrix multiplication (or the Dower transform). The omega function, simulating the heart rhythm, can then be shared between the three components as they each have the same pseudo periodicity.

5.2 Considering pathological rhythms

This model has a first obvious limitation, which is that it seems to be restricted to healthy cases. That is, the model is the repetition of "normal" cycles with the same morphology repeating itself indefinitely. It would be more interesting to be able to simulate pathological cases, with abnormal situations occurring on more or less rare occasions. Examples of such pathologies that are immediately coming to mind are T-wave alternans (with alternative T waves morphology), ischemic episodes (with ST elevation,) occurrence of Premature Ventricular Contractions (PVC) or paroxysmal AF episodes...

The model has been extended such as to be able to simulate all the pathologies that have been listed above (Clifford et al., 2010, Oster and Clifford, 2013, Oster et al., 2015c, Petrenas et al., 2017). The possibility of the model to generate pathological cases makes it even more attractive, as one always wants to stress test novel processing techniques in such challenging conditions and that these techniques should be able to cope with pathological (otherwise they are useless in clinical practice).

The method for generating intermittent episodes is detailed in the subsection 5.2.1, whereas the extension for the simulation the morphology of f waves is presented in 5.2.2.

5.2.1 Simulating intermittent episodes

The problematic of pathological cases such as PVC or paroxysmal AF consists in the apparent random apparition (and disappearance) of the phenomenon. The use of probabilistic graphical models allows for the system to switch randomly" between different states. Hidden Markov Model (HMM) have extensively been suggested in the literature for the analysis of ECG signals, one can in particular cite the work of Moody and Mark (1983), who implemented HMM for the detection of AF episodes. The beauty of HMM is that they are generative models, that it is possible to generate or simulate signals following this apparent random switch between states.

The idea of probabilistic graphical model can be explained by a simple graph, where the different modes are represented by nodes, as depicted in figure 5.5. The nodes are connected to each other with arrows. These arrows represent the possibility of the system to pass from one state to the other. The arrow are usually weighted with the weight representing the probability of the system passing from the state j to the state i at a given time t (or mathematically $p_{ij} = P(State(t) = j | State(t - 1) = i)$). Given that these weights correspond to probabilities, one can easily conclude that for every i , $\sum_j p_{ij} = 1$, as the system has always to be in one state at any given time.

A first order Markov model can then be mathematical reduced to a single matrix representing these transitions, and called the State Transition Matrix, $STM_{i,j} = p_{ij}$. For example, the matrix of the system represented in figure 5.5 is given by:

$$STM = \begin{bmatrix} p_{11} & p_{12} & p_{13} \\ p_{21} & p_{22} & p_{23} \\ p_{31} & p_{32} & p_{33} \end{bmatrix}. \quad (5.2)$$

How can these models be used for the generation of pathological ECG signals?

Let consider the AF case. As for healthy recordings, the simulation starts with the generation of the heart rhythm given by a RR interval time-series. Let describe a two-state system, the first describing a normal rhythm, whereas the second describes AF. The system can switch states at

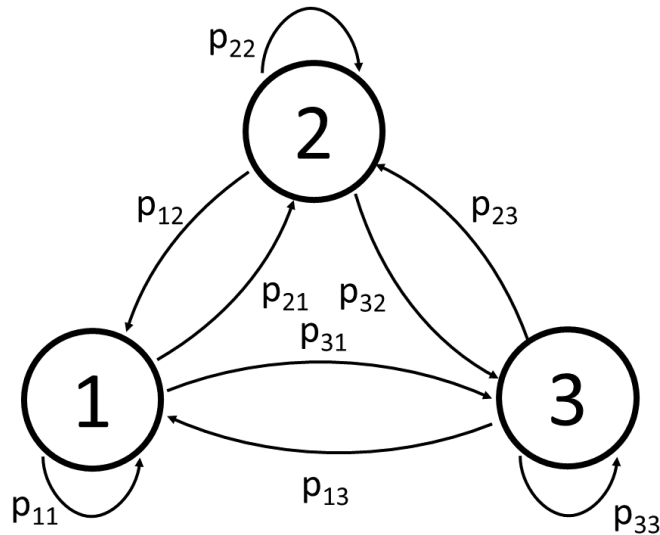


Figure 5.5: State transition graph for a first order Markov model with three modes. p_{ij} being the probability of the system to transition from mode i to mode j at any time t .

each new cycle, n . The model will then from one cycle to the next, whether to model a normal ECG morphology, or an AF morphology (that is an ECG for which the T wave has disappeared and is replaced by f waves – a morphological model for f waves is introduced in the next subsection 5.2.2 –). By doing so, one has simulated the apparition of episodic episodes of arrhythmia, characteristic of paroxysmal AF. Nevertheless, at this stage the mechanism of arrhythmia has not yet been simulated, as the RR interval time-series initially generated does not simulate any arrhythmia, i.e. abnormal variations of the heart rhythm.

This simulation of abnormal rhythm can be handled by another HMM model, which will adjust the length of each cycle (Oster and Clifford, 2013). Let consider a three state system, the different modes representing short, regular or long heartbeats respectively. The HMM will then attribute a mode to each heartbeat, and the RR interval is adjusted accordingly. For regular beats the original RR interval is kept unchanged, the RR interval of a short heartbeat is shortened by multiplying its value by a factor $\alpha \sim \mathcal{N}(2/3, 0.02)$, and the RR interval of a long heartbeat is lengthened by multiplying its value by a factor $\beta \sim \mathcal{N}(4/3, 0.02)$. That is short (resp. long) RR intervals are approximatively reduced (resp. increased) by 33%. The state transition matrix has therefore to be different whether in normal or AF rhythm. These matrices can be estimated on real data, and it is afterwards possible to use them in order to detect AF episodes as suggested by Moody and Mark (1983).

Moody and Mark (1983) estimated these state transition matrices on the data from the MIT BIH arrhythmia database Goldberger et al. (2000), and the resulting matrices are given by:

$$STM_{SRL\{AF\}} = \begin{bmatrix} 0.25 & 0.11 & 0.15 \\ 0.51 & 0.74 & 0.65 \\ 0.24 & 0.15 & 0.20 \end{bmatrix}, \text{ and } STM_{SRL\{normal\}} = \begin{bmatrix} 0.21 & 0.02 & 0.21 \\ 0.21 & 0.96 & 0.48 \\ 0.59 & 0.02 & 0.31 \end{bmatrix}. \quad (5.3)$$

Short interpretations of these matrices can be given. Regarding the normal rhythm, it can be noted that the probability of staying in the regular mode is really high (96%) once in the regular mode (second column). The phenomenon of compensation after an ectopic beat is also reflected by the almost 60% chance of having a long heartbeat following a short one. The interpretation of the matrix in the AF is a bit more complicated, and highlight the chaos of this rhythm. The probability of staying in the regular mode is lower than for the normal matrix, which shows the irregularity of the heart rhythm during AF.

Another probabilistic graphical model has been introduced more recently (Corino et al., 2011, 2013, Henriksson et al., 2016). This model is trying to simulate the behaviour of the AV node,

under rapid firing from the atria due to their fibrillation. This firing rate is modelled with a Poisson distribution with a mean arrival rate λ_{AI} , which is a parameter of the dominant frequency of AF in the vicinity of the AV node. Each excitation can then follow one of the two pathways of the AV node (short –1– with a refractory period τ_1 or fast –2– refractory period τ_2) with a probability of ϵ (or $1 - \epsilon$)

The likelihood of this excitation generating a ventricular activity depends on the length of the time since the last ventricular activity, x , and is given by:

$$p_i(x) = \begin{cases} 0, & r < \tau_i \\ \frac{\lambda_{AI}(x-\tau_i)}{\tau_\rho} \exp\left(-\frac{\lambda_{AI}(x-\tau_i)^2}{2\tau_\rho}\right), & \tau_i \leq x < \tau_i + \tau_\rho \\ \lambda_{AI} \exp\left(-\frac{\lambda_{AI}\tau_\rho}{2} - \lambda_{AI}(x - \tau_i - \tau_\rho)\right), & x > \tau_i + \tau_\rho \end{cases}, \quad (5.4)$$

where τ_ρ describes the maximal refractory period prolongation due to concealed conduction and/or relative refractoriness. This model is a more accurate representation of the ventricular activity rate during AF, and has therefore been suggested by (Petrenas et al., 2017).

5.2.2 f-waves

The previous subsection was aimed at showing how intermittent pathological rhythms can be generated, and how the rhythm (i.e. the length of RR intervals) could be modified so to generate more realistic arrhythmic heart rhythm. In this subsection, the way to generate abnormal morphologies is presented.

As explained in the previous subsection, the model for the morphology of the QRST waves of the ECG signal can be modelled identically whether the heartbeat belongs to the normal sinus rhythm or AF. The only difference rests in the fact that for normal rhythm the P wave is modelled as a sum of Gaussians, while there is the need to introduce a new model for the f waves. These f waves have a different pseudo-periodicity than the rest of the ECG but also have a relative large variation of their morphology over a short period of time. This explains what it is not suited for modelling with a sum of Gaussian waves as described in the subsection 5.3.

The model for the generation of f waves has been proposed by Stridh and Sörnmo (2001), and has been recently improved by Petrenas et al. (2012). This model consists of a sawtooth signal, on which has been added a random component (in order to add to the realism of the model, as it was proved that neural networks were able to learn the predictable pattern of the initial version of the model). The model can then be written as:

$$f_j(t) = d_j(t) + \varepsilon_j(t), j \in \{X, Y, Z\}, \quad (5.5)$$

where the sawtooth function $d_j(t)$ is given by:

$$d_j(t) = \sum_{i=1}^l a_{j,i}(t) \sin\left(2\pi f_{j,0}t + i \frac{\Delta f}{f_m} \sin(2\pi f_m t)\right), \quad (5.6)$$

where $f_{j,0}$ is the dominant AF frequency in the j^{th} direction, l the number of harmonics, Δf the range of variation of AF frequency, and f_m the frequency modulation. It can be noted that the dominant frequency depends on the direction, which simulates the fact that the dominant frequency depends on the location of measurement.

The amplitude series needs to be defined, and is computed such as the overall signal has a sawtooth shape, that is:

$$a_{j,i}(t) = \frac{2}{i\pi} (a_j + \Delta a_j \sin(2\pi f_a t)), i = 1, \dots, l, \quad (5.7)$$

with a_j being the sawtooth amplitude, Δa_j the maximum amplitude deviation, and f_a the amplitude modulation frequency.

Chapter 5. Modelling

Finally, the noise component, $\epsilon_j(t)$, consists of coloured noise, that is white noise having been filtered. The filter for generation of this component consists in a double band passband filter, the first band being centred at $0.8f_{j,0}$ and the second centred at $1.2f_{j,0}$. Interested readers are referred to [Petrenas et al. \(2017\)](#) for further details along with tables containing the range of values for the different parameters.

The figure 5.6 depicts simulated signals. It can be noted how irregular the RR intervals are during the AF episodes.

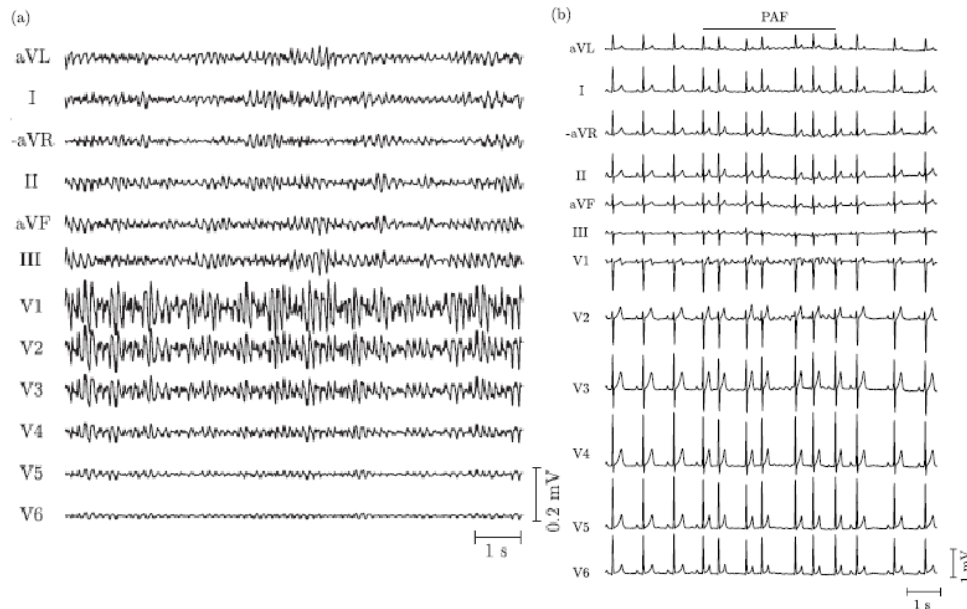


Figure 5.6: Simulation of an ECG signal with Paroxysmal AF (PAF) using the model. (a) Simulated f waves. (b) Simulated ECG with a brief AF episode, indicated on top of the plot. ([Petrenas et al., 2017](#))

5.3 Adding other pseudo-periodic components

In the previous subsections, it was showcased how the ECG signals can be modelled, even during pathological cases. The presented simulations consist of regular applications, that is usual 12-lead recordings or single lead. The noise, which usually consists of baseline, electrode motion, or muscle artefact, is in these circumstances modelled as coloured noise, or by using real noise recordings. There are however some applications, for which unusual noise superimposes onto the signal. Two examples of such applications are foetal ECG or ECG in the MRI. In the former case the noise (depending on how one is looking at the problem) consists of the maternal components, whereas in the latter case the noise consists of the MagnetoHydroDynamic effect. These components as will be seen and detailed further are also pseudo-periodic components, following the same rhythm of the ECG signal or not.

This section is detailing the Foetal ECG application, with a short introduction of the problem and a description of the model and simulator, which was made freely available on-line and called FECGSyn ([Andreotti et al., 2016](#), [Behar et al., 2014b](#)). The section 5.4 is introducing the specificities of the acquisition of ECG (or other electro-physiological) signals in an MRI environment, and how the MHD effect has been modelled.

5.3.1 Foetal monitoring

Despite the first recording of foetal ECG having been performed as early as 1906 by [Cremer \(1906\)](#), the field of fECG is still in its infancy, mainly due to the large difficulties of recording a

clean signal. The development of digital medical acquisition device, along with the development of computation sciences and technology has allowed the advent of new techniques for a more robust and accurate extraction of the foetal ECG components.

Foetal ECG main application consists in the monitoring of the foetal heart rate during delivery (as a replacement for Cardiotocography), in order to detect foetal distress and trigger a Caesarean section. But other applications are currently emerging, for antenatal cardiac diagnosis, with methods suggesting the use of Heart Rate Variability or either using morphological analysis for the detection of conduction pathologies such as AV node block [Lakhno et al. \(2017\)](#).

Foetal ECG can be recorded either in an invasive or non invasive manner. The invasive acquisition consists in "screwing" an electrode in the foetal scalp, therefore during delivery. It provides a high quality signal, but can only be used during delivery but invasive and carries a small additional risk. This technique is denoted scalp ECG. Another way of recording the foetal ECG consists in placing standard ECG electrodes on the belly of the pregnant women. The system therefore records a combination of electro-physiological signals (maternal ECG, electromyogram, and the foetal ECG,...). Figure 5.7 represents an example of signals recorded during foetal monitoring, according to the position of the electrodes (chest, abdomen or scalp). There is therefore a need to develop processing techniques able to extract the component of interest.

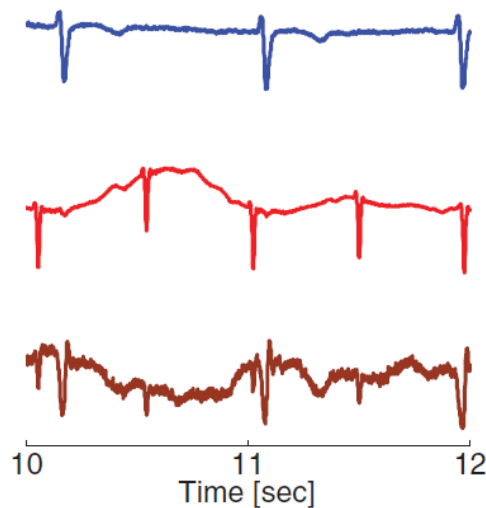


Figure 5.7: From top to bottom: chest ECG (largely dominated by maternal ECG –mECG–), scalp EEG (sECG), and abdominal ECG (mixture of mECG and foetal ECG (fECG)) ([Clifford et al., 2014](#))

The Foetal ECG can be measured from the 20th week of pregnancy until delivery. There is however a period between the 28th and the 37th week of pregnancy during which the quality of the signal will deteriorate, due to the formation of an additional but highly non-conductive layer around the foetus (called vernix caseosa). The cost of such a medical device is relatively low, but the complexity stems from the signal processing and analysis required for accurate extraction of the signal of interest. Figure 5.8 represents the amplitude and frequency range of the different electro-physiological signals recorded during fECG acquisitions, which reflects the difficulty of extracting the fECG components from this mixture of sources.

Interested readers are referred to two reviews detailing the field of foetal ECG analysis ([Behar et al., 2016](#), [Sameni and Clifford, 2010](#)). One of the main limitations that has been identified in both reviews is the lack of freely available clinical data, with validated annotations. The 2013 Physionet/Cinc challenge was devoted to this problem, and allowed for the sharing of a first dataset with annotation and aimed at two objectives (extraction of foetal Heart Rate and foetal QT intervals) ([Clifford et al., 2014](#)). This is a good start, but the datasets lack pathological data, or cases of multi-foetal pregnancy. There is therefore a need for simulation of more and "interesting" cases of foetal ECG recordings. This simulator has been recently proposed and published, along with a datasets of simulated cases with a procedure of stress-testing foetal ECG extraction techniques ([Andreotti et al., 2016](#), [Behar et al., 2014b](#)).

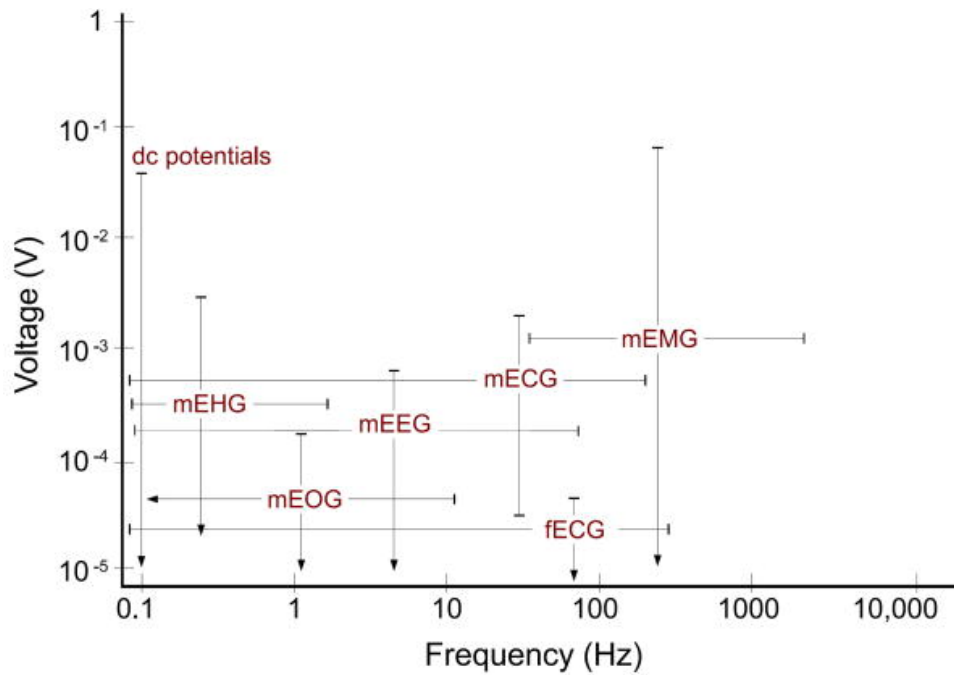


Figure 5.8: Amplitude and frequency range of different electro-physiological signals: maternal ECG (mECG), maternal EEG (mEEG), maternal Electrooculogram (mEOG), electromyogram (mEMG), electrohystogram (mEHG) and foetal ECG (fECG) (Sameni and Clifford, 2010)

5.3.2 Foetal ECG simulation

The abdominal recording consists as can be seen on figure 5.7 a mixture of the maternal ECG, on which the foetal ECG has been added, and with additional noise components. These noise components are highly non stationary (which is usual in biomedical applications), and can reflect the physiological changes occurring during delivery. For example, a contraction is usually accompanied by a decrease of the foetal Heart Rate, the increase of maternal Heart Rate, but also a lower SNR with higher electromyogram components. Another example of extreme noise condition lies in the fact the foetus can move (more or less freely) within the uterus of the mother, the fECG resulting might therefore change drastically as the result of this extreme baseline wander.

In order to analyse fECG, including pathological cases but also noisy situations, it is essential to create a versatile tool. Doing so is possible by using the same model for generating an electrical dipole (and therefore one heart activity), but simply duplicating it and locating it in different positions in a torso model.

In FECGsyn, it was decided to use a simple model for the human torso, a homogeneous cylinder (see figure 5.9). The maternal heart is located at a relative fixed position, but is allowed to move (small rotations and translations) in order to simulate the maternal respiration. The foetal heart is however allowed to move more freely, with complete rotation and translation freedom in the lower part of the cylinder. The software allows for generating of multiple foetal heart, in order to simulate multi-foetal pregnancy. A mixture of noise components can be generated, with the noise dipole location being located at different (and possibly different from the heart dipoles) positions in the volume. The software offers also the possibility of simulating the formation of the vernix caseosa by selecting two factors (or different levels of SNR). The SNRs are defined by the ratio of the energy of the foetal ECG on the energy of maternal ECG, but also the ratio of foetal ECG on the energy of the noise components.

This tool is essential for the simulation of pathological or rare cases, against which the foetal ECG extraction are never tested. However these clinical situations are the cases for which the methods should be robust and accurate. There is no clinical need for a foetal monitoring technique unable to cope with contractions during delivery... Andreotti et al. (2016) presented a method for testing foetal ECG extraction techniques, and generated a dataset of simulated interesting cases

against which to test the analysis techniques. These cases included foetal movement, maternal and foetal Heart Rate acceleration/deceleration, uterine contractions, multi-foetal pregnancies. All these cases were generated using FECGsyn and the model presented here.

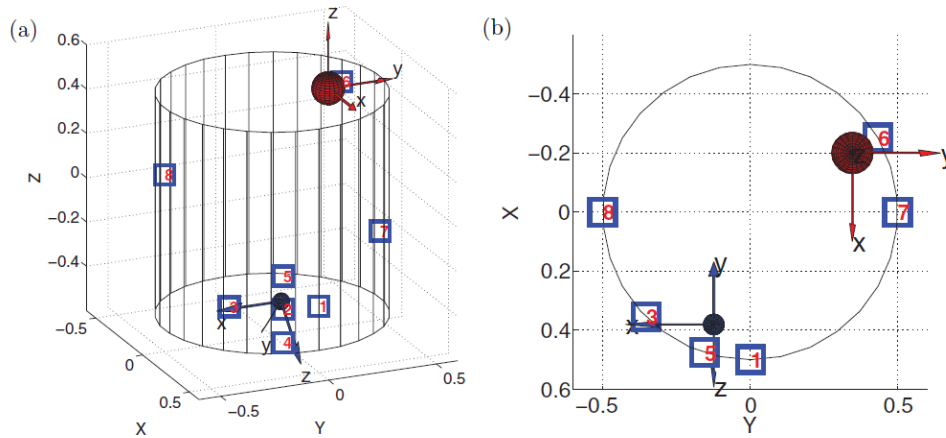


Figure 5.9: Simple cylindrical model representing the mother torso. The two red circles represent the mother and the foetal hearts. The axis for each heart represent the orientation for the electrical dipole. The blue rectangles represent the location of the electrodes and their number denomination.

5.4 Incorporating imaging information

In the previous section, the use of multiple dipoles for simulating multiple pseudo-periodic electro-physiological signals overlapping each others. The example of fECG presented previously introduce multiple dipoles, each of them having their own rhythm as the maternal and the foetal hearts are beating at different rhythms. There are nevertheless examples of applications for which multiple components with the exact same periodicity are overlapping on the same signal. Such an example is given by the acquisition of the ECG signals during an Magnetic Resonance Imaging (MRI) examination. An introduction of the field will be given in the next subsection, whereas a model for such recordings by using imaging information will be introduced in subsection 5.4.2.

5.4.1 Acquisition of ECG signals during MRI

It may seem quite eccentric to even consider recording an ECG signal during an MRI examination, nevertheless the ECG is acquired routinely in the clinical setting. There are two main reasons for such acquisitions:

1. Synchronising the image acquisition with heart activity. MRI is a relatively slow process, and multiple excitations are necessary for building an MRI image. When imaging a moving organ, such as the heart, it is therefore essential to synchronise the MRI measurements with the heart activity as shown in figure 5.10. Triggering of the MRI excitation from the detection of R waves on ECG signal is the state-of-the-art for this task (Scott et al., 2009).
2. Patient monitoring. Undergoing an MRI examination is a clinical act, and the patient safety is therefore the priority. Shellock (2000) has detailed a lost of circumstances under which patient monitoring is mandatory. One of the most important signal when monitoring a patient is the ECG signal, as it reflects the status of the heart (and its electrical activity).

There is therefore a need for the acquisition of ECG signals during MRI, unfortunately the environment of the MRI is probably the worst condition for the recording of an electro-physiological signal.

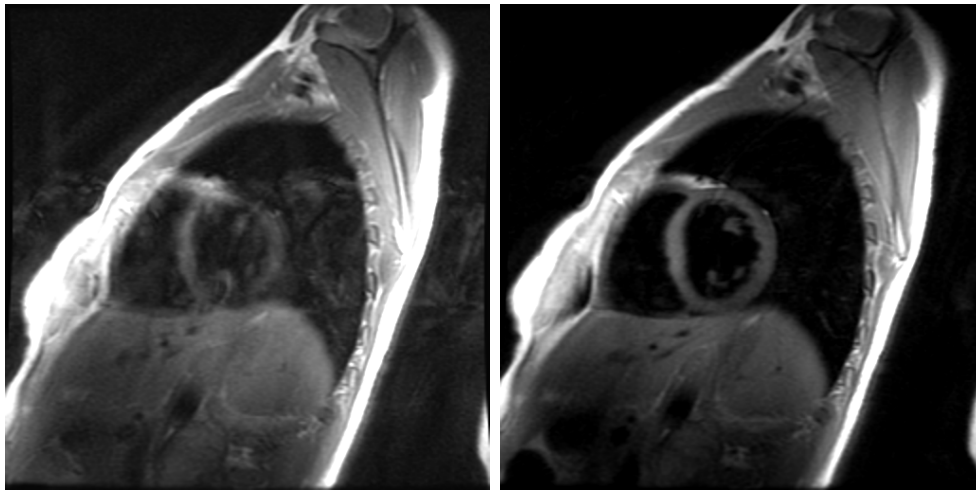


Figure 5.10: Influence of the synchronisation on image quality. Example of failed synchronisation (left) and good synchronisation (right).

The MRI environment consists of a complex electro-magnetic fields divided in three "independent" components:

1. RadioFrequency field. The acquisition of an image in MRI requires successive RF excitations. These RF pulses are highly energetic and are concentrated around a given frequency depending of the MRI scanner (and its static field strength). Commercial scanners use RF pulse at 64 MHz or 128MHz. As these pulses are concentrated at higher bandwidth, and do usually not overlap on the ECG signal. Nevertheless, the presence of these RF pulses require the development of specific hardware, as electronics could be damaged, and cables should be shortened or avoided as much as possible. Cables are antennas that can catch the energy of the pulses, they could therefore heat or induce burns in the patient. The shortening of the cable lead to the use of specific electrode positions, close form each other and the heart.
2. Gradients. To encode the image properly, and to image only one region or slice of interest, RF pulses are usually accompanied by a fast varying magnetic field, denoted as "gradients" in the MRI community. This term is a shortening of spatial gradient of magnetic field, and their purpose is to allow for a localised excitation of the patient. These gradients as they consist of a varying magnetic field induce an electrical field (even in the patient subject) and have to be controlled and restricted to avoid the stimulation of the patient nerves (or worse the heart). The gradients but also the induced electrical field are in the range between a few Hz to a a few tens of kHz. They overlap with the ECG signal bandwidth, and ECG recordings are therefore distorted by artefacts representing the contribution of this induced electrical field by the ECG recording device.
3. Static magnetic field. The last component of the MRI environment is the large static magnetic field, which in clinical scanners have usually a value of 1.5 or 3 T. The most obvious of the effect of this field is the attraction force on metallic objects. There is also another effect , which is less known and is called the MagnetoHydroDynamic effect. The blood is carrying electrically charged particles. These moving (flowing) electrical particles are subject to the Lorentz Force, \vec{F} , due to the presence of \vec{B}_0 , $\vec{F} = q\vec{v} \wedge \vec{B}_0$, where q is the electrical charge of the particle and \vec{v} its speed. This force applied on the charges induces another electrical field, which can characterised. By approximating a section of an artery by a cylinder of diameter d , the voltage V_{MHD} across the artery is given by:

$$V_{MHD} = -vdB_0 \sin \theta, \quad (5.8)$$

with θ being the angle between the particle displacement and the magnetic field (figure 5.11). Given this simplistic model, it can be assumed that the maximal contribution of this MHD

effect stems from the blood flow in the aortic arch, as it is perpendicular to the \vec{B}_0 , the size of the aortic cross-section, and the blood velocity being maximal. This extra electrical field will superimpose onto the ECG signal. The periodicity of this "artefact" is the same as the heart rhythm, as this artefact is indeed an electrical measurement of the pulsatile blood flow in the aortic arch. It was indeed proven that the main contribution of the MHD effect stems from the blood flow in the aortic arch (Gupta et al., 2008, Tenforde, 1992, Tenforde et al., 1983). The main distortion occurs therefore during the ST segment, preventing the detection of ischemic episodes with ST elevation measurements.

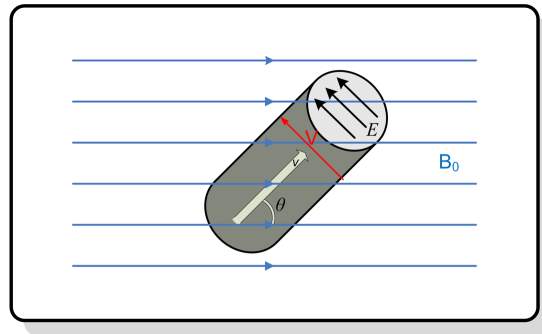


Figure 5.11: Simplified flowchart of induction voltage due to MHD effect.

The MRI environment is therefore hugely distorting the ECG signal (as can be seen in figure 5.12), and specific signal processing tools are therefore necessary and were introduced in order to cope with these distortions. Such solutions were introduced and some are presented in the next chapter 6. Interest readers are referred to an extensive review of this singular application Oster and Clifford (2017).

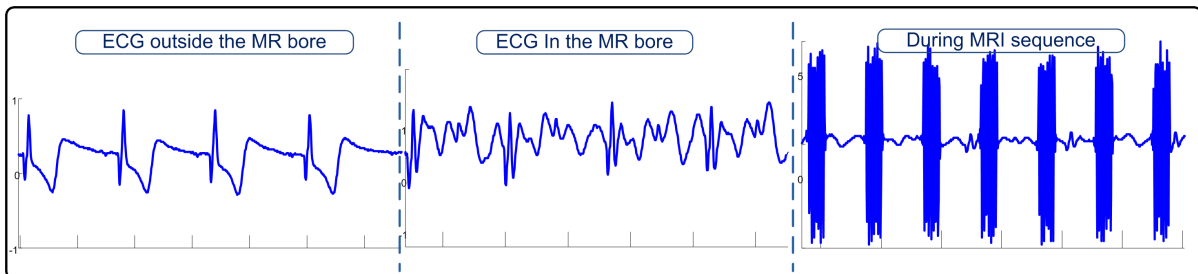


Figure 5.12: Distortion of the ECG signal by the MRI environment, with clean ECG signal (left) distortion of the ECG by the MHD effect (centre) and distortions by the gradients $G_{\{X,Y,Z\}}$ (right).

5.4.2 Modelling of the MagnetoHydroDynamic effect

As seen in the previous subsection, the ECG is highly distorted by the different components of the MRI electro-magnetic environment. Models have been proposed for both gradient artefacts (Felblinger et al., 1999) and the MHD models. The problem of gradient artefacts is easier as they are independent from the heart activity, an efficient way of dealing with those consists of an Adaptive Noise Cancellation scheme. The MHD effect is more complicated to tackle, as both signals (ECG and MHD) are cardiac signals, with close sources. Moreover, the MHD superimposes onto the ECG signal, and there is no possible way of accessing a ground-truth (the underlying clean ECG signal) in order to evaluate an ECG or MHD extraction technique. The development of a model is therefore required for stress-testing techniques for the suppression of the MHD effect.

The MHD effect could be simulated by introducing a dipole, with the same rhythm than the ECG, and located slightly above the heart. The MHD dipole can also be simulated as a sum of Gaussians, however a study is required in order to assess how many waves are necessary. Existing

Chapter 5. Modelling

databases are also required in order to estimate a number of parameters in order to get accurate MHD morphologies.

Different models were suggested in the literature, there are all based on solving the physical equations governing the blood flow in the aorta. Most studies in the literature wanted to assess the impact of the magnetic field on blood velocity or pressure. These models started with geometrical model of the aorta, from a simple rigid cylinder to more complicated 3D model, and tried to solve the Navier Stokes equation given below either analytically or using numerical methods (Gupta et al., 2008, Keltner et al., 1990, Kinouchi et al., 1996, Kyriakou et al., 2012, Martin et al., 2012, Tenforde, 2005).

$$\rho \left(\frac{\partial \vec{v}}{\partial t} + (\vec{v} \cdot \nabla) \cdot \vec{v} \right) = -\nabla \rho + \eta \nabla^2 \vec{v} + \frac{1}{\mu} (\vec{v} \wedge \vec{B}) \wedge \vec{B}, \quad (5.9)$$

where ρ is the blood density, η its viscosity and ρ the blood pressure.

A similar approach was taken for the model proposed by Oster et al. (2015a). First realistic 3D models of the heart, torso and aortic arch were used. The torso and heart models were provided by the ECGSim software (van Oosterom and Oostendorp, 2004), whereas the equation for modelling the aortic arch geometry was suggested by Gupta (2007), Gupta et al. (2008). The figure 5.13 shows the different models being used.

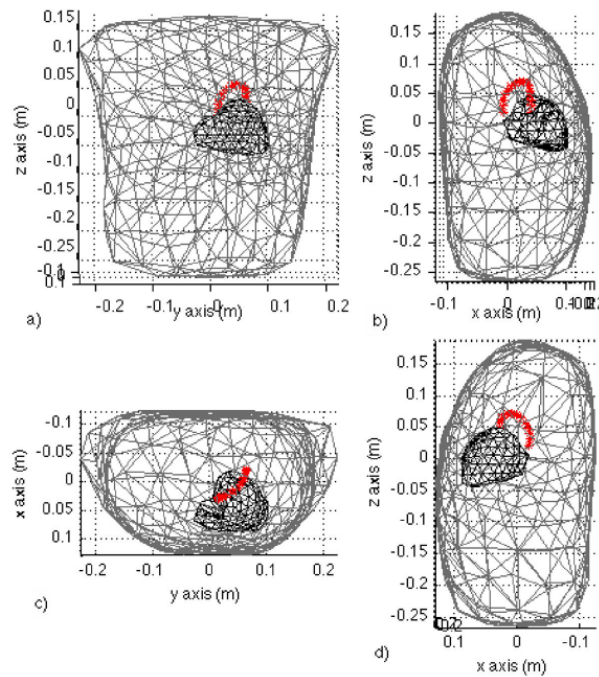


Figure 5.13: Multiple view of the geometrical models, torso in grey, heart in black and aortic arch in red. a) frontal view, b) lateral view, c) top view, d) lateral view.

The blood flow was not modelled by solving the Navier Stokes equation, but by measuring it experimentally. Blood flow velocity measurements has been made possible in MRI, using phase contrast imaging (Markl et al., 2005). It is therefore possible to characterise the blood flow across the aortic arch in the real conditions. Blood flow has been measured in four planes across the aortic arch, as depicted in figure 5.14

In order to enhance the realism of the MHD model, beat to beat variability was introduced in order to link the "strength" of the MHD model with the RR variability (as is the Stroke Volume). The proposed model was compared to the "real" MHD effect as extracted from ECG signals, a theoretical solution (solving the Navier Stokes equation analytically using a simple Windkessel model), and the INRIA's model suggested by Martin et al. (2012) (using a measured blood pressure profile). The figure 5.15 depicts the comparison of the different models. Although the proposed model does not allow a perfect match between the extracted and the simulated effect, it allows

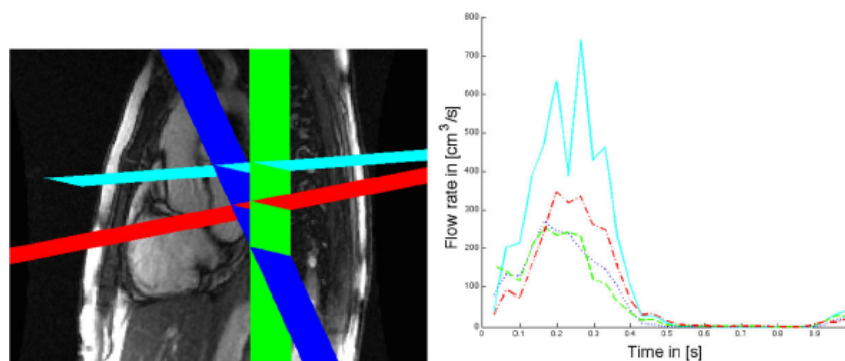


Figure 5.14: MRI image of the chest region (left), with the four hand selected planes for the measurement of the blood flow, in the ascending aorta (cyan) ascending aortic arch (blue) descending aortic arch (green) and descending aorta (red). The four corresponding flow rate measurements over one cardiac cycle, with the time $t = 0$ corresponding the QRS trigger point (right).

for good representation of the complexity of the phenomenon, and is used for stress-testing MHD extraction techniques. Simulation of ischemic episodes is made possible by combining this MHD and the ECG model, and is essential for testing in challenging conditions.

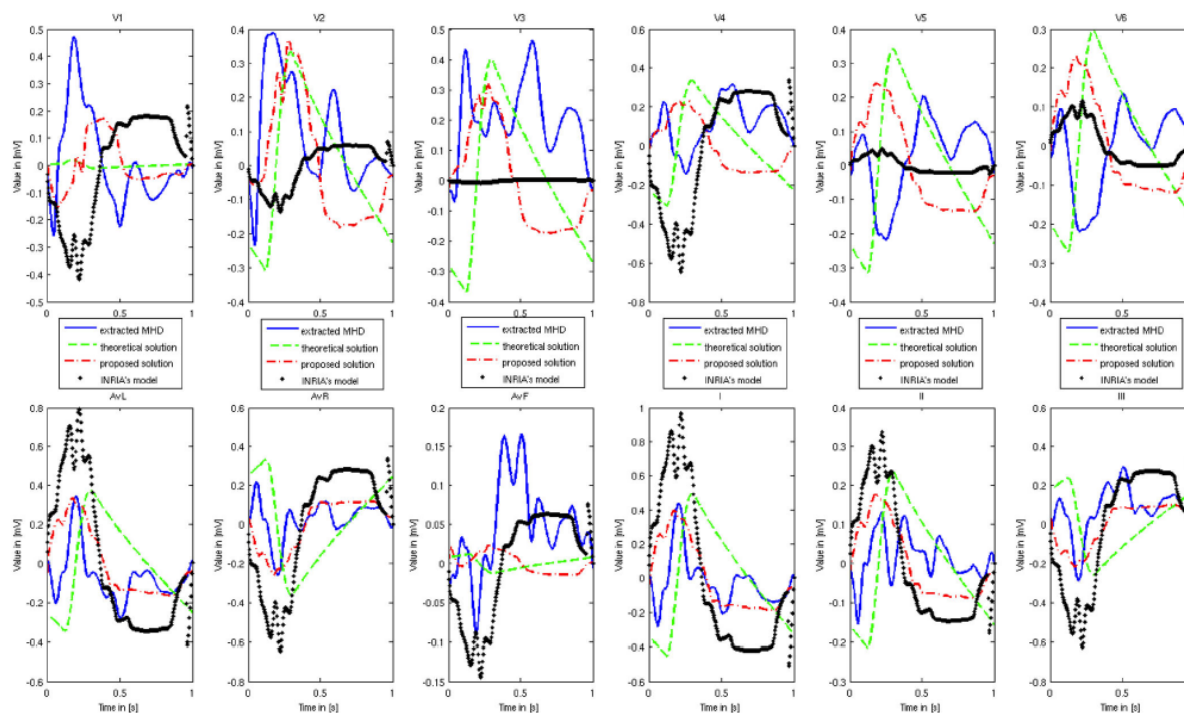


Figure 5.15: Template of the estimated and simulated MHD effects on the standard 12-lead derivations. (blue: extracted MHD effect, green: theoretical solution, black: INRIA's model, red: proposed model)

5.5 Synthesis

The methods described in this chapter were developed in the period spanning over my PhD thesis and my time as a post-doctoral research fellow in Oxford until 2016.

The main research outputs of this avenue of research consisted in:

1. **A. Petrėnas, V. Marozas, A. Solosenko, R. Kubilius, J. Skibarkienė, J. Oster, L. Sörnmo**, "Electrocardiogram modeling during paroxysmal atrial fibrillation: application to

Chapter 5. Modelling

the detection of brief episodes", *Physiological Measurement*, 2017. This paper is the result of a collaboration with Prof Leif Sörnmo (Lund University, Sweden) and the Kaunas University of Technology (Lithuania).

2. **J. Behar, F. Andreotti, S. Zauneder, Q. Li, J. Oster, G.D Clifford**, "An ECG Model for Simulating Maternal-Foetal Activity Mixtures on Abdominal ECG Recordings," *Physiological Measurement*, 35, 1537-50, 2014. This paper is the result of two PhD students I either co-supervised or mentored. I am particularly proud of the open-sourcing of the software for generating the simulations, fecgsyn.com .
3. **J. Oster, R. Llinares, S. Payne, Z. Tse, E.J. Schmidt and G.D. Clifford**, "Comparison of three artificial models of the MHD effect on the electrocardiogram," *Computers Methods in Biomechanics and Biomedical Engineering*, 18(13), 1400-1417, 2015. This model originated from a collaborative work between the University of Oxford, Harvard University, and Valencia. This approach was quite interesting as it showed the added-value of fusing image-based knowledge for the creation of a model of fluid dynamics that allowed for more realistic simulated ECG signals.

Chapter 6

Processing

The previous chapter was devoted to the presentation of an ECG morphological model, which proved to be flexible enough to simulated many situations, pathologies, foetal ECG or even ECG acquired during MRI. As it turns out, the model is even more powerful and can be used as the basis for a full set of analysis techniques. This chapter is devoted to the presentation of a range of processing techniques based on Bayesian filtering, and using the ECG model as the underlying representation of the system.

The first section is introducing the theory lying behind Bayesian filtering, the second section presents an application of denoising the ECG signal, whereas the last section shows how signal separation or extraction can be performed with this approach, on applications such as foetal ECG or ECG acquired in MRI.

6.1 Introduction of Bayesian filtering

Bayesian filtering is a paradigm aiming at the estimation of hidden or latent variables that control a system. Modelling this system, and deriving what is called a state-space model, is the pre-requisite for the application of this filter. The state-space model describes the evolution of the latent variables but the also link between these latent variables and the observations (or measurements) of the system. As will be seen later, Bayesian techniques are powerful tools, which offer more than only point estimates of the latent variables, but also provides information of the uncertainty of these estimations.

6.1.1 Bayesian filtering

Bayesian filtering relies on a state-space modelling, meaning that it is assumed the system is completely controlled by an internal state \mathbf{x}_k . The model is given by its general form by a set of two equations:

$$\begin{cases} \mathbf{x}_k = f(\mathbf{x}_{k-1}, \mathbf{u}_{k-1}, \mathbf{w}_{k-1}, k-1) \\ \mathbf{y}_k = g(\mathbf{x}_k, \mathbf{v}_k, k) \end{cases}, \quad (6.1)$$

where \mathbf{y}_k is the observation vector (or measurements), \mathbf{w}_k is the state (or process) noise, \mathbf{v}_k is the observation (or measurement) noise, \mathbf{u}_k is a control (or input) vector, and finally k is the current timestamps.

The upper equation is the evolution (or process) equation, and the lower the observation (or measurement) equation. It can be noted that both f and g functions are dependent of the time (hence the input k) and can also be noted f_k and g_k . A time independent version of these equations can exist, and the model is then called stationary. Please note the control input \mathbf{u}_k will not be considered further in this thesis.

Bayesian filtering aims at estimating the posterior probability $p(\mathbf{x}_k | \mathbf{y}_{1:k}, \theta_k)$, with θ_k being the parameters of the system $\{f_k, g_k, \mathbf{v}_k, \mathbf{w}_k\}$. This estimation is done recursively in two steps, a

Chapter 6. Processing

prediction step estimating the prior probability $p(\mathbf{x}_k | \mathbf{y}_{1:k-1}, \theta_{k-1})$ by using the evolution equation, which is followed by correction step by using the observation equation and gives $p(\mathbf{x}_k | \mathbf{y}_{1:k}, \theta_k)$.

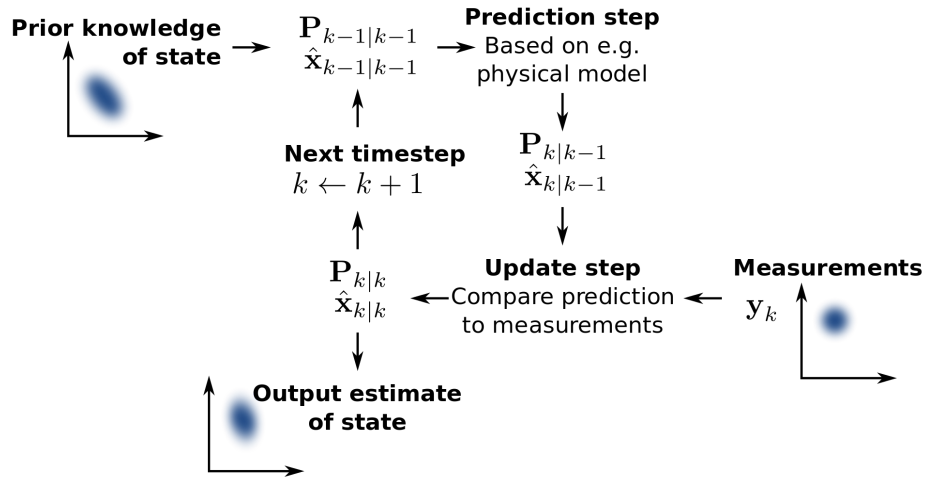


Figure 6.1: Flowchart of Bayesian filtering. The recursive process is depicted, starting from a prior knowledge of the state one get updated statistics of the hidden variabl, which are finally updated when new measurements come in. (source Wikipedia).

A special case of Bayesian filtering occurs when both f_k and g_k are linear and when the random variables are Gaussian. The problem is then called linear-Gaussian state-space model or a linear dynamical system, and the system can then be described by:

$$\begin{cases} \mathbf{x}_k = A_{k-1}\mathbf{x}_{k-1} + F_{k-1}\mathbf{w}_{k-1} \\ \mathbf{y}_k = C_k\mathbf{x}_k + G_k\mathbf{v}_k \end{cases}, \quad (6.2)$$

where both functions f and g are replaced by linear algebra operations (matrices).

The estimation of the posterior probability is then performed with the well-known Kalman Filter equations (or algorithm) (Kalman, 1960):

$$\begin{aligned} & \text{Prediction} \\ & \hat{\mathbf{x}}_{k|k-1} = A_{k-1}\hat{\mathbf{x}}_{k-1|k-1}, \\ & R_{k-} = A_{k-1}R_{k-1}A_{k-1}^T + F_{k-1}Q_{k-1}^w F_{k-1}^T, \\ & \text{Correction} \\ & K_k = R_{k-}C_k^T (C_k R_{k-}C_k^T + G_k Q_{k-1}^v G_k^T)^{-1}, \\ & \hat{\mathbf{x}}_{k|k} = \hat{\mathbf{x}}_{k|k-1} + K_k (\mathbf{y}_k - C_k \hat{\mathbf{x}}_{k|k-1}), \\ & R_k = (I - K_k C_k) R_{k-}, \end{aligned} \quad (6.3)$$

where Q_{k-1}^w is the covariance matrix of the process noise, $Q_{k-1}^w = \text{cov}(\mathbf{w}_{k-1}) = E[\mathbf{w}_{k-1}\mathbf{w}_{k-1}^T]$, $Q_{k-1}^v = \text{cov}(\mathbf{v}_{k-1})$, $R_{k-} = \text{cov}(\hat{\mathbf{x}}_{k|k-1})$, $R_k = \text{cov}(\hat{\mathbf{x}}_{k|k})$, and K_k is called the Kalman gain.

6.1.2 Nonlinear Bayesian Filtering

The Kalman filter has been applied to a wide range of applications, and has been notoriously associated to the Apollo Space program (Grewal and Andrews, 2010) therefore allowing humankind to land on the Moon. Nevertheless, the linear hypothesis is one of the biggest restrictions of its applications and several solutions have been proposed to overcome this limitation.

One of these solutions, called the Extended Kalman Filter (EKF), consists of the linearisation of both evolution and observation equations around the current estimates. The equations 6.1 are

then linearised and rewritten as:

$$\begin{cases} \mathbf{x}_k = f(\hat{\mathbf{x}}_{k-1}, \hat{\mathbf{w}}_{k-1}, k-1) + A_{k-1}(\mathbf{x}_{k-1} - \hat{\mathbf{x}}_{k-1}) + F_{k-1}(\mathbf{w}_{k-1} - \hat{\mathbf{w}}_{k-1}) \\ \mathbf{y}_k = g(\hat{\mathbf{x}}_k, \hat{\mathbf{v}}_k, k) + C_k(\mathbf{x}_k - \hat{\mathbf{x}}_k) + G_k(\mathbf{v}_k - \hat{\mathbf{v}}_k) \end{cases}, \quad (6.4)$$

where

$$\begin{aligned} A_k &= \left. \frac{\partial f(\mathbf{x}, \mathbf{w}, k)}{\partial \mathbf{x}} \right|_{\mathbf{x}=\hat{\mathbf{x}}_k} \\ F_k &= \left. \frac{\partial f(\mathbf{x}, \mathbf{w}, k)}{\partial \mathbf{w}} \right|_{\mathbf{w}=\hat{\mathbf{w}}_k} \\ C_k &= \left. \frac{\partial g(\mathbf{x}, \mathbf{v}, k)}{\partial \mathbf{x}} \right|_{\mathbf{x}=\hat{\mathbf{x}}_k} \\ G_k &= \left. \frac{\partial g(\mathbf{x}, \mathbf{v}, k)}{\partial \mathbf{v}} \right|_{\mathbf{v}=\hat{\mathbf{v}}_k}. \end{aligned} \quad (6.5)$$

Using this linearised version, it is possible to get updates on the state by applying the Kalman Filter algorithm 6.3.

EKF however also has some limitations, mainly the fact that all functions are not differentiable, and as the derivatives cannot be computed, the different matrices can therefore not be estimated. A new range of Kalman Filter has therefore been introduced and called Unscented Kalman Filter (UKF) (Julier and Uhlmann, 2004). UKF introduces σ -points (\mathbf{x}^i) and associated weights (ω_i), which represent a deterministic sampling of the state vector. The Kalman equations are then used to propagate the first and second order of the state, where the first order of the state $E[\mathbf{x}] = \sum_i \omega_i \mathbf{x}^i$, and the second order being $R_x = \sum_i \omega_i (\mathbf{x}^i - E[\mathbf{x}])(\mathbf{x}^i - E[\mathbf{x}])^T$. The advantage of this approach is that first and second order of $\mathbf{y} = g(\mathbf{x})$ can be easily computed as $E[\mathbf{y}] = \sum_i \omega_i g(\mathbf{x}^i)$, and $R_y = \sum_i \omega_i (g(\mathbf{x}^i) - E[\mathbf{y}])(g(\mathbf{x}^i) - E[\mathbf{y}])^T$.

Another class of nonlinear Bayesian filtering has also recently been introduced. It consists of a random sampling of the state vector, and letting these samples evolve according to the process equation and correct them according to the new observations being made. This class of techniques is called particle filters, or Sequential Monte Carlo (Arulampalam et al., 2002, Doucet et al., 2001). It offers the advantage of getting a more complete representation of the state vector distribution, than only taking into account the first and second orders (therefore allowing non Gaussian distributions).

6.2 Denoising

As it turns out, the dynamical model of the ECG morphology introduced by McSharry et al. (2003) is extremely well suited for the state-space representation, and therefore a nonlinear Bayesian approach. This was first proposed by Sameni et al. (2007), as an excellent denoising tool.

6.2.1 Formulation

In order to apply the Bayesian filtering framework, the state and observation vectors needs to be defined. This design is preponderant and is offering the versatility of this approach, as will be seen by the many possible applications.

Let first define the state vector $\mathbf{x}_k = [\theta_k, z_k]$, where θ_k is the angular position in the cylindrical coordinates (or the phase in the cardiac cycle), and z_k represents the ECG value in mV at time k . The state-space formalism of this technique is defined by the following set of equations:

(i) the evolution equations are given by

$$\begin{cases} \theta_k = (\theta_{k-1} + \omega\delta) \bmod 2\pi \\ z_k = - \sum_i \delta \frac{\omega \Delta \theta_{i,k-1}}{b_i^2} g(\alpha_i, \Delta \theta_{i,k-1}, b_i) + z_{k-1} + \eta \end{cases}, \quad (6.6)$$

Chapter 6. Processing

where $\omega = 2\pi/RR$ the angular speed, δ the sampling period. and α_i, b_i, ξ_i are the amplitude, width and angular position of the i^{th} Gaussian respectively, with $\Delta\theta_{i,k-1} = (\theta_{k-1} - \xi_i) \pmod{2\pi}$ and with $g(a, b, c) = a \exp(-\frac{b^2}{2c^2})$ a Gaussian wave.

(ii) the observation equations are defined by

$$\begin{cases} \varphi_k = \theta_k + v_{1,k} \\ s_k = z_k + v_{2,k} \end{cases}, \quad (6.7)$$

The observed signals, s_k is the ECG signal and φ_k is an artificial phase signal assigned linearly from 0 to 2π between two consecutive R waves and then rescaled between $-\pi$ and π .

There is therefore a need to create an artificial signal, which represents the cardiac phase. The R peaks are detected in a pre-processing step, and it is therefore assumed that this detection is possible and accurate even in noisy detections.

6.2.2 Parameter intialisation

The denoising technique, and the Bayesian filtering, depends heavily on a set of initial parameters. These parameters have a huge importance for the success of the technique, as they give us *prior* knowledge on the evolution of the signal. The main parameters to be determined are the three parameters associated to each of the Gaussian wave (α_i, b_i, ξ_i).

To be successfully applied, Bayesian filtering rely on a good parameter initialisation, which is usually performed on a small portion of the data at the beginning of the recording. A small number (usually 30) of ECG cycles represented as a function of the cardiac phase are stacked up. These stacks are used to determine a mean ECG template, and the standard deviation as function of the phase.

Once this mean ECG template has been estimated, it is possible to determine the Gaussian parameters by using a nonlinear optimisation algorithm, as was suggested for the offline applications (Clifford, 2006, Clifford et al., 2005).

6.2.3 Benchmarking and results

Sameni et al. have created a small dataset of ECG signals in order to assess the denoising performance (Sameni et al., 2007). They extracted 190 30-second ECG segments from the MIT-BIH Normal Sinus Rhythm (NSR) database (Goldberger et al., 2000). These segments were selected visually, by ensuring low noise level on the segments. The MIT-BIH NSR database contains long-term recordings from 18 subjects without significant arrhythmias.

Noise was added on top of these high quality segments, by using Muscle Artifact from the MIT-BIH Noise Stress Test (NST) database Goldberger et al. (2000). The noise amplitudes were adjusted in order to simulate different levels of noise with SNR ranging from 6 to 18dB.

The Bayesian filtering approach results were compared to state-of-the-art techniques, such as simple Finite Impulse Response (FIR) filtering, Adaptive Filtering (AF), and wavelet decomposition (WD). Different Bayesian filter techniques were also compared, as the authors implemented Extended Kalman Filter (EKF), Extended Kalman Smoothing (EKS), and Unscented Kalman Filter (UKF). The results obtained on this small dataset are assembled on table 6.1.

The results demonstrated that the Bayesian filtering approaches outperform other techniques, especially in low SNR situations. It was also shown, that EKS gave best denoising results. Sameni et al. have also studied the effect of adaptive noise covariance parameters in order to cope with non stationary noise levels, and interested readers are referred to their paper Sameni et al. (2007).

6.3 Signal Extraction

In the previous sections, we have demonstrated the power of a model-based approach for the analysis of the ECG, for a better denoising but also for the estimation of some clinical parameters.

SNR (dB)			
Input	6.0	12.0	18.0
FIR	5.9	9.7	11.7
AF	5.0	5.4	5.5
WD	6.9	12.9	18.9
EKF	10.0	14.1	18.8
EKS	12.0	15.5	19.5
UKF	9.5	13.8	18.7

Table 6.1: SNR Results for the denoising with real muscle artifacts *Sameni et al. (2007)*.

In the previous applications, no *prior* knowledge on the noise has been added in the state-space equations, and the observation noise was a simple additive noise. However for some applications noise level could be higher, and could more structured than simple white or coloured noise. In this section, we will describe the extension of the model-based approach for problems such as source separation. We will therefore assumed that the “noise” has a pseudo-periodical structure as has the ECG. This pseudo-periodicity could be either identical or different from the ECG rhythm, that is the noise rhythm might be different from the cardiac rhythm.

6.3.1 Problem formulation

Some applications imply the simultaneous acquisition of multiple pseudo-periodical biosignals at once. These signals will therefore overlap, and for an accurate analysis of the signal of interest it will be necessary to separate all the sources. Different approaches have been suggested for source separation in biomedical applications, one of the most popular consists in applying ICA and relies on the assumption that each of the sources are statistically independent (*James and Hesse, 2005*). It is nevertheless possible to make stronger assumptions on the underlying sources, *Sameni et al. (2008)* have suggested a semi-blind approach using some *prior* knowledge on the rhythm of the biosignal to be analysed.

It is possible to make some stronger assumptions, and to imagine that the rhythm of both noise and signal are known, and that both their template can be estimated. Based on these assumptions, it is possible to apply the model-based filtering for an online estimation of the contribution of each of these sources. The state vectors have therefore to be extended, in order to integrate the parameters of the pseudo-periodical noise. The parameters for this state-space formalism are:

$$\begin{aligned}
 \mathbf{x}_k &= [\theta_k^z, \theta_k^n, z_k, n_k, \{\alpha_{i,k}^z\}, \{b_{i,k}^z\}, \{\xi_{i,k}^z\}] \\
 \mathbf{y}_k &= [\varphi_k^z, \varphi_k^n, s_k, s_k] \\
 \mathbf{w}_k &= [\omega^z, \omega^n, \eta_k^z, \eta_k^n, \{\varepsilon_{\alpha,i}\}, \{\varepsilon_{b,i}\}, \{\varepsilon_{\xi,i}\}, \{\alpha_{i,k}^n\}, \{b_{i,k}^n\}, \{\xi_{i,k}^n\}] \\
 \mathbf{v}_k &= [v_{1,k}, v_{2,k}, v_{3,k}, v_{4,k}],
 \end{aligned} \tag{6.8}$$

which gives rise to the following process equations

$$\left\{ \begin{array}{l}
 \theta_k^z = (\theta_{k-1}^z + \omega^z \delta) \bmod 2\pi \\
 \theta_k^n = (\theta_{k-1}^n + \omega^n \delta) \bmod 2\pi \\
 z_k = z_{k-1} - \sum_i \delta \frac{\omega^z \Delta \Theta_{i,k-1}}{(b_{i,k-1}^z)^2} g(\alpha_{i,k-1}^z, \Delta \Theta_{i,k-1}, b_{i,k-1}^z) + \eta_k^z \\
 n_k = n_{k-1} - \sum_i \delta \frac{\omega^n \Delta \theta_{i,k-1}}{(b_i^n)^2} g(\alpha_i^n, \Delta \theta_{i,k-1}, b_i^n) + \eta_k^n \\
 \alpha_{i,k}^z = \alpha_{i,k-1}^z + \varepsilon_{\alpha,i} \\
 b_{i,k}^z = b_{i,k-1}^z + \varepsilon_{b,i} \\
 \xi_{i,k}^z = \xi_{i,k-1}^z + \varepsilon_{\xi,i}
 \end{array} \right. , \tag{6.9}$$

Chapter 6. Processing

and the observation equations

$$\begin{cases} \varphi_k^z = \theta_k^z + v_{1,k} \\ \varphi_k^n = \theta_k^n + v_{2,k} \\ s_k = z_k + n_k + v_{3,k} \\ s_k = n_k + \sum_i g(\alpha_{i,k}^z, \Delta\Theta_{i,k}, b_{i,k}^z) + v_{4,k}, \end{cases} \quad (6.10)$$

It is interesting to note the observation equations have been extended as well. The presence of this fourth equation can be explained by a drifting phenomenon when this extra observation equation was missing, separation of the contribution of each sources on a new observation. Some instabilities were leading to a drift on the signal and noise components. The idea behind the fourth equation is that a first “rough” approximation of the pseudo-periodical noise could be performed by suppressing the signal template from a new observation, that is $s_k - \sum_i g(\alpha_{i,k}^z, \Delta\Theta_{i,k}, b_{i,k}^z) = n_k + v_{4,k}$. This rough estimation could then be used in a second time to estimate the signal contribution z_k , by suppressing the rough estimate of the noise form the new observation. The elegance of the Bayesian filtering approach allows to replace this iterative process by a single step, by adding this fourth equation. In order to account for the fact, that this extra-equation is a rough estimation of the noise component and less precise that equation two, one has only to increase the uncertainty of this equation, that is setting a higher noise covariance for v_4 than v_3 .

6.3.2 Benchmarking and results

This approach has already been applied to two problems.

The first one consists in the acquisition of ECG during an Magnetic Resonance Imaging examination [Oster et al. \(2013\)](#). During such a procedure, the patient is located in a high static magnetic field. The movement of electrically charged particles, ions inside the blood flow, creates an electrical field which is picked up by the electrodes. This phenomenon, called MagnetoHydro-Dynamic (MHD) effect, superposes onto the ECG signal. The MHD effect is synchronised with the ECG, as the heart’s electrical activity is triggering its contraction and therefore the blood flow. For this problem, there is no need to introduce φ_k^n , as the same phase variable could be used for both the signal (z_k) and the “noise” (n_k).

The performance of this approach was assessed on a very small subset of simulated pathological cases, using an in-house MHD generator [Oster et al. \(2015c\)](#). The inversion of the T wave was simulated in one of these cases. It was assessed whether it is possible to automatically detect this inversion, the results are depicted on figure 6.2. It can be seen that the T wave inversion has been automatically detected fifteen cycles after the inversion.

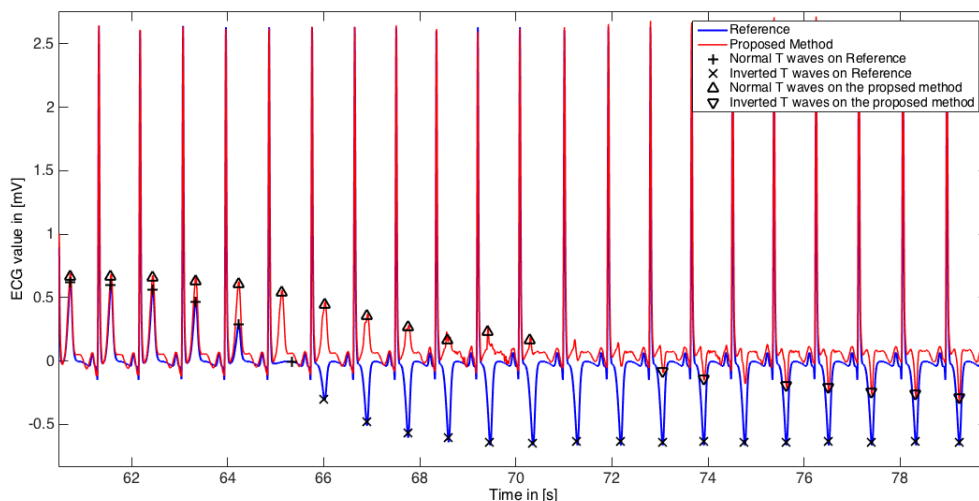


Figure 6.2: Results of ECG signal extraction, and automatic detection of a simulated T wave inversion. The annotations were obtained by using an automatic technique (*ecgpuwave*) Jané et al. (1997).

The second application consists in the extraction of the foetal ECG signal from abdominal signals Behar et al. (2014a). These abdominal signals contain a mixture of both maternal ECG and foetal ECG, and it is therefore necessary to introduce the extra phase signal (φ_k^n), as the foetal cardiac rhythm is usually in the order of magnitude of twice the maternal ECG. The performance of this approach was assessed with SNR and QT interval measurements on a small dataset of simulated data, by using an in-house simulator Behar et al. (2014b), which is available on PhysioNet Goldberger et al. (2000). The Bayesian filtering approach outperformed other techniques, with a 14.1dB SNR improvement and a median absolute error on QT measurements of 4.0ms, well within the manual annotation error range.

6.4 Synthesis

This chapter was devoted to the description of an elegant model-based filtering solution for the analysis of ECG signals. This approach has been shown to be particularly well-suited for the denoising of ECG signals acquired during MRI with accurate suppression of both main MRI induced artefacts:

1. Magnetic Field Gradients (MFG). During my PhD thesis, I suggested the use of the ECG model-based Bayesian filtering for the removal of MFG artefacts on ECG acquired during MRI. The use of the ECG model allowed to account for the ECG contribution during the estimation of the body response to the MFG. This result was published in **J. Oster, O. Pietquin, M. Kraemer and J. Felblinger**, "Nonlinear Bayesian Filtering for Denoising of Electrocardiograms acquired in a Magnetic Resonance Environment," *IEEE Transactions on Biomedical Engineering*, 57, 1628-38, 2010.
2. MHD. At the end of my PhD, I secured funding through the Newton International Fellowship to work on the development of statistical signal processing techniques for the removal of blood flow artifacts in cardiac electrophysiological data recorded during magnetic resonance imaging. The extended ECG model-based filtering was published in **J. Oster, M. Geist, O. Pietquin and G. D. Clifford**, "Filtering of pathological rhythms during MRI scanning," *International Journal of Bioelectromagnetism*, 15, 54-59, 2013.

Chapter 7

Classification

This chapter is devoted to the use of ECG signals as the input for different classification tasks. In the first section, I demonstrate how the versatile ECG model can be used for the classification of heartbeat, while the second section describes how classical machine learning and deep learning can be used for the identification of AF on a large population.

7.1 Detection of pathological beats

As described in the previous chapter, the ECG model-based filtering has been shown to be a powerful tool for the processing and analysis of ECG signals. Nevertheless, the performance of the different techniques relies on feeding the system with the correct *prior* knowledge, that is the morphology of the beats. However, the ECG can also be pathological, and therefore contains beats with a different morphology. The accuracy of the denoising and any other analysis would be greatly affected by such beats, and necessitate an improvement to the approach.

Bayesian filtering is a very versatile tool, in that it not only allows for estimating the hidden variables, but also informs on the level of confidence in these estimations. It offers the possibility to assess how a new observation is likely to have been generated by the ECG model and its given parameters. Bayesian filtering, relying on this property, have been proposed for novelty detection, that is detecting unexpected measurements in a time-series [Pimentel et al. \(2014\)](#). In our context, such an approach could therefore be used for the detection of noisy segments or episodes, but also pathological beats. This was the approach suggested by [Sayadi et al. \(2010\)](#) in order to detect Premature Ventricular Contraction, for whom the ECG morphology is different from the normal beats, which have been parametrised.

This technique is interesting, able to detect non-normal beats, but the processing or analysis of such beats is not possible as no *prior* information is known for such beats. Some patients have very pathological rhythm, and the amount of pathological beats can be high (50% in case of bigeminy). An approach, which deals with such beats as being extremely unlikely and rare events, is therefore not optimal. It is thus necessary to extend this methodology to model pathological beats as well. Switching Kalman Filters (SKF) ([Murphy, 1998](#)) offers the possibility for such an extension, where the morphology of the normal and pathological beats can be modelled as different modes, and the mode with the highest likelihood over a given cardiac cycle can be selected. In this section, the heartbeat classification and filtering technique suggested in [Oster et al. \(2015b\)](#) will be described.

7.1.1 Switching Kalman Filters

Bayesian filtering offers more than just a point estimate of the state vector. At each step, not only the latent variable estimate is updated, but also the uncertainty of this estimate (or the spread), which is given by the covariance matrix. Given the parameters of the state-space model, it is also possible to estimate the likelihood of a new observation having been generated by a given model, i.e. $p(\mathbf{y}_k | \mathbf{x}_k, \mathbf{y}_{1:k-1}, \hat{\mathbf{x}}_k)$. It is therefore possible to estimate how likely a new observation

Chapter 7. Classification

has been generated by the given state-space modelling. In a system, where the state vector could jump between a finite number of modes (and be modelled with different state-space models), it would be possible to estimate the mode being the most likely to have generated a given observation. Such an approach is called Switching Kalman Filter (SKF).

SKF can be seen as an extension of Hidden Markov Models (HMM) [Murphy \(1998\)](#). As for HMM, there are (generally) finite number of latent states, called mode, and one aims at detecting the most likely latent mode from a set of observations. Nevertheless, SKF is more "advanced" than HMM, since each mode can be modelled by its own state-space formalism as a linear (or non-linear) dynamical system. In this section, we will briefly introduce the mechanism of SKF allowing for the selection of the most likely latent mode.

Let call $C_k^{(i)}$ the observation matrix of the i^{th} mode, such that $\mathbf{y}_k = C_k^{(i)} \mathbf{x}_k^{(i)} + G_k^{(i)} \mathbf{v}_k^{(i)}$ and let denote $Q_k^{v(i)} = cov(\mathbf{v}_k^{(i)})$, the covariance matrix of the observation noise. The innovation at time k , is denoted $\tilde{\mathbf{y}}_k^{(i)} = \mathbf{y}_k^{(i)} - C_k^{(i)} \hat{\mathbf{x}}_k^{(i)}$ and $R_{\varepsilon,k}^{(i)}$ its covariance matrix, which can be computed with:

$$R_{\varepsilon,k}^{(i)} = G_k^{(i)} Q_k^{v(i)} G_k^{(i)T} + C_k^{(i)} R_{k-}^{(i)} C_k^{(i)T}, \quad (7.1)$$

with $R_{k-}^{(i)}$ being the *prior* state covariance matrix, which is computed step by step during the Kalman filter algorithm.

The residual likelihood for the i^{th} mode, $l_k(i)$, can then be computed by:

$$l_k(i) = \frac{1}{\alpha} \frac{1}{\sqrt{2\pi \det(\mathbf{R}_{\varepsilon,k}^{(i)})}} \exp\left(-\frac{1}{2} \tilde{\mathbf{y}}_k^{(i)T} \mathbf{R}_{\varepsilon,k}^{(i)-1} \tilde{\mathbf{y}}_k^{(i)}\right), \quad (7.2)$$

with α being a normalization factor, so that $\sum_i l_k(i) = 1$.

Monitoring this likelihood allows to select the most probable mode to have generated the new observations. Section 7.1 will show how this theory can be applied to ECG analysis for the detection of ventricular rhythms.

7.1.2 Problem formulation

Let assume that a given number M of modes, which represent the morphology of each of the main type of heartbeats for one patient, is known. These morphologies being known, it is possible to estimate the state-space models for each of these modes. These M different Bayesian filtering can be run in parallel, and the likelihood can be computed for each new measurement as described in equation 7.2. Standard SKF allows to switch modes for every new samples, but physiologically such a switch only occurs at the start of a new heartbeat, that is the mode remains the same over a whole cardiac cycle. In order to simulate this behaviour, the mode cycle likelihood (I^C) computed over the cardiac cycle is given by:

$$I^C(i) = \int_{k_1}^{k_2} \exp\left(-\left(\frac{\varphi_k - \pi/3}{\sigma_\theta}\right)^2\right) \times l_k(i) dk, \quad (7.3)$$

where φ is the artificial observed phase signal, k_1 is the sample such that $\varphi_{k_1} = -\pi$ and k_2 defined such that $\varphi_{k_2} = \pi$, and σ_θ is a parameter defining the width of an exponential window.

The classification of the heartbeats is therefore achieved by selecting the mode with the highest cycle likelihood (I^C).

However, the ECG signals can be corrupted by noise or artefacts, or they might be some very unusual or rare events, which cannot be modelled easily. The SKF technique can be extended in order to allow some flexibility by including the possibility for novelty detection. Taking inspiration from [Quinn et al. \(2009\)](#), an extra mode was introduced and called X-factor. The X-factor is a mode for which no *prior* information on the dynamics of the heartbeat is incorporated. The X-factor only relies on the smoothness of an ECG signal, and attacks the filtering problem with a target tracking angle. The ECG value is assumed to be the target, whose position (x_k) is evolving

according to its speed (dx_k), which is modelled as following a random walk. The state-space formalism can be written as follows:

(i) evolution equations

$$\begin{cases} x_k = x_{k-1} + \frac{dx_{k-1}}{f_s} + \nu_{1,k} \\ dx_k = dx_{k-1} + \nu_{2,k} \end{cases}, \quad (7.4)$$

f_s being the sampling frequency, and ν_k being the state noise.

(ii) observation equations

$$\{s_k = x_k + v_{1,k} \quad , \quad (7.5)$$

s_k being the observed signal (ECG) and $v_{1,k}$ the observation noise.

The SKF is finally run over $M + 1$ modes, and for each heartbeat the mode with the highest cycle likelihood is selected.

7.1.3 Parameter initialisation

In the previous subsection, we have assumed that the different modes were known, and that Gaussian parameters have been initialised properly. The procedure for this semi-automatic initialisation is described here.

First, the ECG signal has to be segmented around the R-peaks, which are detected using standard detection algorithms. The segmentation is performed by mapping the RR intervals to a cyclic phase as described in [Sameni et al. \(2007\)](#), each cycle is then segmented from $-\pi$ to π radians.

Let assume that a dominant class (heartbeat) and its typical morphology is known, if not this dominant class is supposed to be the first heartbeat of a given signal. Each new heartbeat is then compared to the dominant class morphology using a cross correlation measure. If this value is over a given threshold, t_c , then the heartbeat is added to the dominant class. If not, a new class containing this new heartbeat is created. Subsequent cross correlations are then performed on both classes. If the cross correlation is not above t_c for either of the two new groups, then the heartbeat is put in a third class. This process continues for all heartbeats.

At the end of this step, all the heartbeats have been assembled into different clusters. Only the relevant modes are kept for the estimation of the Gaussian parameters. The relevant modes are determined by counting the number of cycles in each cluster, and keeping only the clusters with a given number of cycles (t_r). The Gaussian parameters for each of the relevant modes are then estimated using the same process as described in the subsection 6.2.2.

The different classes have therefore been parameterised at this stage, and the only missing parameter is their label, that is whether the heartbeat is ventricular or normal. This labelling relies on the cardiologist or local expert to interpret the type of each cluster, although automated approaches could also be possible. For instance, a heartbeat classifier based on features such as QRS width could be used [Llamedo and Martínez \(2012\)](#), followed by a majority voting among all the heartbeats constituting a cluster.

7.1.4 Benchmarking and results

The method was assessed with respect to the performance of ventricular heartbeat classification. Confusion matrices were created for the SKF approach on a test sets (DS2 of the MIT-BIH arrhythmia database) separated from the train set. The proposed SKF approach was compared to state-of-the-art beat classification techniques described by [de Chazal et al. \(2004\)](#), [Llamedo and Martínez \(2011\)](#), and the two techniques described in ([Llamedo and Martínez, 2012](#)). Although these techniques provide complete heartbeat classification, we have only considered their capability of ventricular beat classification, in order to compare with the SKF approach presented in this article.

The proposed technique detection of ventricular beats was assessed using the sensitivity (Se) and positive predictive values ($+P$) as suggested in [ANSI/AAMI:EC57 \(2012\)](#), but also in terms of

Table 7.1: Scores obtained on the DS2 (MIT-BIH arrhythmia database)

Technique	Se	$+P$	F_1
de Chazal et al. (2004)*	86.5	42.7	57.1
Llamedo and Martínez (2011)*	95.3	28.6	44.0
automatic Llamedo and Martínez (2012) ^{a,*}	82.1	77.9	79.9
assisted Llamedo and Martínez (2012) [‡]	91.4	96.9	94.1
SKF with X-factor ^{b,†} Oster et al. (2015a)	90.5	99.96	95.2

^a 0.12% of the heartbeats were not classified.

^b 3.2% of the heartbeats were classified as X-factor, and therefore discarded for the computation of these statistics.

* These techniques are completely automatic.

[‡] 12 cluster centroids were annotated by an expert.

[†] An average of 3 cluster centroids were annotated by an expert, with a 5th percentile of 1 beat and a 95th of 6 beats.

F_1 (which is the harmonic mean of Se and $+P$, and penalises False Positives and False Negatives equally).

The results are assembled in table 7.1. It can be seen that the SKF results are higher than the other state-of-the-art techniques, the scores could even be improved if the Fusion beats were considered separately. Interested readers are referred to Oster et al. (2015a) for further results and analysis. Examples of the processing are depicted in the figure 7.1. A special emphasis on the interpretation of the X-factor and his role as signal quality index has been put in another book chapter Oster and Clifford (2015).

7.2 Rhythm classification: AF detection

The automated detection of AF has an extensive literature, recently reviewed from an engineering perspective by Sörnmo (2018). AF is characterised by a highly irregular ventricular response (or heart rate), but also by ECG morphological changes such as the presence of small f-waves (small oscillations with a dominant frequency around 5Hz with amplitudes of few μV), which replace the P wave. In this section, I will describe how a classical machine learning with specifically designed hand-crafted features, a deep learning model, and a hybrid model combining both models can deal with this problem of AF detection.

7.2.1 Rhythm classification, Atrial Fibrillation

7.2.1.1 Classical Machine Learning

This technique takes inspiration from Colloca's technique Colloca et al. (2013). For many real applications, such as mHealth or recordings during exercise, the presence of high level of noise (for instance of muscle artefacts) renders the accurate extraction of f-waves impossible. So the proposed technique was designed to focus only the ventricular response or rhythm. It was decided to restrict the analysis to only five features: the first consists in a coefficient derived from the sample entropy of the RR-interval time series, denoted COSEn and proposed by Lake and Moorman (2011). The four other features are presented by Sarkar et al. (2008), and are derived from the Poincaré representation of the RR-interval time series. This Poincaré representation space is then divided in several bins following a Union-Jack pattern, and the number of heartbeats in each bin is counted. We included the evidence of AF (AFE), which is a combined coefficient of three subfeatures and was proposed by the authors for the classification of AF (Sarkar et al., 2008). We also included the following three subfeatures: (i) the numbers of beats in the Origin bin (OrC),

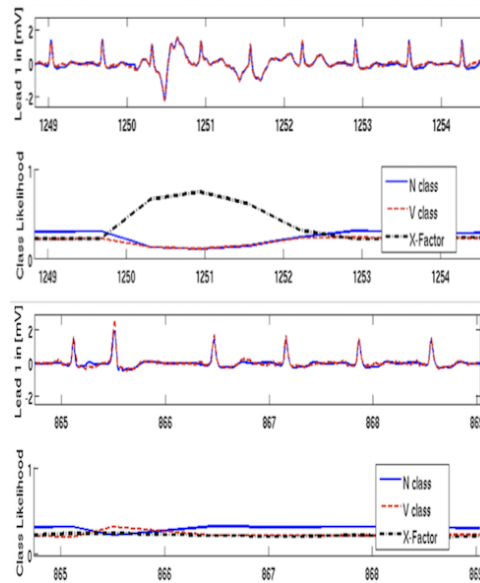


Figure 7.1: Example of the SKF filtering. The top row contains the ECG signal with both the raw signal (solid line) and the denoised signal (dashed line). The second row shows the class likelihood for each mode: normal beat (solid line), ventricular beat (dashed line) and X-factor (dash-dotted line). The example on the bottom highlights an example of ventricular beat classification, and the example on the top highlights an example of a noisy segment classified as X-factor.

representing the number of normal heartbeats; (ii) Irregularity Evidence (IrE), which counts the number of irregular heartbeats; and (iii) Premature Atrial Contraction Evidence (PACE), which counts the number of heartbeats which seem indicative of atrial arrhythmia. The features based on the heart rate were excluded given the inherent presence of tachycardia during exercise. A SVM with a radial basis function (RBF) kernel was used as the classifier, which was trained on the 2017 PhysioNet/Computing in Cardiology challenge training dataset [Clifford et al. \(2017\)](#). The classifiers were trained using cross-validation. Random search was performed to determine the SVM hyperparameters: soft margin constant C and RBF kernel hyperparameter γ .

The AF detector was suggested for the analysis on windows of the ECG signals (around 1-minute long). The use of a sliding window could however introduce an increase in the false positive rate, especially as the SVM classifier was trained to allow for the detection of short episodes of AF (or occult paroxysmal atrial fibrillation). Nevertheless, the shorter the AF episodes targeted, the more likely the classifier is to detect noisy episodes as well as other types of arrhythmia [Petrénas et al. \(2015\)](#). The proposed method was therefore finally applied to the whole ECG recording instead of being applied to sliding windows.

7.2.1.2 Deep Learning Model

A deep-learning (DL) approach, combining convolutional and recurrent networks, was trained on the 2017 PhysioNet/Cinc challenge dataset and obtained a score of 0.85 during cross-fold validation using the same training set. This work was done by a MSc student, Nora Vogt, during her thesis under my co-supervision ([Vogt, 2019](#)).

The network architecture consisted in a standard convolutional neural network (CNN), with 15 layers of a block with Batch Normalisation, a convolution layer, a ReLu activation layer and average pooling. The CNN was followed by a Long Short-Term Memory (LSTM) network with 64 hidden units. This network contained about 3.7 million parameters to be optimised.

Some of the novelty of her work consisted in the use of a two-stage procedure for the training of the overall network. In a first step, the CNN was trained by replacing the LSTM with Global Max Pooling. This enabled the CNN to learn a good representation of the ECG signal. The second step consisted in training the LSTM layer, while also fine tuning the CNN (by adjusting the learning

rate).

7.2.1.3 Hybrid model

The use of hybrid models, that is combining a DL model with hand-crafted features and the aggregation of multiple entries was shown to be able to increase the classification performance for the 2017 PhysioNet/Computing in Cardiology challenge [Clifford et al. \(2017\)](#).

The DL model was therefore combined with the SVM-based approach, with an ensemble (or voting) approach. Unanimous voting is needed to identify a subject with AF, and the method will later be denoted as “hybrid”. This approach is equivalent to the combination of a high sensitivity screening tool with a second technique with a high Positive Predictive Value (PPV) for discarding most of the false detections.

7.2.2 Data and annotations

7.2.2.1 Data

The aim of the study is to evaluate the possibility to automatically identify AF patients on a large population. The method was evaluated on a large database, namely the UK Biobank for which 77,202 ECG signals were available acquired from 75,778 individual subjects ([Sudlow et al., 2015](#)).

Manual annotations were not available, and given the size of the database it was not possible to ask expert cardiologists to annotate all recordings. A subset of the UK Biobank data was first selected for manual annotations by three experts. Automated AF detection algorithms were then trained on the 2017 PhysioNet/CinC challenge database and then evaluated on the subset of manually annotated UK Biobank data. The proposed methodology is illustrated in figure 7.2.

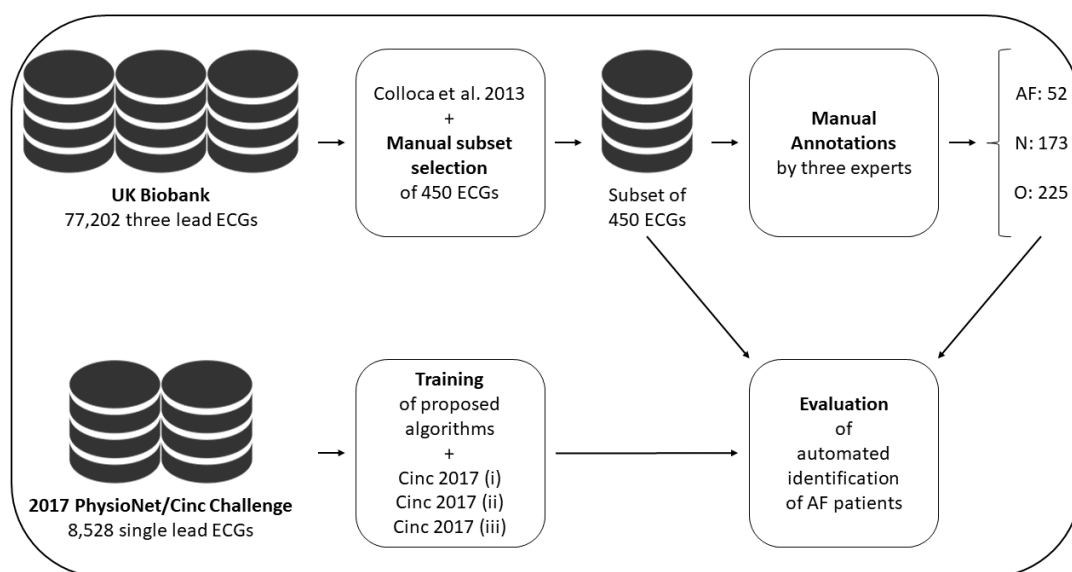


Figure 7.2: Flowchart of the proposed methodology. The top row illustrates the expert annotation process including the manual subset selection, while the bottom row represents the automated identification of AF patients with the evaluation performed on a subset of the UK Biobank database, and the training of the evaluated techniques performed on the 2017 PhysioNet/Cinc challenge database.

7.2.2.2 Data

Two expert cardiologists visually analysed and manually annotated a subset of 450 “randomly” ECG recordings. Finally, a third expert was invited to adjudicate whenever there was a discrepancy

between the AF annotations of the first two experts.

The 450 subjects were then classified in three groups:

1. Atrial Fibrillation, when there is at least one AF episode.
2. Other rhythm, when there is at least one episode of ventricular or atrial ectopics.
3. Normal rhythm in all other cases.

The inter-observer agreement between the first two experts, who acted independently, was evaluated with Cohen’s Kappa coefficient, with special emphasis on the AF annotations (cf. table 7.2). The Cohen’s kappa coefficient for inter-observer agreement on AF was 0.78. On this small subset, experts disagreed for 23 subjects with suspected AF episodes (out of 450). Further analysis showed that the disagreement came from potential AF episodes in short and noisy segments. The adjudication process identified 3 additional subjects with suspected AF.

The final expert annotations in this study classified 52 subjects with AF out of 450 subjects.

	P_{obs2}	N_{obs2}
P_{obs1}	49	8
N_{obs1}	15	378

Table 7.2: Inter-observer agreement on the annotation of AF rhythm, where P_{obsi} (resp. N_{obsi}) stands for positive (resp. negative) subjects as identified by the i^{th} expert

7.2.3 Results

The DL technique outperforms the classical SVM method with hand-crafted features in terms of Sensitivity. Applying the SVM-based classifier on the whole record does significantly decrease the number of false positives, with a PPV of 83.3%, and leads to an increased F1 score (80%) despite a reduction in the sensitivity (77%). As shown by Clifford et al. (2017), combining several techniques increases the overall performance, with the hybrid model reaching an F1 score of 85%.

Method	Se %	PPV %	F1 %
SVM	76.9	83.3	80.0
DL model	96.2	60.2	74.1
hybrid	75.0	97.5	84.8

Table 7.3: AF detection performance on the manually annotated sub-population of 450 subjects.

Cohen’s Kappa coefficient for the hybrid method is 0.83, which is similar to the inter-observer agreement reached by two experts on the same, which demonstrates the usability of the approach in real applications. The confusion matrix for the combined method is given in table 7.4.

	SVM		DL model		hybrid	
	P_{pred}	N_{pred}	P_{pred}	N_{pred}	P_{pred}	N_{pred}
P_{true}	40	12	50	2	39	13
N_{true}	8	390	33	365	1	397

Table 7.4: Confusion tables for three different approaches, where P_{true} (resp. N_{true}) stands for positive (respectively negative) AF subjects as observed by human experts and P_{pred} (respectively N_{pred}) are positive (respectively negative) AF subjects as predicted by automated techniques.

7.3 Synthesis

This chapter presented some of the work done during my time as a postdoctoral research fellow at the University of Oxford. I first demonstrated how the model-based Bayesian filter could be extended in order to work as a ventricular heartbeat classifier. This was made possible through the use of a switching Kalman filter approach, where it was possible to select the ECG dynamical model that most likely generated the measurements. A second important contribution of this period consisted in the development of an hybrid model (hand-crafted + DL) for the detection of AF subjects among a huge database of ECG signals

1. **J. Oster, J. Behar, O. Sayadi, S. Nemati, A.E.W. Johnson, G.D. Clifford**, "Semi-supervised ECG Ventricular Beat Classification with Novelty Detection Based on Switching Kalman Filters," *IEEE Transactions on Biomedical Engineering*, 62(9), 2125-2134 ,2015.
2. **J. Oster, J.C. Hopewell, K. Ziberna, R. Wijesurendra, C.F. Camm, B. Casadei, L. Tarassenko**, "Identification of patients with Atrial Fibrillation, a Big Data exploratory analysis of the UK Biobank," *Physiological Measurement*, 41 (2), 025001, 2021.

Part III
Research Proposal

*You are today where your thoughts have brought you;
you will be tomorrow where your thoughts take you.*
James Allen

The focus of my research is the use of modeling and signal-processing methods to extract novel clinical parameters from large databases of physiological signals, and the use of machine-learning techniques to provide predictive actionable information to clinicians. I have been applying these techniques to electrocardiographic (ECG) (and other physiological) data for more than 10 years.

My research project consists in developing novel machine-learning techniques combined with and/or inspired by modelling in order to create interpretable automatic decision-making systems in healthcare, with a particular focus to cardiovascular health data.

Clinical assessment of the cardiovascular health requires the acquisition of multimodal data, two of the most important modalities being Magnetic Resonance Imaging (MRI) and ECG. I therefore aim at developing tools for the joint analysis of electrophysiological and imaging data. To reach this goal, it is important to develop an efficient representation for both imaging data, and electrophysiological data. These representations will then be used as a starting point for unravelling a joint representation of this multimodal data, therefore representing the physiological phenomenon in a personalised manner.

These techniques and representations of data will offer solutions for concrete clinical problems such as better risk stratification for patients, whether for Atrial Fibrillation catheter ablation outcome prediction, and the risk of presenting Ventricular Tachycardia (VT). This research project aims at finding new ways to fuse the information provided by the MRI and the cardiac physiological information provided by signals such as ECG (or Electrograms –EG–).

This project is divided in three complementary axis focusing on:

1. the analysis of electrophysiological data,
2. the analysis and reconstruction of MR images by accounting for motion, and
3. investigating cutting edge machine learning approaches for bimodal representation of electrophysiological and imaging data.

Chapter 8

Analysis of electrophysiological data

8.1 Electrocardiogram

Deep learning has shown great potential for the automated analysis of ECG signal as demonstrated by cardiologist-level performance for arrhythmia detection [Hannun et al. \(2019\)](#). The development of such approaches requires large amount of data, as no prior knowledge (with the crafting of features performed by experts) is incorporated in the model. The model has therefore to learn from scratch how to represent the the ECG data in such a way to understand the underlying rhythm or pathology. The existence of worldwide competitions, such as the Computing In Cardiology/ PhysioNet challenge, are of tremendous help as they allow for the sharing of big datasets of annotated data. Both the 2017 and 2020 CinC/PhysioNet challenges focused on the classification of heart rhythm from short ECG segments, and these challenges have given researchers around the globe acces to shor ECG segments for more than 50,000 patients. Researchers have therefore been able to develop and test several CNN models for the automatic detection of arrhythmia and other cardiac abnormalities.

Most existing methods apply a deep convolutional classification network with a final global output layer to a fixed-length window of a single ECG and are able to learn a multi-scale latent representation of the electrophysiological signal, as has been suggested by [Hannun et al. \(2019\)](#). We have also started to experiment developing Convolutional Neural Network (CNN)-based approaches [Vogt \(2019\)](#) for the automated classification of rhythm for short ECG signals (either single lead or 12-lead signals). We worked on new models that leverage forms of recurrent neural networks (RNN), allowing us to incorporate temporal information and therefore improve the detection of abnormal rhythm [Clifford et al. \(2017\)](#) (fig. 8.1).

Nevertheless, such abnormal rhythm can be paroxysmal, meaning that short episodes of abnormality can be found in longer recordings. I will be working on attention models ([Zhao et al., 2017](#)) for CNN-based ECG arrhythmia analysis, our method will enable the automatic detection and accurate localisation of arrhythmic events. An interesting avenue of research will consist in inves-

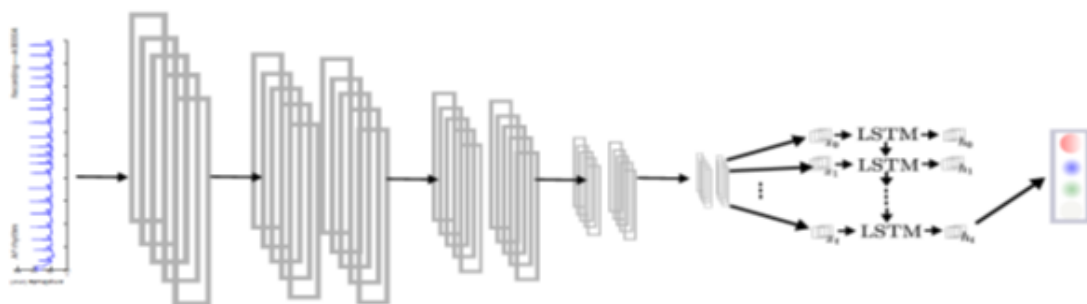


Figure 8.1: Architecture of the CNN-LSTM network developed for ECG rhythm analysis³. The CNN network extracts multilevel morphological features at different time-steps, which are inputted in a LSTM network extracting temporal information, and returns the final rhythm label.

investigating Transformers model [Vaswani et al. \(2017\)](#), which have been recently successfully proposed for ECG signal analysis [Natarajan et al. \(2020\)](#). Contrary to what has been done and studied at the moment, I aim to emphasise on the study of long ECG recordings, especially Holter or wearable devices. A collaboration has already been initiated on this topic, with long-time collaborator (Prof Joachim Behar) at the Technion Institute of Technology (Haifa, Israel). (P. Aublin's PhD thesis will be focused on this topic.)

8.2 Representation Learning

As detailed in the previous section, DL solutions require to be trained on large datasets, which need to be curated, cleaned, and most importantly annotated. There exists currently to my knowledge no large datasets of ECG signals with annotations other than a global label containing presence of arrhythmia or other abnormalities such as myocardial infarction and so on.

However there exists many clinical applications which could benefit hugely from DL approaches in order to automate the ECG analysis or provide help or assistance for the clinical decision. One can for example think of automatically detecting R peaks for heart rate monitoring, ECG delineation for the automated extraction of known biomarkers such as QT intervals for the clinical studies on drug toxicity, or ST level for post myocardium patients or primary Percutaneous Coronary Interventions. Manually validated annotations performed by expert clinicians at the scale required for the training of DL models would be near to impossible to collect given the enormous amount of time needed for such annotation. It is therefore essential to find alternative ways of training DL models for solving the aforementioned clinical problems but with fewer annotations.

I will therefore be investigating the use of self-supervised (or semi-supervised) methods as a pre-training of different models that will be transferred for the analysis of electrophysiological signals.

Representation learning is currently a hot topic in the machine learning community as the availability of large annotated datasets is scarce (especially biomedical data), and even for tasks such as image recognition (for which large annotated datasets are available) the use of self-supervised techniques allows for performance on par with fully-supervised techniques by training on fewer annotated data, but also builds more robust models with better generalisability and less sensitive to transformations. One class of self-supervision techniques consists in contrastive learning, where a set of transformations are applied to the initial data, and positive or negative pairs are clustered together or discriminated using a specific contrastive estimation loss. One of the most popular examples of contrastive learning is SimCLR, which has been introduced for learning visual representation [Chen et al. \(2020\)](#). And contrastive learning has recently also been suggested for electrophysiological signals, namely ECG signals, with the so-called CLOCS technique [Kiyasseh et al. \(2021a\)](#). The elegance of CLOCS relies on benefiting from the multiple views of the same phenomenon offered by multiple leads of the ECG time-series on 12-lead ECG databases. The representation learnt using CLOCS is therefore independent from the recorded lead, which offers robustness for mHealth single lead applications for which lead positioning can be faulty, or MRI acquisitions with the use of nonstandard leads positioning.

Another exciting self-supervised technique is BYOL, which is an iterative training of two models; one for the update of targets used for the training of an enhanced representation, and which was shown to be outperforming SimCLR for visual representation and does not require negative examples [Grill et al. \(2020\)](#). A final interesting avenue of research consists in leveraging the availability of large sets of weakly annotated physiological data in order to develop a deep learning model for multiple tasks, such as rhythm classification for ECG signals, sleep staging for EEG, and so on. The main aim of this multi-task pretraining is to uncover a latent representation of these electrophysiological time-series which will be transferable to signals acquired in an MRI environment. Such approaches have already been suggested for ECG signals [Sarkar and Etemad \(2020\)](#), and more interestingly an extension of the CLOCS techniques has also been suggested for clustering and attribute retrieval, and allowed to further benefit from the usual availability of weak

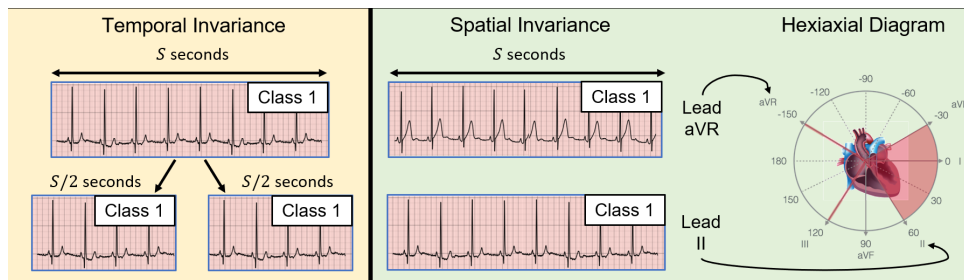


Figure 8.2: Illustration of the temporal and spatial invariance properties of the ECG signals. These properties allow for elegant and realistic data augmentation. Figure provided from Kiyasseh et al. (2021a).

labels or attributes (such as gender, age and some pathology classes) Kiyasseh et al. (2021b).

These techniques will be particularly helpful for the training of models for the analysis of signals and applications for which acquisitions are scarce, this can be either because of the use of a specific sensor (newly developed ECG patches with specific positions and signal quality) or with very limited clinical application (ECG in MRI). A collaboration has been started with Prof Gari Clifford (Emory University, Georgia Tech, Atlanta, USA) to investigate these approaches for the analysis of electrophysiological signals in MRI.

8.3 Interpretability

Machine Learning techniques, more specifically Deep Learning, have been touted as a major breakthrough for healthcare. It is namely envisioned that such techniques will be able to make sense and extract useful information out of the huge trove of medical data routinely acquired by physicians in hospital, in their practice, but also at home with the explosion of medical wearable solutions. This data is currently being under-used, either because clinicians cannot spend enough time to analyse this data or because existing image or signal-based biomarkers are not powerful enough. However, one of the main explanations behind the slow uptake of ML or DL based techniques in medicine lies in the fact that clinicians do not want to blindly rely on automated tools, and want to be provided with explanations along with the diagnosis in diagnostic support systems.

One of the major drawbacks of modern ML and DL lies in the absence or difficulties to interpret how the model is taking his decisions. I will therefore focus on developing new tools in order to better understand how the developed model is making its choice. Several small projects have already started exploring this avenue of research.

A first technique was developed for the interpretability of classical machine learning models, and was applied for the classification of heart rhythm from short single-lead ECG signals Rouhi et al. (2021). In this study, we explored how different global and local explanation techniques can be implemented for classical ML models for both feature selection, and provide an explanation of the decision making process. We showed that SHapley Additive exPlanations (SHAP) values were able to provide a more compact model, and serve as an efficient feature selection technique. But most importantly, SHAP values were also shown to provide additional information to the end-users, cardiologists in our application, with the knowledge of which feature have been the more important in the classification. SHAP values are based on game theory, and are aimed at determining which features are contributing the most in the decision making process.

Examples of SHAP values for four recordings with different rhythms are depicted in figure 8.3. The values depicted in red are the ones contributing the most in favor to the final classification, while the ones in blue are the ones most contradicting the final decision. Example C in figure 8.3 depicts that this recording belongs to the “Other” class because the HR (max_{rr}) is either too high or too low, but that the number of outliers (nb_{out}) is probably too low and seems to be indicating a normal rhythm.

Chapter 8. Analysis of electrophysiological data

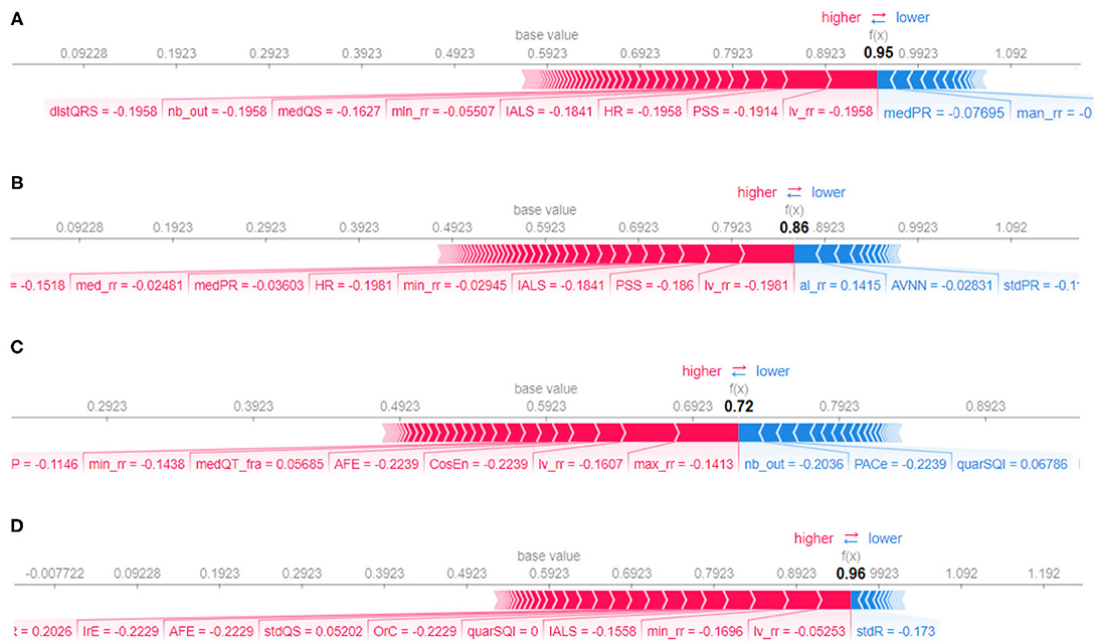


Figure 8.3: Examples of SHAP values, and most important features for the decision on local ECG recordings, with examples from top to bottom of AF, Sinus rhythm, other abnormal rhythm or a noisy recording. On the examples A and B, it can be seen that the features lv_{rr} and PSS are contributing the most to the decision making, while medPR, in the example A, is the one contributing the most negatively (that is by decreasing the most the confidence of the decision). Figure extracted from Rouhi et al. (2021).

Such techniques can be useful for classical ML models, for which features are hand-crafted, and which can therefore more or less easily be explained. However, the same is not true for DL models. The simplicity of DL is that features are learnt directly from the data, which means that those techniques can learn automatically from the data how to represent the input, and which features to extract from images or signals without requiring domain knowledge. The drawback is evidently that given features are data-driven and automatically engineered, it is much harder to interpret them, and understand the properties of the input data being investigated. It is therefore essential to find other ways to provide interpretation for the decision making process.

One of the previously suggested approach is to provide the end-users with the regions in the images or segments in the signals that have influenced the most the DL model. Such techniques have been investigated during Nora Vogt's MSc thesis (Vogt, 2019), they were based on attention mechanism techniques. Preliminary results were interesting, examples of good classification of abnormal rhythms were able to highlight accurately a PVC in the short recording. However, evaluating how accurate and indicative this information is not an easy task. What should we conclude if the attention mechanisms points to f-waves for AF, or a normal QRS for normal rhythm? Quantifying this extra piece of information is a complicated task. One solution would be to ask a team of cardiologists to review the interpretation information, and score the technique as to how much it added confidence to the automated decision making process.

8.4 Electrogram

Finally, I aim at extending DL and modern ML techniques for the analysis of intracardiac electrical signals or Electrograms (EGMs).

The first interesting avenue of research consists in exploring how Physics-Informed Neural Networks (PINN) could be used for the analysis of such signals. PINN have been introduced for the simulation of physical phenomenon such as fluid dynamics. PINNs are neural networks aimed at solving problems subject to Partial Derivative Equations (PDEs). The models are trained to

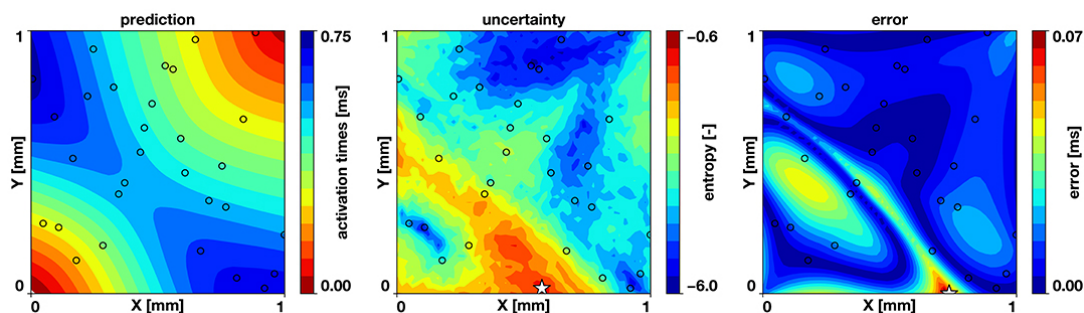


Figure 8.4: Example of the use of active learning scheme for optimal placement of intracardiac measurements. Figure is extracted from *Sahli Costabal et al. (2020)*

find a solution that respect the PDEs, and therefore respecting the laws of Physics, by adding different Loss terms corresponding to the PDEs. One of the interesting aspect of PINN is that they can inherently incorporate measurements performed sparsely and in irregular points. They can therefore account for the fact that EGM measurements are acquired on few datapoints at a precise location, and inherently respect the geometry of the physical phenomenon (in our application, the propagation of electrical activity inside the heart chambers).

PINN have already been suggested for the analysis of EGMs, and combined with active learning in order suggest optimal placement of intracardiac measurements *Sahli Costabal et al. (2020)*.

One of the main problematic of EGM consists in the fact that they represent multi-lead electro-physiological signals, which have been recorded at specific datapoints whose coordinates are highly influential, so is the geometry of the heart. It is therefore important to develop a technique that can reflect that. Conventional Convolutional Neural Networks are not able to deal properly with such information. Another interesting avenue of research would be to use Graphical Convolutional Networks (GCN), which elegantly combines Graph structures for accounting for the heart geometries with CNN for analysing time-series. The use of such GCN have already been suggested for EGMs, and for reconstruction high density Intracardiac maps from sparse measurements *Meister et al. (2020)*.

8.5 Synthesis

The funding for part of the research proposal, presented in this chapter, has been secured through the ERA-CVD Joint Translational Call for cardiovascular research projects driven by Early Career Scientists 2019. This grant is a collaboration between the IADI lab, the University of Luebeck and the Technion. Pierre Aublin is working during his PhD thesis on the development of representation learning approach for the analysis of ECG signals during MRI examination. With our Israeli partner, we are also working on the development and assessment of generalisable techniques.

Another important aspect of the research proposal consists in developing interpretable methods. This avenue of research has been explored during the LUE Mirabelle+ project, during which Dr Rouhi assessed the use of SHAP values for providing explanations on the classifier's decision-making process. Mously Diaw, is also currently exploring other solutions for providing feedback during automated QT estimation. Her PhD is funded through a collaboration with the company Banook through a CIFRE fellowship.

Chapter 9

MRI image analysis and reconstruction integrating the motion

9.1 Cardiac segmentation and heart model extraction

End-to-end deep learning approaches using CNNs have recently been proposed for medical image segmentation (Oktay et al., 2017) (cardiac MRI), but require large amounts of training data and are affected by subtle changes in acquisition protocols. To obtain accurate segmentations generalisable to new patients that are robust against potential motion artefacts and consistent across subjects with respect to the underlying heart anatomy for subsequent motion tracking, current feed-forward CNN networks may be insufficient. We believe that accounting for the motion of the heart will help overcoming current limitations of end-to-end deep learning approaches. Recent work in cine-MR modelling demonstrated promising early results for clustering cardiac motion for dense fields (Krebs et al., 2018), these dense fields could be used for simulation of pathological images of the heart and such approach has been shown to be a very promising data augmentation procedure (Acero et al., 2019).

Krebs et al. (2021) proposed an interesting generative model for the analysis of Cardiac MRI Cine images. In their approach, morphological information is encoded in low dimension latent space using a CNN. Those latent features are then fed into a motion model, which is a combination of a Temporal Convolutional Network, and a multivariate Gaussian Process priors (cf figure 9.1).

The use of such motion model-based representation can also be employed in order to automatically estimate some physiological parameters, such as T1 map or perfusion parameters. Current approaches require the use of registration tools, which could be suppressed by incorporating the motion modelling in an automated end-to-end solution.

Another interesting avenue of research consists in estimating patterns of cardiac motion using the newly arising concepts of learning graph convolutions (Bronstein et al., 2017) together with advanced machine learning regression strategies (e.g. heatmap regression (Hansen et al., 2019)). A preliminary concept to combine graph convolutions with correspondence regression was proposed by Ha et al. (2019). Graph convolutions have the potential to achieve potentially very high robustness and accuracy and will capture shared characteristics, as well as differences of abnormal cardiac motion. A low dimensional non-linear motion and deformation model will be obtained by designing a shape modelling based on deformable convolutions (Heinrich et al., 2019), in both encoder and decoder part of a deep learning architecture.

A collaboration has been initiated on this thematic with Prof. Heinrich at the University of Luebeck, and funding has been obtained through a Joint Transnational Call of the ERA-CVD in 2019. (Nora Vogt has been recruited to work on these aspects.)

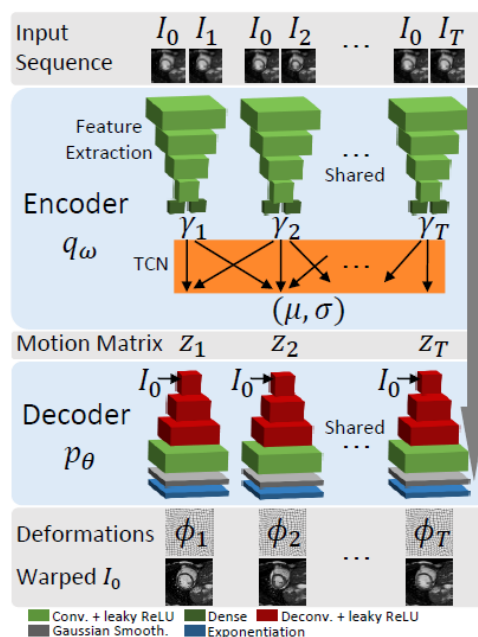


Figure 9.1: Example of the use of a motion (deformation) model for the simulation of clinical data. Two cases are shown where a pathological deformation is applied on a healthy original heart image, allowing for the simulation of four pathological cases. (figure reproduced from Krebs et al. (2021)).

9.2 Cardiac image reconstruction pipelines

I will also be exploring the possibility of incorporating these deformable models in an end-to-end deep learning reconstruction pipeline Zhu et al. (2018b) in order to develop a new strategy for a 3D free-breathing acquisition of the heart

The use of data-driven models to improve MRI image reconstruction schemes with deep learning has become popular within the research community (Schlemper et al., 2017). A DL-based reconstruction pipeline relies either on the convolutional networks to learn the regularization term more effectively (Hammernik et al., 2018) or to model the iterative optimization block within a reconstruction pipeline (Aggarwal et al., 2018). With an increased openness to sharing data and the organization of challenges, a number of larger scale datasets for static 3D MRI reconstruction have been made available, e.g. (Zbontar et al., 2018). However, the currently available datasets are restricted to static images and hence the developed DL algorithms and models do not yet fully account for motion. There are a few exceptions such as the use of (4D) spatio-temporal convolutional networks for the reconstruction of cardiac CINE images (Küstner et al., 2020), or the use of respiration binning technique for free-breathing motion-resolved cardiac MRI based on DL (Qi et al., 2020). However, to our knowledge there exists so far no technique that aims at reconstructing free-breathing cardiac MRI based on DL by integrating a motion model.

DL-based reconstruction schemes rely on the ability of DL to find a nonlinear embedded representation of the images in order to regularize the reconstructed data so it belongs to this compact space. One of the most important aspects of this project will be to develop new techniques for the representation of both the morphological images but also a model of motion using DL-based image and shape analysis approaches (Blendowski et al., 2020, Krebs et al., 2021, Lucas et al., 2018) as described in the previous section. For the technical challenge of reliably estimating motion from limited data (e.g. accelerated k-space acquisition in cardiac MRI), new geometric learning concepts are necessary to advance the ability of AI models beyond conventional CNNs. The use of external motion sensors could be linked to or incorporated as priors on the Gaussian process or motion model, whereas image regularisation will be based on the morphological encoding (cf. figure9.2).

Moreover, the transfer of DL-based reconstruction techniques into clinical practice will only be

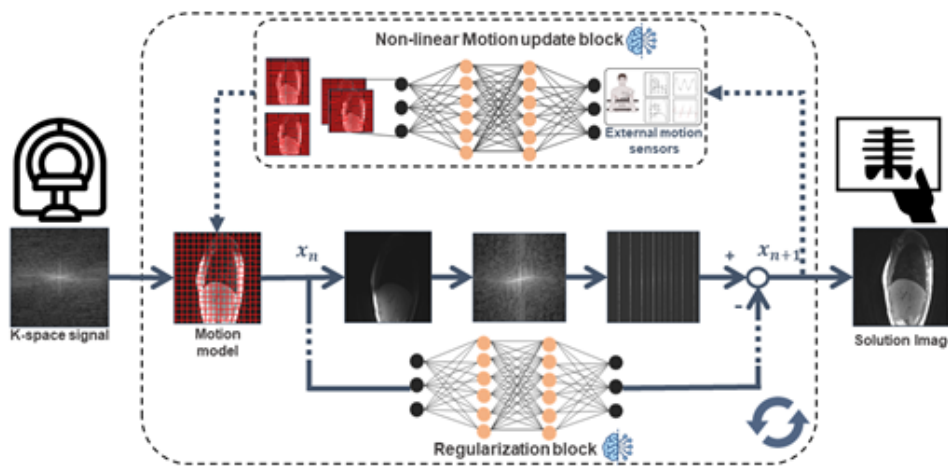


Figure 9.2: Flowchart of the reconstruction pipeline combining a motion model with external physiological sensor, and an integrated DL-based MRI reconstruction regularisation.

possible if radiologists trust that the reconstructed images are reliable, and that the DL regularization scheme does not introduce additional artefacts or is biased towards healthy tissues, and suppressed real pathological features. An interesting avenue of research consists in quantifying the uncertainty of reconstructed images (Edupuganti et al., 2020), providing the radiologists an uncertainty (or confidence) map along with the reconstructed image will help gaining their trust and increase their confidence during the diagnosis process.

Funding for this research project has been obtained, in collaboration with Prof Heinrich (University of Luebeck), through the first joint German-French Call on Artificial Intelligence. (L. Quillien's PhD thesis will be focused on this topic.)

9.3 Autonomous cardiac MRI acquisition

The two previous sections presented how Machine learning will be explored for the analysis of already acquired images or MR raw data, and motion models could be incorporated in ML pipelines especially for cardiac applications. However, one of the most exciting avenue of research consists in investigating how ML could optimise the acquisition of MR data.

When faced with respiratory and cardiac motion, "static" (non-adaptive) acquisition schemes are surely non-optimal and even the best post-processing or MRI reconstruction techniques will face difficulties dealing with out-of-plane motion and low contrast or signal to noise ratios.

Two interesting aspects have already been suggested, (i) use of active learning or reinforcement learning for optimal sampling strategy (ii) the use of supervised or reinforced learning for automated pulse sequence generation.

(i) In order to accelerate the acquisition of MRI data, several techniques have suggested partial sampling of the k-space combined with advanced reconstruction techniques parallel imaging or compressed sensing (Fessler, 2019). Different strategies were suggested for the undersampling of the k-space, acquisition of a subset of lines, radial or propeller (for accessing motion information), higher sampling of central k-space lines, or random sampling for compressed sensing-based techniques. Each of these sampling strategies were associated with specific reconstruction noise, and/or aimed at providing navigator or motion information. More recently, the use of active learning or reinforcement learning has been suggested for automatically determining the most informative sampling strategy in conjunction of specific MRI reconstruction (Jin et al., 2019, Pineda et al., 2020). I believe such approaches could be interesting, especially if associated with a motion model linked to external sensors, which could allow for optimal sampling strategy and prospective motion correction (Maclaren et al., 2013).

(ii) One could even envision going one step further and building a ML system able to automat-

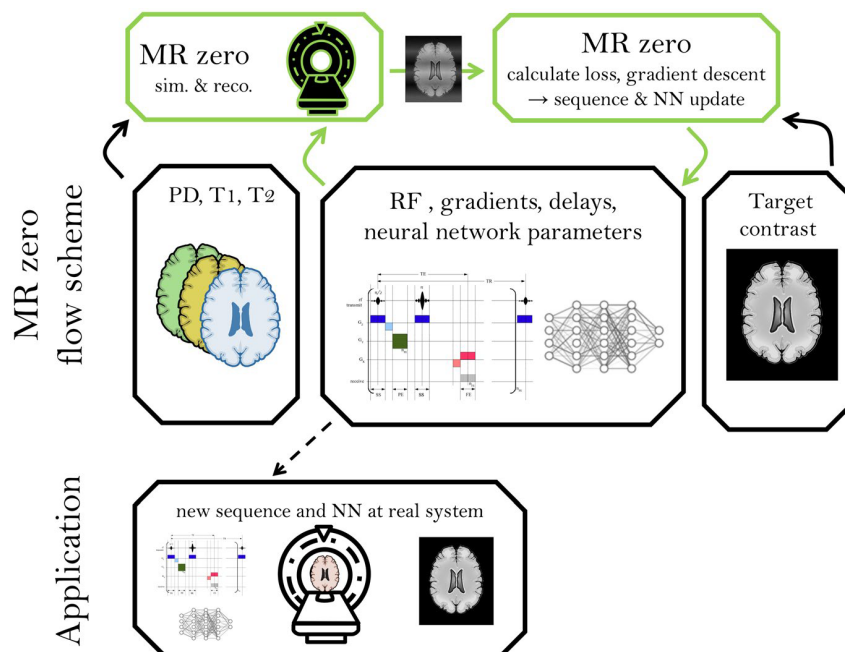


Figure 9.3: Flowchart of the technique for autonomous pipeline of MR acquisition and reconstruction. Figure reproduced from (Loktyushin et al., 2021).

ically select or optimise the multiple pulse sequence parameters required for the acquisition of MR raw data. Such techniques have already been suggested, first by applying Bayesian reinforcement learning in a MRI physics simulation environment (Zhu et al., 2018a), and more recently using a supervised approach (which is less computationally costly than reinforcement learning) also trained on a simulated environment (Loktyushin et al., 2021). The development of such techniques require huge amount of training data, and the possibility of interacting with the acquisition and reconstruction process, which explains the necessity to work on a simulated environment (strategy which has shown its huge potential with several DeepMind solutions). It would be extremely interesting to develop such a simulated environment integrating respiratory and cardiac motion, in order to develop an optimal acquisition and reconstruction strategy for fast whole-heart imaging. Such studies might pave the way towards a fully autonomous acquisition of cardiac MRI data, and provide the radiologists with robust and accurate physiological parameter estimation for better diagnoses.

9.4 Synthesis

A collaboration with Prof Mattias Heinrich at the University of Luebeck has been kick-started since 2016. This collaboration started with the exchange of Master students, and this collaboration led to securing two major grants:

1. MEIDIC-VTACH, through the 2019 ERA-CVD JTC call. The project aims at developing novel strategy for the acquisition of cardiac MRI for irregular heart rhythm. Prof Heinrich's team is looking to develop 3D+t heart models from MRI data, while Nora Vogt is currently looking to develop super-resolution techniques combined with real-time cardiac techniques for the acquisition of high resolution cardiac images during irregular heart rhythm
2. MEDICARE, through a joint French-German call for IA. Lucile Quillien will be working during her PhD thesis to develop a novel MRI reconstruction technique combining physiological information with MRI raw data with DL techniques.

Chapter 10

Multimodal Deep Learning

10.1 Smart fusion of the multimodal information

The final research axis will consist in the smart fusion of the information provided by medical images (MRI, echocardiography, CT,...) and the electrophysiological signals.

In a first step, I will explore how to build on the developments of previous research axes for fusing images and electrophysiological information. This data-driven solution will aim at solving concrete clinical problems, with personalised models integrating electrical, morphological or mechanistic information provided by the different modalities.

Some of the foreseen applications include better risk stratification or prediction for patients at risk of VT [Goldberger et al. \(2014\)](#), or the risk prediction of AF or recurrence of Stroke, or for the prediction of AF catheter ablation outcome.

Such ML-based models have already been suggested, but are usually based on a single modality. Several studies have demonstrated the potential of deep learning analysis of 12-lead ECG signals. The analysis of these signals have shown potential to determine the risk of presenting AF in the future (with a 3 or 5 years follow-up). [Attia et al. \(2019b\)](#) have used a fully DL model for the prediction of AF, while [Biton et al. \(2021\)](#) suggested of an hybrid model combining both hand-crafted features, clinical features and a DL model. The added value for the prediction of EMR for this task has been inspired from studies like the CHARGE-AF ([Alonso et al., 2013](#)).

Other studies have shown the predictive value of imaging biomarkers for such applications. Morphology of the atria extracted from CT images was shown to be an independent predictor of the recurrence of AF after catheter ablation ([Jia et al., 2021](#)). Geometrical properties of ischemic scars extracted from cardiac MRI data was shown to be predictive of the risk of VT in post-ischemic population, with higher predictive value than Left Ventricle Ejection Fraction (LVEF) ([de Chillou et al., 2021](#)). [Krebs et al. \(2021\)](#) demonstrated that the motion model extracted from Cardiac Cine Images (already discussed in 9.1) could also be used a survival predictor for Heart Failure patients (that is patients with low LVEF), highlighting the potential of mechanistic information for patient risk stratification (cf. figure 10.1).

Another interesting study successfully attempted at linking functional information, namely the LVEF, usually extracted from imaging modalities (echocardiography or MRI) by training a DL model with standard 12-lead ECG signals as inputs ([Attia et al., 2019a](#)). I will aim at replicating such results, and try to find a joint representation of motion models extracted from Echocardiography and ECG signals. The previously mentioned motion model has already been evaluated on a large Echocardiography dataset ([Krebs, 2020](#), [Ouyang et al., 2020](#)). One could envision training a joint model using approaches such as a deep canonical correlation analysis. Such a technique would allow to screen patients requiring further imaging exams (Echo or MRI) based on a simple 12-lead ECG signals. A collaboration with Banook Group (Nancy, France) has been initiated to work on such an application. (M. Diaw's PhD thesis will be focused on this topic.)

Combining models developed in previous research axes, should allow to uncover a compact representation of a patient data, which reflects electrical, morphological, functional and mechanistic

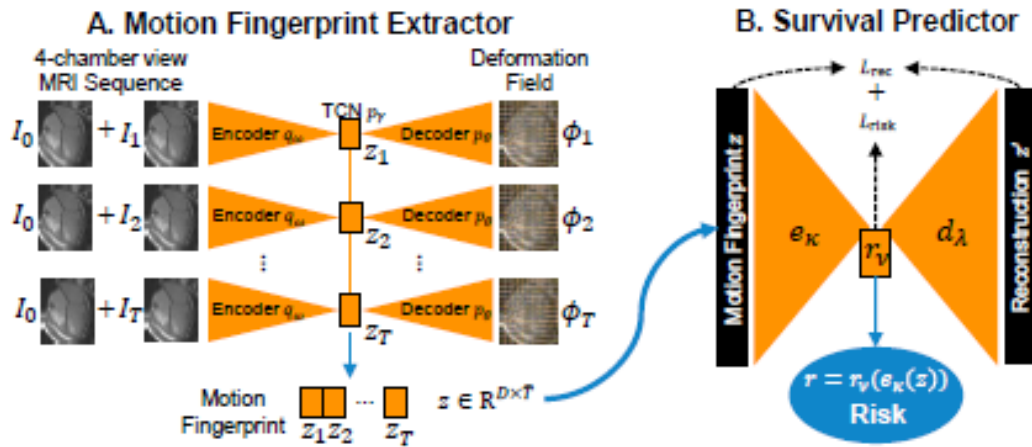


Figure 10.1: Flowchart of the use of motion model features (so-called motion fingerprints) for the prediction of survival. Figure reproduced from (Krebs, 2020).

properties of his/her heart, which can be compared to a purely data-driven digital twin. This compact representation should allow for a true precision medicine, with a fine phenotyping of the at-risk population.

10.2 ECG Imaging

The ability to visualise the electrical cardiac activity in a non-invasive way is of great importance, in order to enable a better characterisation of the heart electrical activity and yield an accurate risk stratification of abnormal and life-threatening rhythms (VT, AF).

Electrocardiographic imaging or electro-imaging (ECGI) enables the non-invasive visualisation of the cardiac electrophysiology (Ramanathan et al., 2004), by measuring a large number of Electrocardiogram (ECG) leads on the body surface, covering the whole torso, and subsequently estimating epicardial potentials. Applications of ECGI include amongst other: the localization of Premature Ventricular Contractions (PVCs), better risk stratification of VT, characterization of atrial fibrillation (Cluitmans et al., 2015), which led to an increased commercial interest and first FDA approved devices (CardioInsight, Medtronic). To date, catheter ablation procedures require invasive placement of electrodes at multiple locations across the atrias and/or ventricles, which are a great burden for both patients and physicians. ECGI can reduce the procedure time by accurately characterising the arrhythmogenic substrate to be targeted, therefore minimising the number of acquisitions of invasive electrograms.

I will aim at developing a fully data-driven fusion of electrophysiological and images for the resolution of the inverse problems in ECGI applications. Current ECGI approaches rely on the modelling of the propagation of the electrical activity, either modelling the electrical sources as dipoles in the heart (using the equivalent dipole layer source model) or modelling biopotential on the surface of the endocardium Cluitmans et al. (2015). Such approaches have proved to be useful for some specific applications (planning of cardiac resynchronisation therapy), but do not seem to be accurately depicting more complex pathologies Duchateau et al. (2019), and therefore require further methodological developments.

Some techniques have recently been proposed for a DL-based ECGI formulation. One of the main difficulties stems from the integration of the heart and torso geometries to solve the inverse problems. Some of the interesting solutions include to transform both the torso and the heart geometries to a plane with a mapping conversion, which makes it more suitable for convolutional neural networks (Wang et al., 2021). Another approach suggested the use of Conditional Variational AUtoEncoder (CVAE), which allowed the integration of volumic imaging data (including substrate (ischemic scar) characterisation) (Bacoyannis et al., 2021). Early results obtained on a

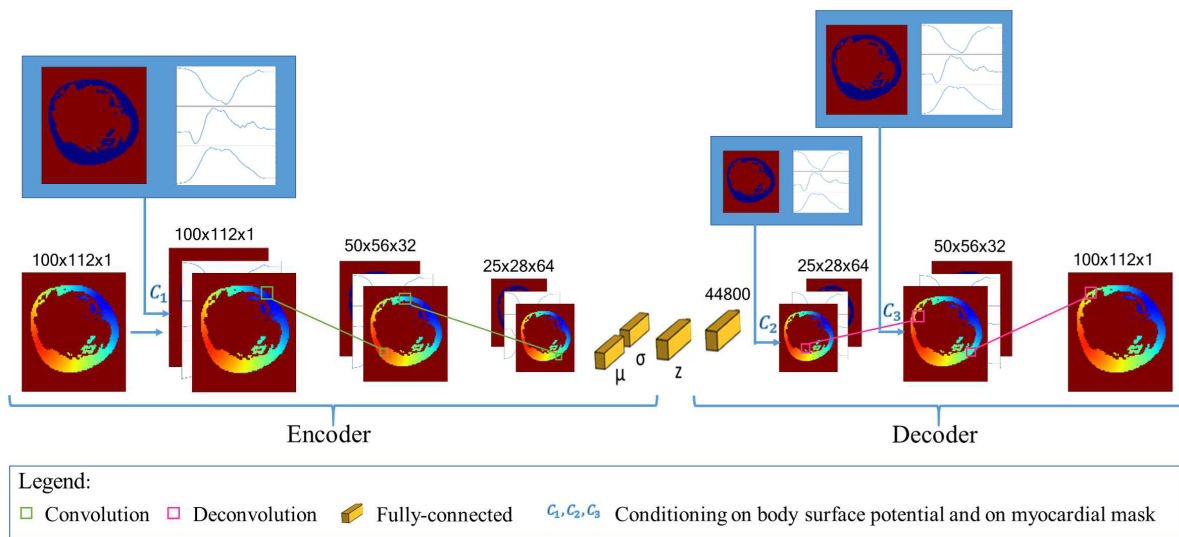


Figure 10.2: Flowchart of the ECGL technique based on CVAE for the fusion of 3D volumes of myocardial images with Body Surface Potentials. Figure reproduced from (Bacoyannis et al., 2019).

limited number of simulations are promising but need confirmation on real data.

I will be investigating the use of PINNs (already introduced in 8.4) for the resolution of this inverse problem. Such an approach will deal elegantly with personalised heart and torso geometries, while also incorporating imaging priors. This technique is currently being investigated by one of my PhD student, Benjamin Roussel, for the analysis of Electrical fields by MRI gradient coils for the estimation of tissue electrical properties.

Another strategy will consist in the use of Graph Convolutional Networks, again as suggested for the analysis of Electrograms 8.4.

10.3 Synthesis

Some early aspects of this research proposal are currently being undertaken by some PhD students currently under my supervision.

1. Mously Diaw is exploring how the analysis of ECG signals could allow the detection of pathological ventricular contraction, especially biomarkers usually extracted for an Echocardiographic examination. This work will be the first in uncover an ECG representation “correlated” with the heart motion, next steps would consist in multimodal analysis of either ECG and Echo or ECG and MRI images.
2. Benjamin Roussel recently proposed the use of PINNs for solving the inverse problem of Current Induced MR Electrical Impedance Tomography. The elegance of the proposed solutions consists in combining different contributions in loss: (i) Maxwell laws (ii) torso electrical measurements (iii) prior MRI-based images (pre-segmentation). The solution of the PINNs therefore respects Maxwell laws (hence the Physics Inspired acronym) but more importantly is an multimodal analysis of electrical measurements and MRI images.

Bibliography

- J. C. Acero, E. Zacur, H. Xu, R. Ariga, A. Bueno-Orovio, P. Lamata, and V. Grau. Smoldata augmentation based on statistical models of deformation to enhance segmentation in 2d cine cardiac mri. In *International Conference on Functional Imaging and Modeling of the Heart*, pages 361–369. Springer, 2019.
- H. K. Aggarwal, M. P. Mani, and M. Jacob. Modl: Model-based deep learning architecture for inverse problems. *IEEE transactions on medical imaging*, 38(2):394–405, 2018.
- A. Alonso, B. P. Krijthe, T. Aspelund, K. A. Stepas, M. J. Pencina, C. B. Moser, M. F. Sinner, N. Sotoodehnia, J. D. Fontes, A. C. J. Janssens, et al. Simple risk model predicts incidence of atrial fibrillation in a racially and geographically diverse population: the charge-af consortium. *Journal of the American Heart Association*, 2(2):e000102, 2013.
- F. Andreotti, J. Behar, S. Zaunseder, J. Oster, and G. D. Clifford. An open-source framework for stress-testing non-invasive foetal ecg extraction algorithms. *Physiological measurement*, 37: 627–648, May 2016. ISSN 1361-6579. doi: 10.1088/0967-3334/37/5/627.
- ANSI/AAMI:EC57. Testing and reporting performance results of cardiac rhythm and ST-segment measurement algorithms, 2012.
- M. S. Arulampalam, S. Maskell, N. Gordon, and T. Clapp. A tutorial on particle filters for online nonlinear/non-gaussian bayesian tracking. *Signal Processing, IEEE Transactions on*, 50(2):174–188, 2002.
- Z. I. Attia, S. Kapa, F. Lopez-Jimenez, P. M. McKie, D. J. Ladewig, G. Satam, P. A. Pellikka, M. Enriquez-Sarano, P. A. Noseworthy, T. M. Munger, et al. Screening for cardiac contractile dysfunction using an artificial intelligence-enabled electrocardiogram. *Nature medicine*, 25(1): 70–74, 2019a.
- Z. I. Attia, P. A. Noseworthy, F. Lopez-Jimenez, S. J. Asirvatham, A. J. Deshmukh, B. J. Gersh, R. E. Carter, X. Yao, A. A. Rabinstein, B. J. Erickson, et al. An artificial intelligence-enabled ecg algorithm for the identification of patients with atrial fibrillation during sinus rhythm: a retrospective analysis of outcome prediction. *The Lancet*, 394(10201):861–867, 2019b.
- T. Bacoyannis, J. Krebs, N. Cedilnik, H. Cochet, and M. Sermesant. Deep learning formulation of ecgi for data-driven integration of spatiotemporal correlations and imaging information. In *International Conference on Functional Imaging and Modeling of the Heart*, pages 20–28. Springer, 2019.
- T. Bacoyannis, B. Ly, N. Cedilnik, H. Cochet, and M. Sermesant. Deep learning formulation of electrocardiographic imaging integrating image and signal information with data-driven regularization. *EP Europace*, 23(Supplement_1):i55–i62, 2021.
- J. Behar, F. Andreotti, J. Oster, and G. D. Clifford. A bayesian filtering framework for accurate extracting of the non-invasive fecg morphology. In *Computing in Cardiology Conference (CinC), 2014*, pages 53–56. IEEE, 2014a.

BIBLIOGRAPHY

- J. Behar, F. Andreotti, S. Zaunseder, Q. Li, J. Oster, and G. D. Clifford. An ecg simulator for generating maternal-foetal activity mixtures on abdominal ecg recordings. *Physiological measurement*, 35:1537–1550, Aug. 2014b. ISSN 1361-6579. doi: 10.1088/0967-3334/35/8/1537.
- J. Behar, F. Andreotti, S. Zaunseder, J. Oster, and G. D. Clifford. A practical guide to non-invasive foetal electrocardiogram extraction and analysis. *Physiological measurement*, 37:R1–R35, May 2016. ISSN 1361-6579. doi: 10.1088/0967-3334/37/5/R1.
- S. Biton, S. Gendelman, A. H. Ribeiro, G. Miana, C. Moreira, A. L. P. Ribeiro, and J. A. Behar. Atrial fibrillation risk prediction from the 12-lead electrocardiogram using digital biomarkers and deep representation learning. *European Heart Journal-Digital Health*, 2021.
- M. Blendowski, N. Bouteldja, and M. P. Heinrich. Multimodal 3d medical image registration guided by shape encoder–decoder networks. *International journal of computer assisted radiology and surgery*, 15(2):269–276, 2020.
- M. M. Bronstein, J. Bruna, Y. LeCun, A. Szlam, and P. Vandergheynst. Geometric deep learning: going beyond euclidean data. *IEEE Signal Processing Magazine*, 34(4):18–42, 2017.
- T. Chen, S. Kornblith, M. Norouzi, and G. Hinton. A simple framework for contrastive learning of visual representations. In *International conference on machine learning*, pages 1597–1607. PMLR, 2020.
- G. Clifford. A novel framework for signal representation and source separation: Applications to filtering and segmentation of biosignals. *Journal of Biological Systems*, 14(2):169–184, 2006.
- G. Clifford, A. Shoeb, P. McSharry, and B. Janz. Model-based filtering, compression and classification of the ecg. *International Journal of Bioelectromagnetism*, 7(1):158–161, 2005.
- G. D. Clifford, S. Nematy, and R. Sameni. An artificial vector model for generating abnormal electrocardiographic rhythms. *Physiological measurement*, 31:595–609, May 2010. ISSN 1361-6579. doi: 10.1088/0967-3334/31/5/001.
- G. D. Clifford, I. Silva, J. Behar, and G. B. Moody. Non-invasive fetal ecg analysis. *Physiological measurement*, 35:1521–1536, Aug. 2014. ISSN 1361-6579. doi: 10.1088/0967-3334/35/8/1521.
- G. D. Clifford, C. Liu, B. Moody, H. L. Li-wei, I. Silva, Q. Li, A. Johnson, and R. G. Mark. Af classification from a short single lead ecg recording: the physionet/computing in cardiology challenge 2017. In *2017 Computing in Cardiology (CinC)*, pages 1–4. IEEE, 2017.
- M. J. M. Cluitmans, R. Peeters, R. Westra, and P. Volders. Noninvasive reconstruction of cardiac electrical activity: update on current methods, applications and challenges. *Netherlands Heart Journal*, 23(6):301–311, 2015.
- R. Colloca, A. E. Johnson, L. Mainardi, and G. D. Clifford. A Support Vector Machine approach for reliable detection of atrial fibrillation events. In *Computing in Cardiology Conference (CinC), 2013*, pages 1047–1050. IEEE, 2013.
- V. D. Corino, F. Sandberg, L. T. Mainardi, and L. Sörnmo. An atrioventricular node model for analysis of the ventricular response during atrial fibrillation. *IEEE Transactions on Biomedical Engineering*, 58(12):3386–3395, 2011.
- V. D. Corino, F. Sandberg, F. Lombardi, L. T. Mainardi, and L. Sörnmo. Atrioventricular nodal function during atrial fibrillation: Model building and robust estimation. *Biomedical Signal Processing and Control*, 8(6):1017–1025, 2013.

- M. Cremer. Über die direkte ableitung der aktionströme des menschlichen herzens vom oesophagus und über das elektrokardiogramm des fotes. *MMW*, 53:190, 1906.
- P. de Chazal, M. O'Dwyer, and R. B. Reilly. Automatic Classification of Heartbeats using ECG Morphology and Heartbeat Interval Features. *Biomedical Engineering, IEEE Transactions on*, 51(7):1196–1206, 2004.
- C. de Chillou, D. Voilliot, S. Amraoui, J. Duchateau, E. Marijon, E. Gandjbakhch, P. Maury, J.-M. Sellal, G. Hossu, H. Cochet, P.-Y. Marie, D. Mandry, E. Mousseaux, A. Redheuil, A. Rollin, O. Lairez, V. Waldmann, G. Soulat, X. Waintraub, M. Pauriah, F. Zannad, N. Girerd, I. Magnin-Poull, M. Beaumont, P. Jaïs, F. Sacher, M. Hocini, P. Bordachar, H. Blangy, N. Sadoul, J. Felblinger, M. Haïssaguerre, and F. Odille. Magnetic resonance imaging screening for postinfarct life-threatening ventricular arrhythmia. *Cardiovascular Imaging*, 2021.
- A. Doucet, N. de Freitas, and N. Gordon. *Sequential Monte Carlo methods in practice*. Springer Science & Business Media, 2001.
- J. Duchateau, F. Sacher, T. Pambrun, N. Derval, J. Chamorro-Servent, A. Denis, S. Ploux, M. Hocini, P. Jaïs, O. Bernus, et al. Performance and limitations of noninvasive cardiac activation mapping. *Heart Rhythm*, 16(3):435–442, 2019.
- V. Edupuganti, M. Mardani, S. Vasanawala, and J. Pauly. Uncertainty quantification in deep mri reconstruction. *IEEE Transactions on Medical Imaging*, 40(1):239–250, 2020.
- W. Einthoven. The different forms of the human electrocardiogram and their signification. *The Lancet*, 179(4622):853–861, 1912.
- J. Felblinger, J. Slotboom, R. Kreis, B. Jung, C. Boesch, et al. Restoration of electrophysiological signals distorted by inductive effects of magnetic field gradients during mr sequences. *Magn Res Med*, 41(4):715–721, 1999.
- J. A. Fessler. Optimization methods for mr image reconstruction (long version). *arXiv preprint arXiv:1903.03510*, 2019.
- A. L. Goldberger, L. A. Amaral, L. Glass, J. M. Hausdorff, P. C. Ivanov, R. G. Mark, J. E. Mietus, G. B. Moody, C.-K. Peng, and H. E. Stanley. Physiobank, physiotoolkit, and physionet components of a new research resource for complex physiologic signals. *Circ J*, 101(23):e215–e220, 2000.
- J. J. Goldberger, A. Basu, R. Boineau, A. E. Buxton, M. E. Cain, J. M. Canty Jr, P.-S. Chen, S. S. Chugh, O. Costantini, D. V. Exner, et al. Risk stratification for sudden cardiac death: a plan for the future. *Circulation*, 129(4):516–526, 2014.
- M. S. Grewal and A. P. Andrews. Applications of kalman filtering in aerospace 1960 to the present [historical perspectives]. *Control Systems, IEEE*, 30(3):69–78, 2010.
- J.-B. Grill, F. Strub, F. Altché, C. Tallec, P. H. Richemond, E. Buchatskaya, C. Doersch, B. A. Pires, Z. D. Guo, M. G. Azar, et al. Bootstrap your own latent: A new approach to self-supervised learning. *arXiv preprint arXiv:2006.07733*, 2020.
- A. Gupta. *Signal processing of an ECG signal in the presence of a strong static magnetic field*. . Phd thesis, University of Central Florida, 2007.
- A. Gupta, A. R. Weeks, and S. M. Richie. Simulation of elevated T-waves of an ECG inside a static magnetic field (MRI). *IEEE T Bio-Med Eng*, 55(7):1890–1896, Jul 2008. doi: 10.1109/TBME.2008.919868. URL <http://www.hubmed.org/display.cgi?uids=18595808>.

BIBLIOGRAPHY

- I. Y. Ha, L. Hansen, M. Wilms, and M. P. Heinrich. Geometric deep learning and heatmap prediction for large deformation registration of abdominal and thoracic ct. In *International Conference on Medical Imaging with Deep Learning—Extended Abstract Track*, 2019.
- K. Hammernik, T. Klatzer, E. Kobler, M. P. Recht, D. K. Sodickson, T. Pock, and F. Knoll. Learning a variational network for reconstruction of accelerated mri data. *Magnetic resonance in medicine*, 79(6):3055–3071, 2018.
- A. Y. Hannun, P. Rajpurkar, M. Haghpanahi, G. H. Tison, C. Bourn, M. P. Turakhia, and A. Y. Ng. Cardiologist-level arrhythmia detection and classification in ambulatory electrocardiograms using a deep neural network. *Nature medicine*, 25(1):65, 2019.
- L. Hansen, J. Diesel, and M. P. Heinrich. Regularized landmark detection with caes for human pose estimation in the operating room. In *Bildverarbeitung für die Medizin 2019*, pages 178–183. Springer, 2019.
- M. P. Heinrich, O. Oktay, and N. Bouteldja. Obelisk-net: Fewer layers to solve 3d multi-organ segmentation with sparse deformable convolutions. *Medical image analysis*, 54:1–9, 2019.
- M. Henriksson, V. D. Corino, L. Sörnmo, and F. Sandberg. A statistical atrioventricular node model accounting for pathway switching during atrial fibrillation. *IEEE Transactions on Biomedical Engineering*, 63(9):1842–1849, 2016.
- A. L. Hodgkin and A. F. Huxley. A quantitative description of membrane current and its application to conduction and excitation in nerve. *The Journal of physiology*, 117:500–544, Aug. 1952. ISSN 0022-3751.
- C. J. James and C. W. Hesse. Independent component analysis for biomedical signals. *Physiological measurement*, 26(1):R15, 2005.
- R. Jané, A. Blasi, J. García, and P. Laguna. Evaluation of an automatic threshold based detector of waveform limits in holter ecg with the qt database. In *Computers in Cardiology 1997*, pages 295–298. IEEE, 1997.
- S. Jia, H. Nivet, J. Harrison, X. Pennec, C. Camaioni, P. Jaïs, H. Cochet, and M. Sermesant. Left atrial shape is independent predictor of arrhythmia recurrence after catheter ablation for atrial fibrillation: A shape statistics study. *Heart Rhythm O2*, 2021.
- K. H. Jin, M. Unser, and K. M. Yi. Self-supervised deep active accelerated mri. *arXiv preprint arXiv:1901.04547*, 2019.
- S. J. Julier and J. K. Uhlmann. Unscented filtering and nonlinear estimation. *Proceedings of the IEEE*, 92(3):401–422, 2004.
- R. E. Kalman. A new approach to linear filtering and prediction problems. *Journal of Fluids Engineering*, 82(1):35–45, 1960.
- J. Keltner, M. Roos, P. Brakeman, and T. Budinger. Magnetohydrodynamics of blood flow. *Magn Res Med*, 16(1):139–149, 1990.
- Y. Kinouchi, H. Yamaguchi, and T. Tenforde. Theoretical analysis of magnetic field interactions with aortic blood flow. *Bioelectromagnetics*, 17(1):21–32, 1996.
- D. Kiyasseh, T. Zhu, and D. A. Clifton. Clocs: Contrastive learning of cardiac signals across space, time, and patients. In *International Conference on Machine Learning*, pages 5606–5615. PMLR, 2021a.

- D. Kiyasseh, T. Zhu, and D. A. Clifton. Crocs: Clustering and retrieval of cardiac signals based on patient disease class, sex, and age. In *Thirty-Fifth Conference on Neural Information Processing Systems*, 2021b.
- J. Krebs. *Le recalage robuste d'images médicales et la modélisation du mouvement basée sur l'apprentissage profond*. PhD thesis, Université Côte d'Azur, 2020.
- J. Krebs, T. Mansi, B. Mailhé, N. Ayache, and H. Delingette. Unsupervised probabilistic deformation modeling for robust diffeomorphic registration. In *Deep Learning in Medical Image Analysis and Multimodal Learning for Clinical Decision Support*, pages 101–109. Springer, 2018.
- J. Krebs, H. Delingette, N. Ayache, and T. Mansi. Learning a generative motion model from image sequences based on a latent motion matrix. *IEEE Transactions on Medical Imaging*, 40(5):1405–1416, 2021.
- T. Küstner, N. Fuin, K. Hammernik, A. Bustin, H. Qi, R. Hajhosseiny, P. G. Masci, R. Neji, D. Rueckert, R. M. Botnar, et al. Cinenet: deep learning-based 3d cardiac cine mri reconstruction with multi-coil complex-valued 4d spatio-temporal convolutions. *Scientific reports*, 10(1):1–13, 2020.
- A. Kyriakou, E. Neufeld, D. Szczerba, W. Kainz, R. Luechinger, S. Kozerke, R. McGregor, and N. Kuster. Patient-specific simulations and measurements of the magneto-hemodynamic effect in human primary vessels. *Physiol Meas*, 33(2):117–130, 2012.
- D. E. Lake and J. R. Moorman. Accurate estimation of entropy in very short physiological time series: the problem of atrial fibrillation detection in implanted ventricular devices. *American Journal of Physiology-Heart and Circulatory Physiology*, 300(1):H319–H325, 2011.
- I. Lakhno, J. A. Behar, J. Oster, V. Shulgin, O. Ostras, and F. Andreotti. The use of non-invasive fetal electrocardiography in diagnosing second-degree fetal atrioventricular block. *Maternal health, neonatology and perinatology*, 3:14, 2017. ISSN 2054-958X. doi: 10.1186/s40748-017-0053-1.
- M. Llamedo and J. P. Martínez. Heartbeat Classification using Feature Selection driven by Database generalization criteria. *Biomedical Engineering, IEEE Transactions on*, 58(3):616–625, 2011.
- M. Llamedo and J. P. Martínez. An automatic patient-adapted ecg heartbeat classifier allowing expert assistance. *Biomedical Engineering, IEEE Transactions on*, 59(8):2312–2320, 2012.
- A. Loktyushin, K. Herz, N. Dang, F. Glang, A. Deshmane, S. Weinmüller, A. Doerfler, B. Schölkopf, K. Scheffler, and M. Zaiss. Mrzero-automated discovery of mri sequences using supervised learning. *Magnetic Resonance in Medicine*, 86(2):709–724, 2021.
- C. Lucas, A. Kemmling, N. Bouteldja, L. F. Aulmann, A. Madany Mamlouk, and M. P. Heinrich. Learning to predict ischemic stroke growth on acute ct perfusion data by interpolating low-dimensional shape representations. *Frontiers in neurology*, 9:989, 2018.
- J. Maclaren, M. Herbst, O. Speck, and M. Zaitsev. Prospective motion correction in brain imaging: a review. *Magnetic resonance in medicine*, 69(3):621–636, 2013.
- M. Markl, M. Draney, D. Miller, J. Levin, E. Williamson, N. Pelc, D. Liang, and R. Herfkens. Time-resolved three-dimensional magnetic resonance velocity mapping of aortic flow in healthy volunteers and patients after valve-sparing aortic root replacement. *The Journal of Thoracic and Cardiovascular Surgery*, 130(2):456–463, 2005.
- V. Martin, A. Drochon, O. Fokapu, and J.-F. Gerbeau. Magneto-hemodynamics in the aorta and electrocardiograms. *Phys Med Biol*, 57(10):3177–3195, 2012. URL <http://stacks.iop.org/0031-9155/57/i=10/a=3177>.

BIBLIOGRAPHY

- P. McSharry, G. D. Clifford, L. Tarassenko, and L. A. Smith. A Dynamical Model for Generating Synthetic Electrocardiogram Signals. *IEEE T Bio-Med Eng*, 50(3):289–294, 2003.
- F. Meister, T. Passerini, C. Audigier, È. Lluch, V. Mihalef, H. Ashikaga, A. Maier, H. Halperin, and T. Mansi. Graph convolutional regression of cardiac depolarization from sparse endocardial maps. In *International Workshop on Statistical Atlases and Computational Models of the Heart*, pages 23–34. Springer, 2020.
- G. B. Moody and R. G. Mark. A new method for detecting atrial fibrillation using rr intervals. In *Computers in Cardiology*, volume 10, pages 227 – 230, 1983.
- K. Murphy. Switching Kalman Filters. *Dept. of Computer Science, University of California, Berkeley, Tech. Rep*, 1998.
- A. Natarajan, Y. Chang, S. Mariani, A. Rahman, G. Boverman, S. Vij, and J. Rubin. A wide and deep transformer neural network for 12-lead ecg classification. In *2020 Computing in Cardiology*, pages 1–4. IEEE, 2020.
- F. H. Netter. *The CIBA collection of medical illustrations.*, volume 5. CIBA Pharmaceutical products,, 1992.
- D. Noble. Cardiac action and pacemaker potentials based on the hodgkin-huxley equations. *Nature*, 188:495–497, Nov. 1960. ISSN 0028-0836.
- D. Noble, A. Garny, and P. J. Noble. How the hodgkin-huxley equations inspired the cardiac physiome project. *The Journal of physiology*, 590:2613–2628, June 2012. ISSN 1469-7793. doi: 10.1113/jphysiol.2011.224238.
- O. Oktay, E. Ferrante, K. Kamnitsas, M. Heinrich, W. Bai, J. Caballero, S. A. Cook, A. De Marvao, T. Dawes, D. P. OâRegan, et al. Anatomically constrained neural networks (acnns): application to cardiac image enhancement and segmentation. *IEEE transactions on medical imaging*, 37(2):384–395, 2017.
- J. Oster and G. Clifford. Signal quality indices for state space electrophysiological signal processing and vice versa. *Advanced State Space Methods for Neural and Clinical Data*, 15:345–366, 2015.
- J. Oster and G. D. Clifford. An artificial model of the electrocardiogram during paroxysmal atrial fibrillation. In *Computing in Cardiology Conference (CinC), 2013*, pages 539–542. IEEE, 2013.
- J. Oster and G. D. Clifford. Acquisition of electrocardiogram signals during magnetic resonance imaging. *Physiological measurement*, 38:R119–R142, June 2017. ISSN 1361-6579. doi: 10.1088/1361-6579/aa6e8c.
- J. Oster, M. Geist, O. Pietquin, and G. Clifford. Filtering of pathological ventricular rhythms during mri scanning. *International Journal of Bioelectromagnetism*, 15(1):54–59, 2013.
- J. Oster, J. Behar, A. E. W. Johnson, O. Sayadi, S. Nemati, and G. D. Clifford. Semi-supervised ECG beat Classification and Novelty Detection based on Switching Kalman Filters. *Biomedical Engineering, IEEE Transactions on*, 62:2125–2134, 2015a.
- J. Oster, J. Behar, O. Sayadi, S. Nemati, A. E. Johnson, and G. D. Clifford. Semisupervised ecg ventricular beat classification with novelty detection based on switching kalman filters. *IEEE T Bio-Med Eng*, 62(9):2125–2134, 2015b.
- J. Oster, R. Llinares, S. Payne, Z. T. H. Tse, E. J. Schmidt, and G. D. Clifford. Comparison of three artificial models of the magnetohydrodynamic effect on the electrocardiogram. *Computer methods in biomechanics and biomedical engineering*, 18(13):1400–1417, 2015c.

- D. Ouyang, B. He, A. Ghorbani, N. Yuan, J. Ebinger, C. P. Langlotz, P. A. Heidenreich, R. A. Harrington, D. H. Liang, E. A. Ashley, et al. Video-based ai for beat-to-beat assessment of cardiac function. *Nature*, 580(7802):252–256, 2020.
- A. Petrenas, V. Marozas, L. Sörnmo, and A. Lukosevicius. An echo state neural network for qrst cancellation during atrial fibrillation. *IEEE transactions on bio-medical engineering*, 59: 2950–2957, Oct. 2012. ISSN 1558-2531. doi: 10.1109/TBME.2012.2212895.
- A. Petrėnas, L. Sörnmo, A. Lukošėvičius, and V. Marozas. Detection of occult paroxysmal Atrial Fibrillation. *Medical & biological engineering & computing*, 53(4):287–297, 2015.
- A. Petrenas, V. Marozas, A. Solosenko, R. Kubilius, J. Skibarkiene, J. Oster, and L. Sörnmo. Electrocardiogram modeling during paroxysmal atrial fibrillation: application to the detection of brief episodes. *Physiological measurement*, 38:2058–2080, Nov. 2017. ISSN 1361-6579. doi: 10.1088/1361-6579/aa9153.
- M. A. Pimentel, D. A. Clifton, L. Clifton, and L. Tarassenko. A Review of Novelty Detection. *Signal Processing*, 2014.
- L. Pineda, S. Basu, A. Romero, R. Calandra, and M. Drozdal. Active mr k-space sampling with reinforcement learning. In *International Conference on Medical Image Computing and Computer-Assisted Intervention*, pages 23–33. Springer, 2020.
- J. Pitt-Francis, P. Pathmanathan, M. O. Bernabeu, R. Bordas, J. Cooper, A. G. Fletcher, G. R. Mirams, P. Murray, J. M. Osborne, A. Walter, et al. Chaste: a test-driven approach to software development for biological modelling. *Computer Physics Communications*, 180(12):2452–2471, 2009.
- H. Qi, N. Fuin, T. Kuestner, R. Botnar, and C. Prieto. Accelerated 4d respiratory motion-resolved cardiac mri with a model-based variational network. In *International Conference on Medical Image Computing and Computer-Assisted Intervention*, pages 427–435. Springer, 2020.
- J. Quinn, C. Williams, and N. McIntosh. Factorial Switching Linear Dynamical Systems applied to Physiological Condition Monitoring. *Pattern Analysis and Machine Intelligence, IEEE Transactions on*, 31(9):1537–1551, 2009.
- C. Ramanathan, R. N. Ghanem, P. Jia, K. Ryu, and Y. Rudy. Noninvasive electrocardiographic imaging for cardiac electrophysiology and arrhythmia. *Nature medicine*, 10(4):422–428, 2004.
- R. Rouhi, M. Clausel, J. Oster, and F. Lauer. An interpretable hand-crafted feature-based model for atrial fibrillation detection. *Frontiers in Physiology*, 12:581, 2021.
- F. Sahli Costabal, Y. Yang, P. Perdikaris, D. E. Hurtado, and E. Kuhl. Physics-informed neural networks for cardiac activation mapping. *Frontiers in Physics*, 8:42, 2020.
- R. Sameni and G. D. Clifford. A review of fetal ecg signal processing; issues and promising directions. *The open pacing, electrophysiology & therapy journal*, 3:4–20, Jan. 2010. ISSN 1876-536X. doi: 10.2174/1876536X01003010004.
- R. Sameni, M. B. Shamsollahi, C. Jutten, and G. D. Clifford. A nonlinear Bayesian filtering framework for ECG denoising. *Biomedical Engineering, IEEE Transactions on*, 54(12):2172–2185, 2007.
- R. Sameni, C. Jutten, and M. B. Shamsollahi. Multichannel electrocardiogram decomposition using periodic component analysis. *Biomedical Engineering, IEEE Transactions on*, 55(8):1935–1940, 2008.

BIBLIOGRAPHY

- P. Sarkar and A. Etemad. Self-supervised ecg representation learning for emotion recognition. *IEEE Transactions on Affective Computing*, 2020.
- S. Sarkar, D. Ritscher, and R. Mehra. A detector for a chronic implantable atrial tachyarrhythmia monitor. *Biomedical Engineering, IEEE Transactions on*, 55(3):1219–1224, 2008.
- O. Sayadi, M. B. Shamsollahi, and G. D. Clifford. Robust detection of premature ventricular contractions using a wave-based Bayesian framework. *Biomedical Engineering, IEEE Transactions on*, 57(2):353–362, 2010.
- J. Schlemper, J. Caballero, J. V. Hajnal, A. N. Price, and D. Rueckert. A deep cascade of convolutional neural networks for dynamic mr image reconstruction. *IEEE transactions on Medical Imaging*, 37(2):491–503, 2017.
- O. H. Schmitt. Biological information processing using the concept of interpenetrating domains. In *Information processing in the nervous system*, pages 325–331. Springer, 1969.
- A. D. Scott, J. Keegan, and D. N. Firmin. Motion in Cardiovascular MR Imaging. *Radiology*, 250(2):331–351, 2009.
- F. G. Shellock. Radiofrequency energy-induced heating during mr procedures: A review. *JMRI- J Magn Reson Im*, 12:30–36, 2000.
- L. Sörnmo. *Atrial Fibrillation from an Engineering Perspective*. Springer, 2018.
- L. Sörnmo, P. O. Borjesson, M.-E. Nygard, and O. Pahlm. A method for evaluation of qrs shape features using a mathematical model for the ecg. *IEEE Transactions on Biomedical Engineering*, (10):713–717, 1981.
- M. Stridh and L. Sörnmo. Spatiotemporal qrst cancellation techniques for analysis of atrial fibrillation. *IEEE transactions on bio-medical engineering*, 48:105–111, Jan. 2001. ISSN 0018-9294. doi: 10.1109/10.900266.
- C. Sudlow, J. Gallacher, N. Allen, V. Beral, P. Burton, J. Danesh, P. Downey, P. Elliott, J. Green, M. Landray, et al. UK Biobank: an Open Access resource for identifying the causes of a wide range of complex diseases of middle and old age. *PLoS medicine*, 12(3):1–10, 2015.
- T. Tenforde. Magnetically induced electric fields and currents in the circulatory system. *Prog Biophys Mol Bio*, 87(2-3):279–288, 2005.
- T. S. Tenforde. Interaction mechanisms and biological effects of static magnetic fields. *Automedica*, 14:271–293, 1992.
- T. S. Tenforde, C. T. Gaffey, B. R. Moyer, and T. F. Budinger. Cardiovascular alterations in Macaca Monkeys exposed to stationary fields: experimental observations and theoretical analysis. *Bioelectromagnetics*, 4(1):1–9, 1983.
- L. Tung. *A bi-domain model for describing ischemic myocardial dc potentials*. PhD thesis, Massachusetts Institute of Technology, 1978.
- A. van Oosterom and T. F. Oostendorp. ECGSIM: an interactive tool for studying the genesis of QRST waveforms. *Heart*, 90(2):165–168, Feb 2004. URL <http://www.hubmed.org/display.cgi?uids=14729788>.
- A. Vaswani, N. Shazeer, N. Parmar, J. Uszkoreit, L. Jones, A. N. Gomez, L. Kaiser, and I. Polosukhin. Attention is all you need. *arXiv preprint arXiv:1706.03762*, 2017.

- N. Vogt. Cnns, lstms, and attention networks for pathology detection in medical data. *arXiv preprint arXiv:1912.00852*, 2019.
- T. Wang, P. Bonizzi, J. Karel, and R. Peteers. Ecgj with a deep neural network and 2d normalized body surface potential maps. In *Computing in Cardiology*, page 257. IEEE, 2021.
- J. Zbontar, F. Knoll, A. Sriram, T. Murrell, Z. Huang, M. J. Muckley, A. Defazio, R. Stern, P. Johnson, M. Bruno, et al. fastmri: An open dataset and benchmarks for accelerated mri. *arXiv preprint arXiv:1811.08839*, 2018.
- B. Zhao, X. Wu, J. Feng, Q. Peng, and S. Yan. Diversified visual attention networks for fine-grained object classification. *IEEE Transactions on Multimedia*, 19(6):1245–1256, 2017.
- B. Zhu, J. Liu, N. Koonjoo, B. Rosen, and M. Rosen. Automated pulse sequence generation (autoseq) using bayesian reinforcement learning in an mri physics simulation environment. In *Proc. 26th Annu. Meeting ISMRM*, pages 16–21, 2018a.
- B. Zhu, J. Z. Liu, S. F. Cauley, B. R. Rosen, and M. S. Rosen. Image reconstruction by domain-transform manifold learning. *Nature*, 555(7697):487–492, 2018b.

Titre : *Analyse des signaux Electrocardiogrammes: du modèle à l'apprentissage machine*

Résumé : Mes recherches ont essentiellement porté sur l'utilisation de méthodes de modélisation et de traitement des signaux pour extraire de nouveaux paramètres cliniques de grandes bases de données de signaux physiologiques, et sur l'utilisation de techniques d'apprentissage automatique pour l'aide à la décision clinique. J'applique ces techniques aux données électrocardiographiques (ECG) depuis plus de 10 ans.

Mon projet de recherche consiste à développer de nouvelles techniques d'apprentissage automatique combinées à et/ou inspirées par la modélisation afin de créer des systèmes de décision automatique interprétables dans le domaine des soins de santé cardiovasculaire. L'évaluation clinique de la santé cardiovasculaire nécessite l'acquisition de données multimodales, deux des modalités les plus importantes étant l'imagerie par résonance magnétique (IRM) et l'ECG. Mon objectif sera donc de développer des outils pour l'analyse conjointe de données électrophysiologiques et d'imagerie. Ces techniques et représentations de données offriront des solutions à des problèmes cliniques concrets tels que pour la prédiction des résultats de l'ablation par catheter de la fibrillation auriculaire, ou la stratification de risque de présenter une tachycardie ventriculaire.

Mots clés : .

Title: *Analysis of Electrocardiogram signals: from modelling to classification through signal processing*

Abstract: The focus of my research is the use of modeling and signal-processing methods to extract novel clinical parameters from large databases of physiological signals, and the use of machine-learning techniques to provide predictive actionable information to clinicians. I have been applying these techniques to electrocardiographic (ECG) (and other physiological) data for more than 10 years.

My research project consists in developing novel machine-learning techniques combined with and/or inspired by modelling in order to create interpretable automatic decision-making systems in healthcare, with a particular focus to cardiovascular health data. Clinical assessment of the cardiovascular health requires the acquisition of multimodal data, two of the most important modalities being Magnetic Resonance Imaging (MRI) and ECG. I therefore aim at developing tools for the joint analysis of electrophysiological and imaging data. These techniques and representations of data will offer solutions for concrete clinical problems such as better risk stratification for patients, whether for Atrial Fibrillation catheter ablation outcome prediction, and the risk of presenting Ventricular Tachycardia.

Keywords : .